Title
Characterizing glycans on stem cells for discovery of biomarkers and biological significance

Permalink
https://escholarship.org/uc/item/7vw7k066

Author
Gip, Phung

Publication Date
2010

Peer reviewed|Thesis/dissertation

Characterization of glycans on stem cells for discovery of biological markers and

functional significance

by

Phung Tu Gip

A dissertation submitted in partial satisfaction of the

requirements for the degree of

Doctor of Philosophy

in

Molecular and Cellular Biology

in the

Graduate Division

of the University of California at Berkeley

Committee in charge:

Professor Carolyn R. Bertozzi, Chair
Professor David V. Schaffer
Professor Randy Schekman
Professor Irina Conboy
Professor Andrew Wurmser

Fall 2010

Abstract

Characterization of glycans on stem cells for discovery of biomarkers and
functional significance

by

Phung Tu Gip

Doctor of Philosophy in Molecular and Cell Biology

University of California, Berkeley

Professor Carolyn R. Bertozzi, Chair

A decade after the sequencing of the human genome, there are many biological functions that cannot be discerned from the genetic code. Post-translational modifications that regulate biological functions, such as glycosylation, have become the focus of biological research to help fill in the gaps not filled by genomics. Glycosylation is the process by which oligosaccharides, termed glycans, are appended onto membrane and secreted proteins as well as lipids. Glycans on the cell surface make up the majority of the cellular glycome, and are essential for many biological processes, including cell development and differentiation, cell-cell or cell-matrix communication, and pathogen-host recognition. In addition, they can be powerfully harnessed as cellular markers for distinct cell populations. This thesis focuses on the efforts made to characterize the cell surface glycome of human embryonic stem cells (hESCs) and changes in glycosylation during neural differentiation for

Human embryonic stem cells are derived from human embryos with the capacity to differentiate into any somatic cell type. Since the derivation of hESC lines, there has been an enormous amount of excitement surrounding their use in regenerative medicine and as a model for human development. In the last decade, the properties and behavior of stem cells have been extensively studies. There are still several challenges, however, that remain in understanding hESC biology, such as characterization of the glycome and the functional role of glycans. Glycans and glycoconjugates are ideal candidates for cell surface markers of stem cells as they are easily identified by a wide array of lectins and antibodies. The few stem cell surface markers used are antigens identified, thus, glycome profiling will be extremely useful for specific selection and enrichment of hESCs at various stages of development and for defining the functional roles of glycans in the process.

Because of the heterogeneity and complexity of many glycans, they have been traditionally hard to study. This complexity has presented a significant challenge for obtaining structural information about glycans at the molecular level, particularly in contexts that are relevant to native cellular physiology. Technological advances in the last few decades have allowed for better characterization of these glycans, a major challenge in the past. One such approach is the use of fourier transform (FTICR) mass spectrometry

1

(MS), the most sensitive ion detection method with almost unlimited resolution, surpassing commonmass spectrometric methods. Chapter 2 describes the development of a method using FTICR MS and analytical tools to analyze membrane glycans on hESCs. This method is the first to provide structural detail and quantitation of glycans on hESCs membranes and to reveal an unusual glycosylation pattern not commonly found on mammalian cell surface.

The development of this method allowed for analysis of glycans on different cell types. Since changes in glycans during stem cell differentiation have important roles in self-renewal and differentiation, Chapter 3 focuses on characterizing the changes in the glycosylation pattern of embryoid bodies and neural stem cells derived from hESCs. By analyzing glycans on hESC during neural development, new potential stem cell and cell stage markers were identified as well as the identification of high mannose glycans in all cell stages. These findings have elicited a new investigation into the function of high mannose glycans on hESCs and mammalian cells.

In summary, glycosylation is a fundamental post-translational modification that is important in all cells. The wealth of information contained in the glycome of a cell has yet to be discovered. With existing technological advances, and efforts to optimize methods, various part of the glycome can be characterized. hESCs differentiated along the neural lineage was used as a model system to further understand hESC biology and to find novel biomarkers for the specific cell types. Toward this end, several N-glycans were identified on hESCs, embryoid bodies and neural stem cells by developing an optimized method using state-of-the –art mass spectrometry. Characterization of the hESC glycome should contribute to our understanding of hESC biology, and help to accelerate their use in regenerative medicine.

_____

Professor Carolyn R. Bertozzi, Chair

This thesis is dedicated to my family and friends for all their support. Special thanks to my parents and my sister and brother.

Table of Contents

Chapter 1. Principles of cell surface glycosylation during development

Chapter 2. Optimization of hESC membrane glycans analysis using FTICR MS

Chapter 3. Identification of glycans on hESCs during neural development

List of Figures

Acknowledgments

Chapter 1:
Principles of cell surface glycosylation during development

Chapter 1: Principles of cell surface glycosylation during development

1.1. Introduction

One of the many post-genomic challenges in cell biology is characterizing post-translational modifications of proteins that provide the considerable diversity needed to regulate a variety of biological functions (1). Glycosylation is the most common and complex form of post-translational modifications, and approximately 50% of all proteins are glycosylated (2). In this process, glycans are appended onto membrane and secreted proteins and lipids, as glycoconjugates, to serve important roles in many biological systems mediating cell-cell interactions (3,4,5), such as adhesion (4,6-9) and signaling (4,10). They also can serve as markers for identifying various cellular states. Changes in glycosylation accompany temporal and lineage specificity during embryogenesis, development, and differentiation of various cell types (3,11-17). In addition, differences in glycan profiles between healthy and disease states has been utilized as a method for clinical diagnosis and has provided targets for many novel classes of therapeutics, including those used for cancer chemotherapy, diabetes treatment, and antibiotic and anti-viral medicine (5,18).

While significant progress has been made in elucidating the identity of glycans and their physiological functions, the glycosylation state of most proteins and the role of the glycans on those proteins are mostly unknown. This gap in knowledge is due to the inherent complexity of glycan biosynthesis as well as their structural and chemical heterogeneity. Glycans are highly diverse in nature, varying in the composition of individual monosaccharide building blocks, the positions with which these building blocks link to each other, and the stereochemical disposition of the linkages (α or β) (3). In addition, the biosynthesis of glycans is non-template driven, meaning that their structures cannot be predicted from a DNA template (3). This complexity has presented a significant challenge for obtaining structural information about glycans at the molecular level, particularly in contexts that are relevant to native cellular physiology. For this reason, the technology for elucidating their structures has lagged behind other major classes of biomolecules, such as protein, DNA, and RNA (19). With the development and optimization of new technologies in the last few decades, progress has been made exploring the structures and functions of glycans that make up the "glycome." The information content of the glycome is enormous, however, characterizing and understanding the glycome on different cell populations in various physiological states will provide new developments in basic biology and medicine.

1.2. Different types of glycans make up the glycome

Glycans exist as monosaccharides, oligosaccharides, and polysaccharides that can be covalently attached to other macromolecules, making up the "glycome" of a cell (3). In higher eukaryotes, glycans are convalently attached to their protein or lipid scaffolds forming glycoproteins and glycolipids, orchestrated by several glycosyltransferases and glycosidases in the endoplasmic reticulum (ER) and Golgi apparatus (20,21). There are three major types of glycoproteins: N-glycans, O-glycans, and glycosaminoglycans,
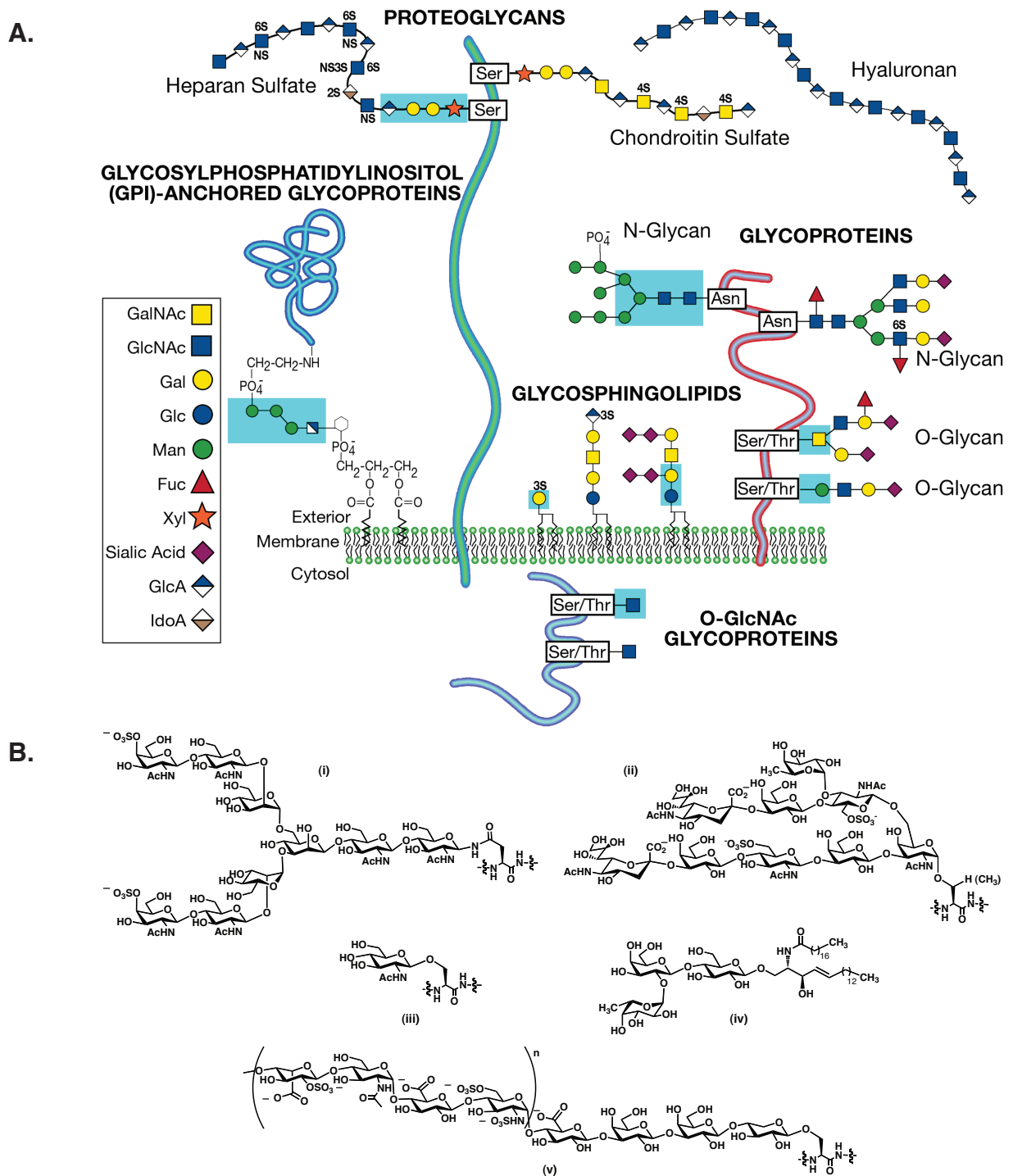
Figure 1.1. Common classes of animal glycans. (A) The monosaccharides in the symbolic representations are N-acetylglucosamine (GalNAc), N-acetylglucosamine (GlcNAc), galactose (Gal), Glucose (Glc), mannose (Man), fucose (Fuc), xylose (Xyl), N-acetylneuraminic acid, glucuronic acid (GlcA) and iduronic acid (IdoA) (Adopted from Varki et al. 2009, Essentials in Glycobiology, 2nd edition). (B) Typicla structures of a N-glycan (i), O-glycan (ii), bO-GlcNAc (iii), glycolipd (iv), and proteglycan (v).

which are defined by their structure and attachment to peptides. N-glycans have an N-acetylglucosamine (GlcNAc) attached to an asparagine residue in the peptide sequence containing Asn-Xxx-Ser/Thr, where Xxx corresponds to any amino acid, except for proline (20). Typically in O-glycans, N-acetylgalactosamine (GalNAc) is linked to serine or threonine residues of proteins (21). Whereas glycosaminoglycans (GAGs) are linear chains of repeating disaccharide units that contain one of the two modified sugars, GalNAc or GlcNAc, with an uronic acid. Proteoglycans are a type of glycosaminoglycan that attach to serine residues of specific core proteins (22). Another type of glycan attachment occurs when glycans are attached to a lipid carrier, providing glycolipds. Glycolipds contain a hydrophobic ceramide anchor, such as N-acylsphingoside, and sugars at the hydrophilic end. In general, glycan structures can vary from highly branched, complex glycans (N- and O- glycans, and glycolipids) to linear glycans (proteoglycans; Fig.1.1). N-glycans are thought to be the most abundant type of glycan. Inside the cell, N-glycans function in protein folding and trafficking of proteins in the secretory and endocytic pathway (23). On the cell surface, N-glycans are involved in several biological functions, such as in cell-cell communication, signaling, adhesion, cell development and differentiation, as well as pathogen-host recognition.

1.3. Protein glycosylation

N-glycans are derived from a previously synthesized precursor containing 14 monosaccharides: 2 GlcNAc, 9 mannose, and 3 glucose (Glc3Man9GlcNAc2) units, at-
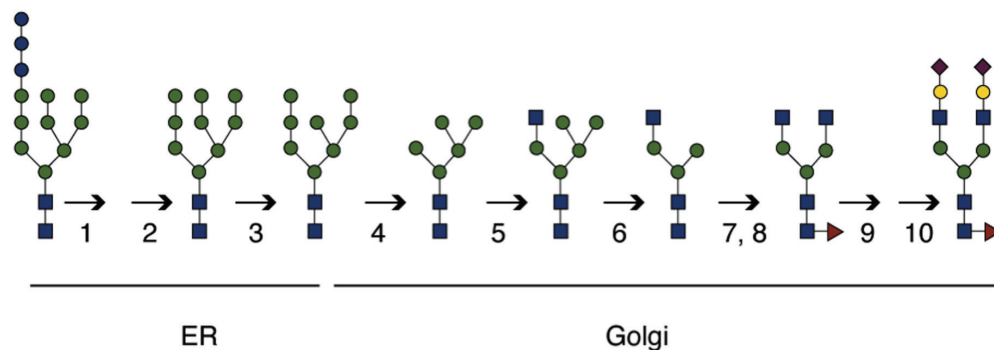
Figure 1.2. Several enzymes are involved in N-glycan processing (1) α-glucosidase I, (2) α-glucosidase II, (3) ER α-1,2 mannosidase, (4) Golgi α-1,2 mannosidase I, (5) N-acetylglucosaminyltransferase II, (8) fucosyltransferase, (9) galactosyltransferase, (10) sialytransferase.

tached to the asparagine residue of a nascent protein in the ER (20). The precursor is subjected to sequential enzymatic modifications, resulting in three types of N-glycan structures with a trimannosyl pentasaccharide core (Man3GlcNAc2): high mannose, hybrid, and complex. In the ER, high mannose structures are formed from the precursor

after the removal of the three glucoses by glucosidases-I and -II, leaving only mannose residues. High mannose glycans are considered "immature" glycans that are further processed to generate hybrid and complex glycans. The activity of α-mannosidases reduces the number of mannose residues, allowing for the generation of hybrid structures in the Golgi appartus, consisting of 3 mannose residues on one branch with the other containing various sugars. The coordinated activity of several other enzymes add or remove sugars to further elaborate and form complex glycans, which can be structures with several branches. Hybrid and complex glycans are further modified with common terminal sugars such as GlcNAc, galactose, sialic acid, and fucose to generate a variety of different structures depending on the enzymes that are expressed in the cell (20; Fig. 1.2).

O-glycans are primarily assembled in the Golgi apparatus (21). There are several different types of O-glycosylation. Contrary to N-glycans, there is no trimming involved that occurs in O-glycan synthesis. Mucin-type glycans are the most abundant form with the attachment of N-acetylgalactosamine (GalNAc) directly onto a serine or threonine residue. Other monosaccharides such as fucose, galactose, glucose, mannose, and xylose can also modify the peptide. A special type of O-glycosylation is the reversible β-O-linkage of GalNAc to cytoplasmic and nuclear proteins (24). Like N-glycans, O-glycans are complex and heterogeneous structures (21).

1.4. Changes in glycans during development

The enzymes involved in the biosynthesis of glycans are sensitive to the various intracellular and extracellular factors governed by the physiological status of a cell. This sensitivity makes the glycome very dynamic, amenable to programmed changes during differentiation and development (12,25, 26,27). In the 1970's, several surface antigens were discovered to be differentially expressed and biologically important in vertebrate embryogenesis (28). Many of these antigens were found to be glycans. Muramatsu et al. (27) studied mouse and human embryonic carcinoma cell lines (EC) derived from teratomas, which resemble multipotential cells and mouse embryos as model systems12,26,27,28. From histochemical analyses using glycan-binding lectins and antibodies, they showed that glycans expressed during development are spatially and temporally regulated, restricted to specific stages early in embryogenesis. As such, some of these surface antigens were appropriately named: stage-specific embryonic antigens (SSEA) (29,30).

In the process of embryogenesis, the fertilization of the egg by sperm forms the zygote, which undergoes several mitotic divisions starting from the 2- to 8- to 16-cell stage to form a blastocyst, a hollow sphere of at least 100 cells, with two distinct tissue types, the trophoblast and the embryoblast (31,32). The trophoblast is the outer layer of cells that eventually form the placenta. The embryoblast, also known as the inner cell mass (ICM), is the cells that develop into the three germ layers, ectoderm, endoderm, and mesoderm to form the embryo and is the source of embryonic stem cells (ES). SSEA-1 was the first SSEA antigen discovered as an important marker in mouse development (29,33). It is a fucosylated trisaccharide, otherwise known as Lexis X antigen (29). In pre-implantation mouse embryos, SSEA-1 first appears at the late 8-cell stage and is highly expressed in cells in the ICM, such as embryonic ectoderm and visceral endoderm. It can be detected in trophoblasts in early post-implantation embryos and later in specific adult tissues (34).

Mouse EC cells also express SSEA-1, which disappears during cellular differentiation (35).

Two other antigenic epitopes discovered were SSEA-3 and SSEA-4 (30, 36). They are glycolipid antigens that are expressed on the zygote until they disappear some time at the blastocyst stage. They are not expressed in the ICM; however, SSEA-3 is expressed on extraembryonic visceral endoderm. Interestingly, these SSEA antigens are differentially expressed in human EC cells and embryos compared to those in mouse (37).

Human EC cells express SSEA-3 and SSEA-4 and only SSEA-1 during differentiation. In pre-implantation human embryos, SSEA-1 is expressed only on trophoblast, and SSEA-3 and SSEA-4 are initially detected and highly expressed on embryonic stem cells in the ICM. Two other surface antigens found were keratan sulfate proteoglycans called TRA-1-60 (38) and TRA-1-81 (12), which are mostly absent in pre-implantation mouse embryos, but appear in the ICM of human embryos (37). Monitoring changes in the glycome have been invaluable in defining stages of development and differentiation.

1.5. The derivation of human embryonic stem cells

The discovery of cell surface glycans in the 1970's has significantly contributed to an exciting line of research on embryonic stem cells that could revolutionize biomedical research. The generation of antibodies SSEA-3, SSEA-4, TRA-1-60, and TRA-1-81 against glycan antigens expressed in the inner cell mass (ICM) has been crucial in characterizing human embryonic stem cells (hESC). The generation of hESC lines has elicited significant attention and excitement with the hopes of treating diseases, use in drug discovery screens, and providing a basic model for human development (39,40, 41). hESCs are derived from the human inner cell mass (ICM) of the blastocyst, the structure formed in early embryogenesis, approximately 5 days after fertilization. Since the first mouse embryonic stem cell lines were derived in 1981 (42,43), the properties and behavior of stem cells have been extensively studied (44-56). What followed almost two decades later in 1998, was the derivation of the first hESC lines by Thomson et al.(39). Since then, several hESCs lines have been derived from donated embryos (41). Embryonic stem cells have the unique ability for unlimited self-renewal and intrinsic capability to differentiate into any of the 220 somatic cell types in the adult body. hESC lines share a similar capacity to self-renew and differentiate into several different cell types. In addition to their developmental potential and similar expression of surface markers in the ICM of human blastocyts, they can be further characterized by their transcriptional and epigenetic profiles.

1.5.1. Glycosylation of hESCs

Significant progress has been made in characterizing the hESC transcriptome (collection of genes expressed as mRNA) (57,58), epigenome (total epigenetic state of a cell) (58,59) as well as the proteome (collection of proteins expressed by the cell) (60), to elucidate the molecular mechanisms underlying hESC biology. The characterization of the glycome, however, and the functional roles of glycans in hESCs have not been fully investigated. While stage-specific embryonic antigens, (SSEA-3 and SSEA-4) are the most established glycan-based markers and are used to characterize hESCs (39), there

is a need for additional markers to positively identify the vast array of cell populations that can arise from differentiation. As a consequence, progress towards answering fundamental questions about the behavior of hESCs and their utilization for therapeutic purposes has been impeded by this lack of cell surface markers. Glycome profiling will be extremely useful for specific selection and enrichment of hESCs at various stages of development and for defining the functional roles of glycans in the process.

The glycosylation of hESCs has been previously studied using lectins and antibodies to identify glycans on hESCs (61,62). Venable et al. was the first to use a panel of lectins on SSEA-4-positive hESCs to assess the presence of their respective glycan antigen on the cell surface. Using flow cytometry and immunocytochemistry, lectins TL, RCA, and Con A, specific for N-acetylglucosamine, galactose, branched mannose, and free glucose, respectively, were found to bind to the majority of hESCs and hESC colonies. These lectins could potentially be used as surface markers for hESCs (61). A complementary study by Wearne et al., using similar techniques and a panel of lectins and antibodies against various glycan antigens, differentiated hESCs into embryoid bodies (EB) to probe for changes in glycosylation patterns (62). Embryoid bodies are aggregates of representative precursor cells from all three germ layers and formed when hESCs are grown in suspension without growth factors (63). The study revealed that hESCs and EBs have an abundance of α-mannosyl-terminated chains, poly N-acetyllactosaminyl residues, α-2,3- and - α-2,6-linked sialic acids, α-1,6-linked fucose, Tn, and sialyl-Tn antigens. Both cell types did not bind to the DBA or Lotus lectins, specific for α-N-acetylgalactosamine, and terminal α-1,2-linked fucose. One lectin that bound to hESCs, but not to EBs was UEA-1, which is specific for α-1,2-linked fucose. Additionally, MAA lectin, which identifies the presence of the disaccharide Neu5Ac-α-2,3-Gal, bound 89% of the EBs, but only 19% of undifferentiated hESCs. This study is the most descriptive analysis of the hESC surface glycome as it changes during differentiation.

Recently, Satomaa et al. performed a more comprehensive study by analyzing the entire N-glycome of hESC, hESC-derived EBs, and uncharacterized differentiated cells using mass spectrometry (64). By analyzing whole cell lysates from the three cell types, hESCs were found to have high levels of high mannose glycans, while low-mannose type and hybrid-type glycans were abundant in EBs. A distinct characteristic of hESCs compared to all differentiated cells was complex fucosylation, meaning that hESC N-glycans were modified by more than one fucose residue. Approximately 25% of the total N-glycan profile of hESCs changed during their differentiation. Because whole cell lysates were used in this study, it is unclear whether glycosylation changes were on the cell surface or intracellular. While these studies have shown that the hESC glycome is dynamic and changes during cellular differentiation, continued investigations are necessary to profile the hESC surface glycome and various cellular lineages.
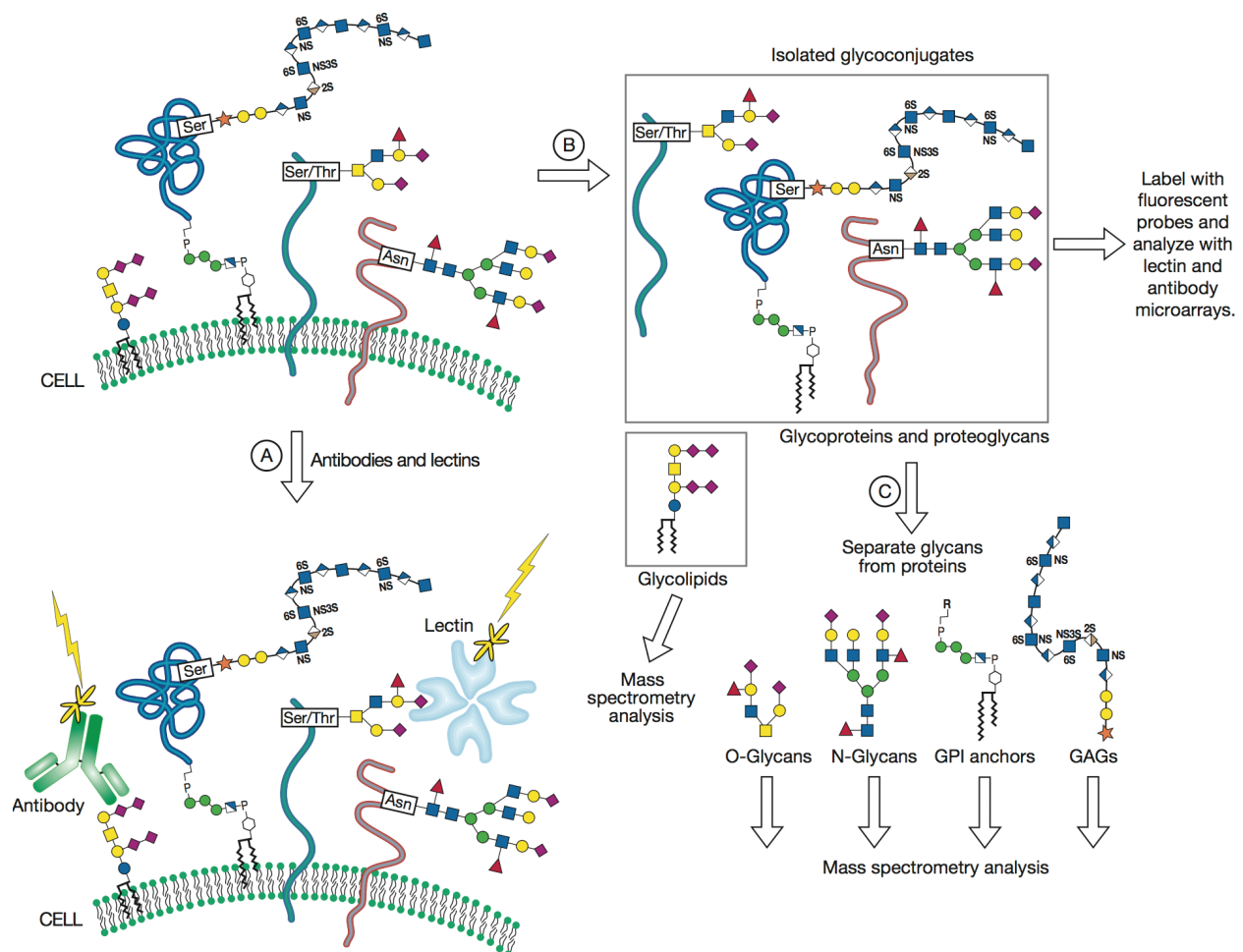
Figure 1.3. Multiple approaches for profiling a cell's glycome at various hierarchical levels of complexity. (Step A) Cells can be directly probed for glycan expression using labeled lectins and glycan-specific antibodies. This top–down experiment provides a global view of the distribution of certain glycan epitopes on cells and tissues but does not afford detailed structural information. (Step B) Glycoproteins and glycolipids can be isolated from cell lysates and then analyzed using lectin and antibody microarrays and mass spectrometry methods. Glycolipids can be sequenced directly, whereas glycoproteins are often further deconstructed into separate glycans and proteins before structural analysis. (Step C) Isolated glycans are separated based on type (i.e., N-glycans, O-glycans, glycosaminoglycans, etc.) and their sequences determined by mass spectrometry. Alternatively, intact glycoproteins can be digested with trypsin and the glycopeptides characterized by mass spectrometry. This approach retains the glycan–peptide linkage and allows assignment of sites of protein glycosylation. Collectively, steps B and C comprise a bottom–up glycomic analysis (Adopted from Varki et al. 2009, Essentials in Glycobiology, 2nd edition).

8

1.6. Methods of analyzing the glycome

Due to the recent technological advances, significant progress has been made in profiling changes in the glycome during development and in other biological systems. Approaches to investigating the glycome depends on what aspect of the glycome is being investigated. The analysis of the glycome can be deconstructed into four levels of investigation (3): (1). Profiling of glycan structures that are separated from its protein or lipid scaffold, (2). Identifying the protein or lipid that is being modified by the glycan and the site of attachment of the glycan, (3). Determining the glycans and glycoconjugates expressed on specific cell types, and (4). Visualizing the organization of glycoconjugates relative to each other on the cell's surface and extracellular matrix. There is no one method that can evaluate the entire glycome. And due to the structural diversity of the glycome, different approaches and techniques are necessary to evaluate the different glycan classes (i.e. N- and O-glycans, glycosaminoglycans, and glycolipids).

1.6.1. Lectins and antibodies

As previously discussed, glycan-binding lectins and antibodies are widely accessible tools to probe glycosylation at a global level (3). Commercially available antibodies and naturally occurring lectins conjugated to fluorophores allow for the detection of diverse glycans using fluorescence microscopy, flow cytometry, and tissue histology (12,61,62). Lectins and antibodies can be useful in profiling glycans with or without their scaffolds or to enrich for specific glycans toward identification of the protein or lipid scaffold. They also can be used to profile the glycome on specific cell types or tissues ex vivo, and serve to identify their cellular and tissue distribution. Lectins and antibodies can be bound on chips, similar to DNA microarrays (65). This microarray technique provides a high-throughput method to analyze cellular glycomes (Fig. 1.3). Unfortunately, the structural information obtained by lectins and antibodies is limited, dependent upon the antigen to which they bind. In addition, the number of lectins and antibodies available do not cover the all the possible glycan structures that exist, some of which are yet to be discovered.

1.6.2. Metabolic and covalent labeling

While lectins and antibodies are mostly used to profile the glycome on specific cell types or tissues ex vivo, metabolic and covalent labeling of glycans is a method for in vivo imaging as well as the enrichment of glycoproteins. Metabolic and covalent labeling of glycans is a technique pioneered in Carolyn Bertozzi's lab for the study of protein glycosylation (66,67,68). This method relies on the use of unnatural monosaccharides (azido sugars), which are structurally very similar to natural sugars, but bear a reactive chemical functionality (the azide). For example, azido sugar N-azidoacetylmannosamine (ManNAz), is taken up by the cell, converted, and incorporated into glycoproteins in the place of the natural sugar, sialic acid. ManNAz becomes azido sialic acid (SiaNAz) (69,70). The azide functionality then can be used to selectively label glycoproteins with affinity tags or fluorescent dyes by the addition of reactive partners bearing a phosphine (e.g. Phos-FLAG) (71), cyclooctyne (e.g. DIFO-Alexa Fluor-488) (72), or an alkyne (e.g. Alkyne-Cy3)
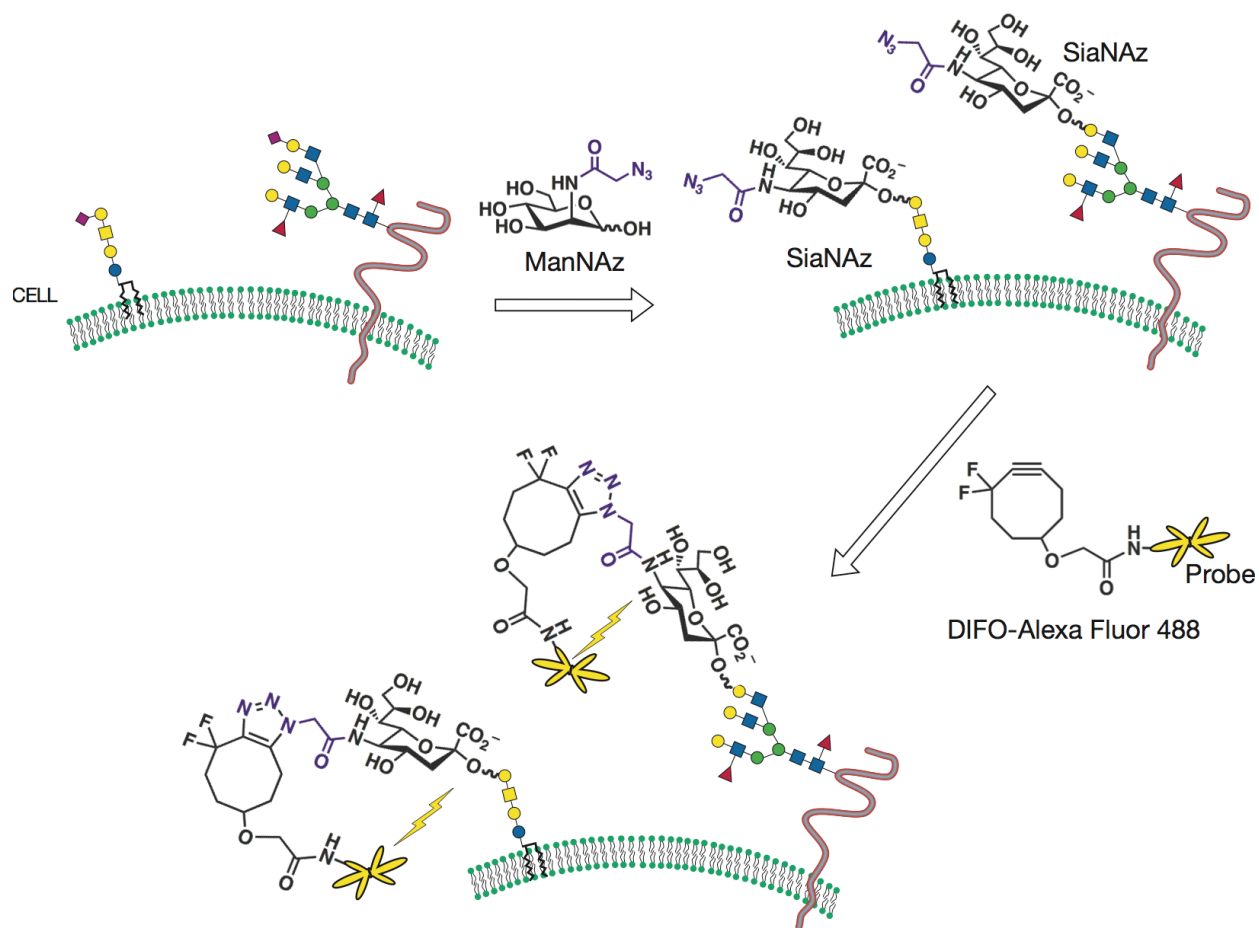
Figure 1.4. Metabolic and covalent labeling of glycans for in vivo imaging of the glycome. Cells metabolize azido sugars such as N-azidoacetylmannosamine (ManNAz), which is converted into the corresponding azido sialic acid (SiaNAz) and incorporated into cellular glycans. The azides are selectively reacted with a fluorescent probe conjugated to a cyclooctyne reagent termed "DIFO." The fluorescent dye-labeled glycans are then visualized. Using this two-step method, changes in the glycome can be probed within the physiologically authentic environment of a live organism (Adopted from Varki et al. 2009, Essentials in Glycobiology, 2nd edition).

(67). This methodology allows covalent labeling of glycoproteins in living cells and organisms with minimal perturbation to physiological processes and has been used by our lab and others to study diverse biological processes (70,73,74). The observed fluorescence is directly related to the number of azides present on the cell surface (Fig. 1.4). As a secondary detection method, Western blots are performed to probe for the presence of azides. Metabolic labeling can be exploited to investigate the metabolic turnover of carbohydrates and to enrich for glycoproteins in preparation for structural analysis.

10

This technique allows for real-time analysis of changes in glycosylation associated with differentiation.

1.6.3. Mass spectrometry

Another method used for glycan analysis is mass spectrometry (MS). In MS, molecules are ionized to generate charged ion fragments using an ionization method such as matrix-assisted laser desorption ionization (MALDI) (75, 76). These ions are then separated in the mass spectrometer according to their mass-to-charge ratio and detected in proportion to their abundance. The mass calculated is used to distinguish the different ions to elucidate and/or validate the identity and structure of the molecule. MALDI sources may be coupled to additional analyzers (e.g. time of flight (TOF) analyzers and fourier transform ion cyclotron (FTICR)) to analyze the mass of ions after further ion fragmentation (19,). These complementary in-line analyzers, in particular FTICR, provide the sensitivity and structural information required for the analysis of complex glycans.

MS is the primary technique for characterizing the structures of individual glycans (3,75,76,77). In a sample of an individual glycan or a mixture of glycans, some of the structural details that MS methods provide are the type of glycans in the sample (e.g., N-glycan, high mannose, hybrid, or complex types), the sites of attachment/glycosylation, the branching pattern, the number and lengths of branches specific to a glycan, the complete sequence of individual glycans with identification of individual monosaccharides, and how they are linked to each other. In the preparation of glycoprotein samples for MS analysis, the glycan is typically separated from its linked protein component. For example, N-glycans can be selectively released using an enzyme called PNGase F, purified, separated by chromatography methods, and sequenced by MS (Fig. 1.3). MS is a very sensitive and a high-throughput method for profiling glycans and providing structural detail; however, the detection of low abundance species is difficult to detect due to the saturation of the most abundant species. Nevertheless, MS methods have been invaluable in glycan analysis.

1.7. Conclusion

The cellular glycome is comprised of several types of glycans, all of which are diverse in their structure, function, and expression. The glycome is dynamic and sensitive to subtle changes in the cell and cellular environment. Monitoring changes in the glycome during embryogenesis has been invaluable in defining stages of development and differentiation. A comprehensive analysis of any one glycome; however, has yet to be achieved. While significant progress has been made in elucidating the identity of glycans and their physiological functions, the glycosylation state of most proteins and the role of the glycans on those proteins are mostly unknown. This lack of knowledge is due in part to the lack of effective tools for visualizing, sequencing, and profiling glycoproteins; a situation remedied by techniques developed in the Bertozzi lab and others.

Changes in glycosylation have been shown to accompany differentiation in human embryonic stem cells; however, detailed molecular structures of the vast majority of glycoforms present on hESCs before and after differentiation is currently unavailable. Because of the potential of hESCs for treating disease, facilitating drug discovery, and providing a basic model for human development, further characterization of the cells and their biology is essential. Glycoconjugates serve many important biological functions and the glycome can be powerfully harnessed for sorting of intact cell populations.

1.8. References

1.   Lebrilla, C. B., Mahal, L. K. Post-translation modifications. Curr Opin Chem Biol 2009, 13, (4), 373-4.

2.   Apweiler, R., Hermjakob, H., Sharon, N. On the frequency of protein glycosylation, as deduced from analysis of the SWISS-PROT database. Biochim Biophys Acta 1999,1473, 4–8.

3.   Varki, A., Cummings, R.D., Esko, J.D., Freeze, H.H., Stanley, P., Bertozzo, C.R., Hart, G.W., Etzler, M.E. Essentials of Glycobiology: Cold Spring Harbor Laboratory Press. 2009.

4.   Haltiwanger, R.S., Lowe, J.B. Role of glycosylation in development. Annu Rev Biochem. 2004, 73, 491-537.

5.   Ohtsubo, K.; Marth, J.D., Glycosylation in cellular mechanisms of health and disease. Cell 2006, 126, (5), 855-867.

6.   Pincet, F., Le Bouar, T., Zhang, Y., Esnault, J., Mallet, J.M., Perez, E., Sinay, P., Ultra-weak sugar-sugar interactions for transient cell adhesion. Biophys J 2001, 80, 1354–8.

7.   Nomoto, S., Muramatsu, H., Ozawa, M., Suganuma, T., Tashiro, M., Muramatsu, T., An anti-carbohydrate monoclonal antibody inhibits cell-substratum adhesion of F9 embryonal carcinoma cells. Exp.Cell Res 1986,164, 49–62.

8.   Sudou ,A., Ozawa, M., Muramatsu, T., Lewis X structure increases cell substratum adhesion in L cells. J Biochem 1995, 117, 271–5.

9.   Zha, Y., Sato, Y., Isaji, T., Fukuda, T., Matsumoto, A., Miyoshi, E., Gu, J., Tnaiguchi, N. Branched N-glycans regulated the biological functions of integrins and cadherins. FEBS Journal 2008, 275, 1939-1948.

10. Wells, L., Vosseller, K., Hart, G.W. Glycosylation of nucleocytoplasmic proteins: signal transduction and O-GlcNAc. Science, 2001. 291: 2376-2378.

11. Laughlin, S.T., Baskin, J.M., Amacher, S.L., Bertozzi, C.R. In vivo imaging of membrane-associated glycans in developing zebrafish. Science 2008, 320, 664-667.

12. Muramatsu, T., Muramatsu, H. Carbohydrate antigens expressed on stem cells and early embryonic cells. Glycocon J. 2004, 21: 41-45.

13. Sato, M., Yonezawa, S., Uehara, H., Arita, Y., Sato, E., Muramatsu, T. Differential distribution of receptors for two fucose-recognizing lectins in embryos and adult tissues of the mouse, Differentiation 1986, 30, 211–9.

14. Kapadia, A., Feizi, T., Evans, M.J. Changes in the expression and polarization of blood group I and i antigens in post-implantation embryos and teratocarcinomas of mouse associated with cell differentiation. Exp Cell Res 1981, 131, 185–95.

15. Yoshida-Noro, C., Heasman, J., Goldstone, K., Vickers, L. ,Wylie, C. Expression of the Lewis group carbohydrate antigens during Xenopus development. Glycobiology 1999, 9, 1323–30.

16. Wianny. F., Perreau, C., Hochereau de Reviers, M.T. Proliferation and differentiation of porcine inner cell mass and epiblast in vitro. Biol Reprod 1997, 57, 756–64.

17. Fukuda, M.N., Dell, A., Oates, J.E., Fukuda, M. Embryonal lactosaminoglycan. The structure of branched lactosaminoglycans with novel disialosyl (sialyl α 2–9 sialyl) terminals isolated from PA1 human embryonal carcinoma cells. J Biol Chem 1985, 260, 6623–31.

18. Fuster, M.M., Esko, J.D. The sweet and sour of cancer: glycans as novel therapeutic targets. Nat Rev Cancer 2005, 7, 526-542.

19. 0. Park, Y., Lebrilla, C.B. Application of fourier transform ion cyclotron resonance mass spectrometry of oligosaccharides. Mass Spec. Rev. 2005 24, 232-264.

20. Kornfeld, R., Kornfeld, S. Assembly of asparagine-linked oligosaccharides. Annu Rev Biochem 1985, 54, 631-664.

21. Van den Steen. P., Rudd, P., Dwek. R., Opdenakker, G. Concepts and principles of O-linked glycosylation. Crit Rev Biochem Mol Biol 1998, 33, 151-208.

22. Bill, R.M., Revers, L., Wilson, I.A. Protein glycosylation. Boston Kluwer, Academic Publishers. 1998.

23. Molinari, M. N-glycan structure dictates extension of protein folding or onset of disposal. Nature Chemical Biology 2007, 3, (6), 313-320.

24. Hart, G.W., Housley, M.P., Slawson, sC. Cycling of O-linked beta-N-acetylglucosamine onnucleocytoplasmic proteins. Nature 2007, 446, 1017-1022.

25. Sudou,A., Muramatsu, H., Kaname, T., Kadomatsu, K., Muramatsu, T. Lex structure enhances myocardial differentiation from embryonic stem cells, Cell Struct Funct 1997,22, 247–51.

26. Muramatsu, T. Cell surface glycoproteins as markers in monitoring in vitro differentiation of embryonal carcinoma cells. Cell differentiation, 1984, 15, 101-108.

27. Muramatsu, T., Gachelin, G., Nicolas, J.F., Condamine, H., Jakob, H., Jacob, F. Carbohydrate structure and cell differentiation: Unique properties of fucosyl glycopeptides isolated from embryonal carcinoma cells. Proc Natl Acad Sci 1978, 75, 2315–9.

28. Muramatsu, T. Developmentally regulated expression of cell surface carbohydrates during mouse embryogenesis. J Cell Biochem 1988, 36, 1-14.

29. Solter, D., Knowles, B.B. Monoclonal antibody defining a stage-specific mouse embryonic antigen (SSEA-1), Proc Natl Acad Sci 1978,75, 5565–9.

30. Kannagi, R., Cochran, N.A., Ishigami, F., Hakomori, S., Andrew, P.W., Knowles, B.B., Solter, D. Stage-specific embryonic antigen (SSEA-3 and -4) are epitopes of a unique globoseries ganglioside isolated from human teratocacinoma cells. EMBO J 1983, 2, 2355–61.

31. Sherman, M.I. (1975). Long term culture of cells derived from mouse blastocysts. Differentiation. 3, 51-67.

32. Gilbert, S. F. Developmental biology (8th ed.) 2006, Sunderland, Mass.: Sinauer Associates, Inc. Publishers.

33. Gooi, H.C., Feizi, T., Kapadia, A., Knowles, B.B., Solter, D., Evans, M.J. Stage-specific embryonic antigen involves α1-3 fucosylated type 2 blood group chains, Nature 1981, 292,156–8.

34. Capela, A., Temple, S. LeX/ssea-1 is expressed by adult mouse CNS stem cells, identifying them as nonependymal. Neuron 2002, 35, 865-875.

35. Artz, K., Dubois, P., Bennett, D., Condamine, H., Babinet, C., Jacob, F. Surface antigens common to mouse cleavage embryos and primitive teratocarcinoma cells in culture. Proc Natl Acad Sci 1973, 70, (10), 2988-2992.

36. Kannagi, R., Cochran, N.A., Ishigami, F., Hakomori, S., Andrews, P.W., Knowles, B.B., Solter, D. Stage-specific embryonic antigens (SSEA-3 and -4) are epitopes of a unique globo-series ganglioside isolated from human teratocarcinoma cells. The EMBO J 2, 1983.

37. Henderson, J.K. , Draper, J.S., Baillie, H.S., Fishel, S., Thomson, J.A., Moore, H., Andrews, P.W. Preimplantation human embryos and embryonic stem cells show comparable expression of stage-specific embryonic antigens. Stem Cells 2002, 20, 329-337.

38. Badcock, G., Pigott ,C., Goepel, J., Andrews, P.W. The human embryonal carcinoma marker antigen TRA-1-60 is a sialylated keratan sulfate proteoglycan. Cancer Res 1999, 59, 4715–19.

39. Thomson, J.A., Itskovitz-Eldor, J., Shapiro, S.S., Waknitz, M.A. Swiergiel, J.J., Marshall, V.S., Jones, J.M. Embryonic stem cell lines derived from human blastocysts. Science 1998, 282: 1145-7.

40. McNeish, J., Embryonic stem cells in drug discovery. Nat Rev Drug Discovery 2004, 3, (1), 70-80.

41. Borstaln, J., Luong, MX., Rooke, H.M., Aran, B., Damaschun, A., Elstner, A., Smith, K.P., Stein, G.S., Veiga, A. International stem cell registries. 2010 46, 242-6. Evans, M. J., Kaufman, M.H. Establishment in culture of pluripotential cells from mouse embryos. Nature 1981, 292, 154-6.

42. Evans, M.J., Kaufman, M.H. Establishment in culture of pluripotential cells from mouse embryos. Nature 1981, 292, 154-6.

43. Martin, G. R. Isolation of a pluripotent cell line from early mouse embryos cultured in medium conditioned by teratocarcinoma stem cells. Proc Natl Acad Sci 1981, 78, 7634-

44. Richards, M., Fong, C.Y., Chan, W. K., Wong, P.C. Bongso, A. Human feeders support prolonged undifferentiated growth of human inner cell masses and embryonic stem cells. Nat Biotechnol, 2002, 20, 933-6.

45. Lee, J. B., Lee, J.E., Park, J.H., Kim, S.J., Kim, M.K., Roh, S.I., Yoon, H.S. Establishment and maintenance of human embryonic stem cell lines on human feeder cells derived from uterine endometrium under serum-free condition. Biol Reprod, 2005, 72,42-9.

46. Ludwig, T. E., Bergendahl, V., Levenstein, M.E., Yu, J., Probasco, M.D., Thomson, J.A. Feeder-independent culture of human embryonic stem cells. Nat Methods, 2006, 3, 637-46.

47. Genbacev, O.,Krtolica, A., Zdravkovic, T., Brunette, E., Powell, S., Nath, A., Caceres, E., McMaster, M., McDonagh, S., Li, Y., Mandalam, R., Lebkowski, J., Fisher, S.J. Serum-free derivation of human embryonic stem cell lines on human placental fibroblast feeders. Fertil Steril, 2005, 83, 1517-29.

48. Amit, M., Margulets, V., Segev, H., Shariki, K., Laevsky, I., Coleman, R., Itskovitz-Eldor,J. Human feeder layers for human embryonic stem cells. Biol Reprod, 2003, 68, 2150-6.

49. Cheng, L., Hammond, H., Ye, Z., Zhan, X., Dravid, G. Human adult marrow cells support prolonged expansion of human embryonic stem cells in culture. Stem Cells, 2003, 21, 131-42.

50. Xu, C., Inokuma, M.S., Denham, J., Golds, K., Kundu, P., Gold, J.D., Carpenter, M.K. Feeder-free growth of undifferentiated human embryonic stem cells. Nat Biotechnol, 2001, 19, 971-4.

51. Xu, C., Jiang, J., Sottile, V., McWhir, J., Lebkowski, J., Carpenter, M.K. Immortalized fibroblast-like cells derived from human embryonic stem cells support undifferentiated cell growth. Stem Cells, 2004, 22, 972-80.

52. Xiao, L., Yuan, X., Sharkis, S.J. Activin A maintains self-renewal and regulates fibroblast growth factor, Wnt, and bone morphogenic protein pathways in human embryonic stem cells. Stem Cells, 2006, 24, 1476-86.

53. Li, Y., Powell, S., Brunette, E, Lebkowski, J., Mandalam, R. Expansion of human embryonic stem cells in defined serum-free medium devoid of animal-derived products. Biotechnol Bioeng, 2005, 91, 688-98.

54. Xu, R. H., Peck, R.M., Li, D.S., Feng, X., Ludwig, T., Thomson, J.A. Basic FGF and suppression of BMP signaling sustain undifferentiated proliferation of human ES cells. Nat Methods, 2005, 2, 185-90.

55. Wang, G., Zhang, H., Zhao, Y., Li, J., Cai, J., Wang, P., Meng, S., Feng, J., Miao, C., Ding, M., Li, D., Deng, H. Noggin and bFGF cooperate to maintain the pluripotency of human embryonic stem cells in the absence of feeder layers. Biochem Biophys Res Commun, 2005, 330, 934-42.

56. Sato, N., Meijer, L., Skaltsounis, L., Greengard, P., Brivanlou, A.H. Maintenance of pluripotency in human and mouse embryonic stem cells through activation of Wnt signaling by a pharmacological GSK-3-specific inhibitor. Nat Med, 2004, 10, 55-63

57. Bhattacharya, B., Puri, S., Puri, R.K. A review of gene expression profiling of human embryonic stem cell lines and their differentiated progeny. Curr Stem Cell Res Ther. 2009, 4, 98-106.

58. Brien, G.L. and A.P. Bracken Transcriptomics: Unravelling the biology of transcriptionfactors and chromatin remodelers during development and differentiation. Sem in Cell Dev Biol, 2009, 20, 835-841.

59. Zhao, X., Ruan, Y., Wei, C.L. Tacking the epigenome in the pluripotent stem cells. J Genet Genomic, 2008, 35, (7), 403-12.

60. Van Hoof D, Heck AJ, Krijgsveld J, Mummery CL. Proteomics and human embryonic stem cells. Stem Cell Res. 2008 Sep;1(3):169-82.

61. Venable, A., Mitalipova, M., Lyons, I., Jones, K., Shin, S., Pierce, M., Stice, S. Lectin binding profiles of SSEA-4 enriched, pluripotent human embryonic stem cell surfaces. BMC Dev Biol, 2005, 5, 1-11.

62. Wearne, K.A., Winter, H.C., O'Shea, K., Goldstein, I.J. Use of lectins for probing differentiated human embryonic stem cells for carbohydrates. Glycobiol. 2006, 10, 981-990.

63. Leahy, A., Xiong, J.W., Kuhnert, F., Stuhlmann, H. Use of developmental marker genes to define temporal and spatial patterns of differentiation during embryoid body formation. J of Exp Zool, 1999 284: 67-81.

64. Satomaa, T., Heiskanen, A., Mikkola, M., Olsson, C., Blomqvist, M., Tiittanen, M., Jaatinen, T., Aitio, O., Olonen, A., Helin, J., Hiltunen, J., Natunen, J., Tuuri, T., Otonkoski, T., Saarinen, J., Laine, J. The N-glycome of human embryonic stem cells. BMC Cell Biol 2009, 10, 42.

65. Liang, PH, Wu CY, Greenberg WA, Wong CH. Glycan arrays: biological and medical applications. Curr Opin Chem Biol. 2008 Feb;12(1):86-92.

66. Saxon, E., and C.R. Bertozzi Cell surface engineering by a modified Staudinger reaction.Science, 2000. 287: 2007-2010.

67. Baskin, J.M., Bertozzi, C.R. Bioorthogonal click chemistry: Covalent labeling in livingsystems. Qsar & Combinatorial Science 2007, 26, 1211-1219.

68. Prescher, J.A.,Bertozzi, C.R. Chemical technologies for probing glycans. Cell 2006,126, 851-854.

69. Laughlin, S.T., Bertozzi, C.R. Metabolic labeling of glycans with azido sugars and subsequent glycan-profiling and visualization via Staudinger ligation. Nat Prot. 2007, 2, 2930-2944.

70. Prescher, J. A., Bertozzi, C.R. Chemistry in living systems. Nat Chem Biol, 2005 1, 13-21.

71. Prescher, J.A., Dube, D.H., Bertozzi, C.R. Chemical remodelling of cell surfaces in living animals. Nature 2004, 430, 873-877.

72. Baskin, J.M., Prescher, J.A., Laughlin, S.T., Agard, N.J., Chang, P.V., Miller, I.A., Lo, A.,Codelli, J.A., Bertozzi, C.R. Copper-free click chemistry for dynamic in vivo imaging. Proc Natl Acad Sci 2007, 104, (43), 16793-7.

73. Dube, D.H., Prescher, J.A., Quang, C.N., Bertozzi, C.R. Probing mucin-type O-linked glycosylation in living animals. Proc Natl Acad Sci, 2006, 103, 4819-4824.

74. Laughlin, S.T., Agard, N.J., Baskin, J.M., Carrico, I.S., Chang, P.V., Ganguli, A.S., Hangauer, M.J., Lo, A., Prescher, J.A., Bertozzi, C.R. Metabolic labeling of glycans with azido sugars for visualization and glycoproteomics, Methods in Enzymology. 2006, 415, 230-250.

75. Harvey, D. J., Quantitative Aspects of the Matrix-Assisted Laser-Desorption Mass-Spectrometry of Complex Oligosaccharides. Rapid Comm in Mass Spectrometry 1993, 7, (7), 614-619.

76. North, S.J., Hitchen, P.G., Haslam, S.M., Dell, A. Mass spectrometry in the analysis of N-linked and O-linked glycans. Curr Opin. In Struct. Biol. 2009, 19, 498-506.

77. Wollscheid, B.; Bausch-Fluck, D.; Henderson, C.; O'Brien, R.; Bibel, M.; Schiess, R.; Aebersold, R.; Watts, J. D., Mass-spectrometric identification and relative quantification of N-linked cell surface glycoproteins. Nat Biotech 2009, 27, (4), 378-386.

78. Park, Y.; Lebrilla, C.B., Application of fourier transform ion cyclotron resonance mass spectrometry of oligosaccharides. Mass Spec. Rev. 2005 24, 232-264.

Chapter 2:
Optimization of hESC membrane glycans analysis using FTICR MS

Chapter 2: Optimization of hESC membrane glycans analysis using FTICR MS

2.1. Introduction

In this study, we present a rapid method for the specific detection and relative quantitation of the glycans present on human embryonic stem cell (hESC) membranes. This method entails the enrichment of membrane components by cellular fractionation followed by glycan structure elucidation using Fourier transform ion cyclotron mass spectrometry (FTICR MS) - one of the most sensitive methods for molecular detection. Briefly, membrane proteins are enriched by ultracentrifugation with buffer conditions developed to be compatible with mass spectrometry analyses. Glycans were enzymatically and chemically released from membrane proteins and captured on graphitized carbon and analyzed with high performance mass spectrometry. Tandem mass spectrometry and nanoflow liquid chromatography (nanoLC) were further used to gain detailed structural information and relative quantitation of glycans, respectively.

Results obtained using our method led to the analysis of a specific type of glycan present in cellular membranes, including cell surface membranes from human embryonic stem cells (hESCs). hESCs hold enormous potential for regenerative medicine, drug discovery, understanding human development, and guiding cancer research (12-14). Progress towards utilization of hESCs for therapeutic purposes has been impeded by the lack of cell surface markers, needed to isolate purified cell populations. By evaluating membrane fractions using state-of-the- art mass spectrometry and analytical tools, we were hoping to identify potential glycans on the cell surface. Structural elucidation of the components present on hESC membranes will provide a basis for understanding their role in hESC maintenance and differentiation. Recent studies suggest that glycans on the surface of hESCs change during differentiation, and such changes can have profound effects on cellular function (15). Using this method, and subsequent analyses, hESC membrane fractions consisted mostly of high mannose glycans Man8 and Man9. This led to investigating whether high mannose glycans are on the cell surface. GNA lectin, which is commonly used for detecting terminal mannose residues, bound to hESC cell surfaces. Further verification of cell surface high mannose glycans and their biological significance is currently under further investigation in our laboratory.

2.2. Results

The experimental strategy including i) membrane fractionation from whole cell lysates by ultracentrifugation, ii) release and enrichment of surface glycans by solid phase extraction (SPE) using a graphitized carbon, iii) glycan profiling by high performance mass spectrometry, and iv) isomer separation and quantitation by nanoflow liquid chromatography (nanoLC) is outlined in the Figure 2.1. These methods were developed and streamlined to profile cell membrane glycans effectively and selectively by mass spectrometry. The methods were further optimized to minimize sample handling and to increase analysis speed.
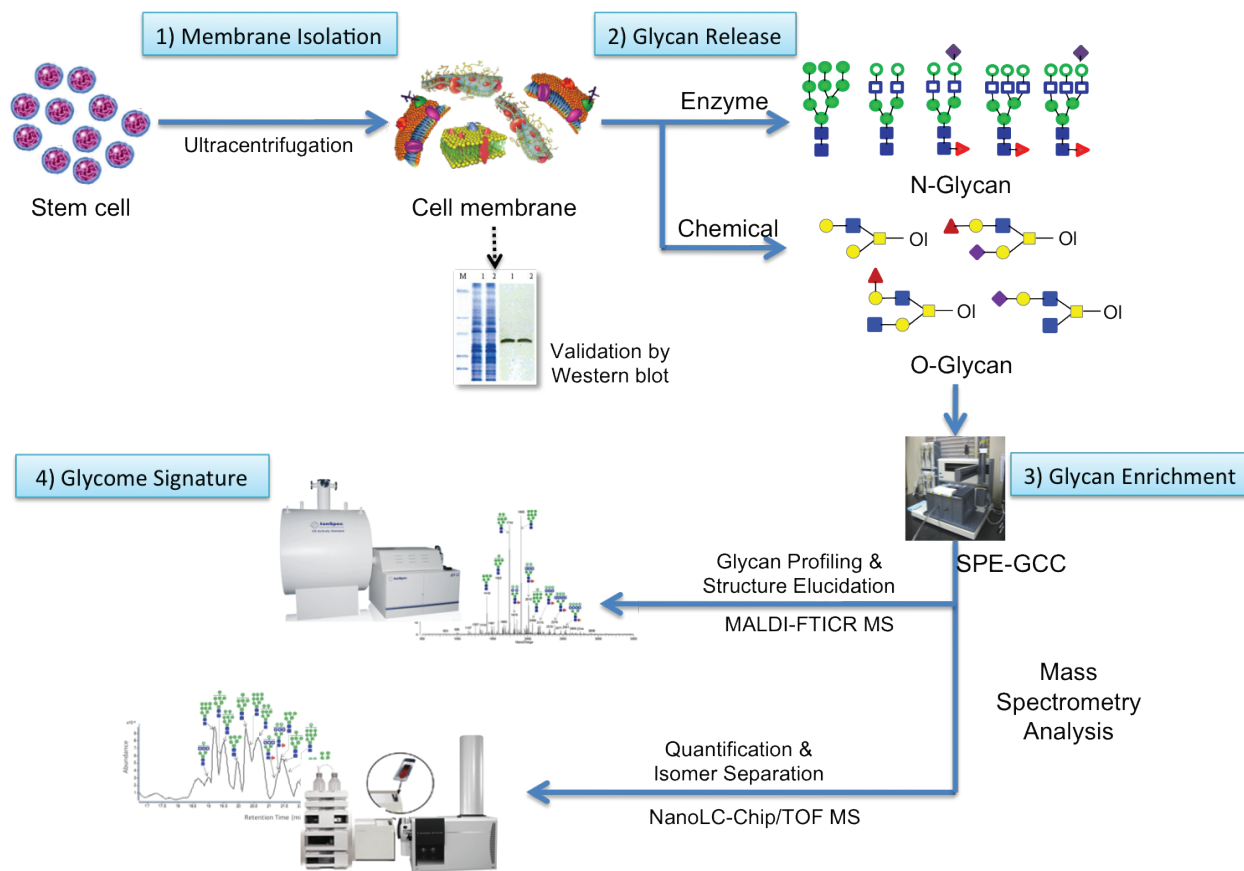
Figure 2.1. Experimental flowchart for the profiling and quantitation of N- and O-glycans in membrane fractions of hESCs.

2.2.1. Isolation of membrane fractions by ultracentrifugation in hESCs

Isolation of membrane fractions from whole cells in a manner that allows sensitive MS detection of glycans was important in our methodology development. We employed the technique of ultracentrifugation – which has been widely used in cell biology and microbiology to separate organelles of interest from whole cells for the analysis of specific cellular components. The typical buffer solution used in ultracentrifugation usually contains detergents and solvents such as sodium dodecyl sulfate (SDS), Triton X-100, EDTA, sucrose, sodium, and protease inhibitors, however, several of these components are known to be deleterious to the mass spectrometry analyses. Mass spectrometry can be a powerful method for analyzing biomolecules because of its intrinsic speed and sensitivity, but coupling the two techniques have proved challenging due in part to such incompatibilities in sample processing (38,39). In this study we optimized the buffer solutions used in ultracentrifugation to render it more compatible with mass spectrometry. Homogenization buffer (HB) consisting of 0.25 M sucrose, 20 mM Hepes-KOH, 1 mM EDTA, 1% SDS, and a protease inhibitor mixture was initially used in this study. However, in the final MS analysis we only observed polymeric material with a regular mass spacing but non-
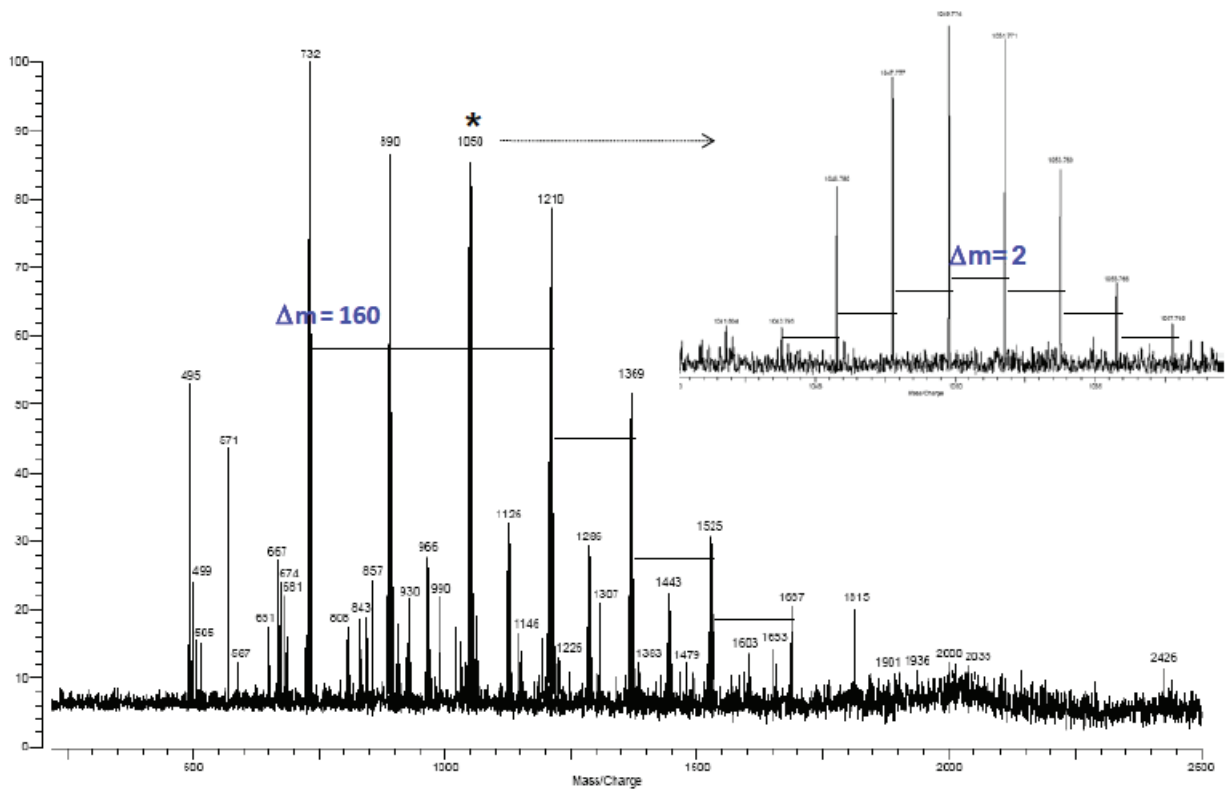
Figure 2.2. MALDI-FT ICR mass spectra of glycans released from membrane fraction of hESCs. Only polymer peaks with non-carbon isotopic distribution were observed instead of glycan peaks.
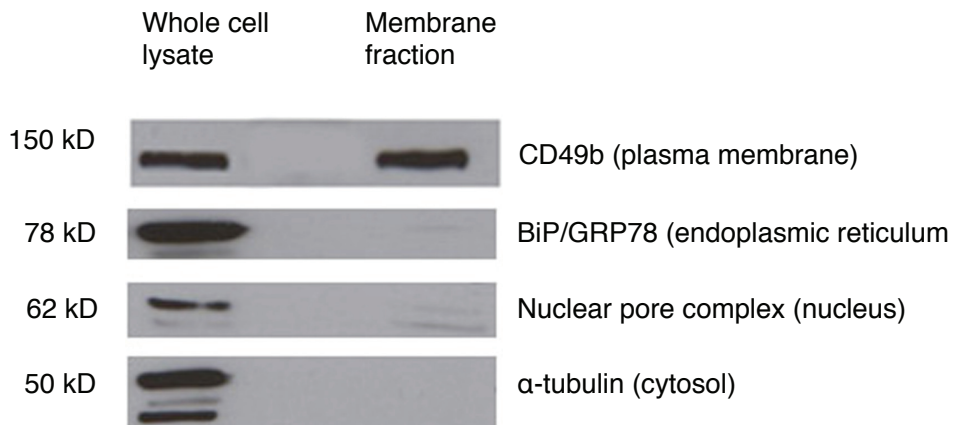
Figure 2.3. SDS-PAGE electrophoresis of membrane fractions followed by Western blotting. Specific proteins from the endoplasmic reticulum, nuclear pore complex and cytosol were not expressed in membrane fractions.

carbon isotopic distribution, indicative of matrix background material only and absence or complete suppression of signal from glycans (Fig. 2.2). To resolve this issue, the buffer conditions were reformulated. One key change was the removal of EDTA from the homogenization buffer - a change that did not affect the quality of the cellular fractionation step (see below) but importantly allowed observation of masses correlating to glycans in the mass spectra. Other changes included eliminating SDS and the addition of rigorous washes with nanopure water. This optimized method allowed for glycans to be readily observed with little background noise (Fig. 2.4). Crude membrane fractions from hESCs were assessed for the presence of other cellular constituents, such as common proteins found in the cytsol, nucleus, plasma membrane and endoplasmic reticulum. These proteins were evaluated by SDS-PAGE gel electrophoresis followed by Western blotting using organelle-specific antibodies (Fig 2.3). While there was minimal contamination of these specific proteins, cross-contaminants such as those from the endoplasmic reticulum needs further evaluation. Proteins such as BiP/(GRP78), a resident chaperone protein in the ER, may have been solublized during the sonication and wash with sodium carbonate, a procedure designed to remove peripheral membrane proteins and organelle luminal content. Thus, the absence of BiP/GRP78 may not reflect an absence of ER components. Antibodies against ER integral membrane proteins, such as ribophorin, Sec22 and p58, will better access the purity of the membrane fraction.

2.2.2. Release and purification of cell membrane glycans

N-glycosylation is the major type of protein glycosylation found on mammalian cell surfaces. N-glycans are attached to the side chain of Asn residues via a nitrogen atom, and the N-glycans present in the membrane fraction were released from their protein carriers using PNGase F – an enzyme that selectively cleaves N-glycans from the polypeptide backbone. The free glycans thus obtained were concentrated and captured on a graphitized carbon. Such solid phase extraction (SPE) techniques are known to provide superior performance to other techniques in that they provide higher recovery of polar cellular components, while allowing reduced handling and automation of the process (40). The glycans were loaded onto a graphitized carbon solid phase and eluted stepwise with solvents of decreasing polarity (10, 20, and 40% aqueous acetonitrile (AcN)). The glycan mixtures eluted from these three SPEs were subsequently analyzed by mass spectrometry.

2.2.3. Mass profiling of glycans from hESC cell membranes

To obtain detailed structural information about the glycans present on hESC membranes, we employed matrix-assisted laser desorption/ionization (MALDI) FTICR MS. FTICR MS is considered one of the most sensitive methods of ion detection with almost unlimited resolution, and surpasses common mass spectrometric methods such as TOF (Time-of-Flight) or quadrapole ion traps by providing more structurally relevant fragments for glycan analysis, and significantly more resolving power, respectively (36). This method as optimized and developed for glycan analysis has already been used for several studies, including the identification of biomarkers for ovarian cancer (37).

In initial studies, we determined the composition of the released glycans with respect to the individual monosaccharides present in each glycan. These components, as denoted by Hex (hexoses), HexNAc (N-acetylhexosamines), NeuAc (N-acetyl sialic acid), and Fuc (fucose), were deduced based on the predicted masses of glycans based on the known biosynthetic routes for glycan assembly and the core oligosaccharide structures present in human glycans. The most abundant glycans were analyzed with tandem mass spectrometry using infrared multiphoton dissociation (IRMPD) to obtain further information about the structural connectivity of the individual monosaccharides within the native glycans. Figure 2.4 shows representative spectra of N-glycans from hESC membranes in the combined fractions (Fig. 2.4A) and in the individual 10, 20, and 40% AcN fractions (Fig. 2.4B)

All N-glycans contain a conserved core pentasaccharide consisting of three mannoses (Man) and two N-acetylglucosamines (GlcNAc), and are further sub-categorized based on the number of additional mannoses. In the three types, N-glycans of the complex type contain only the 3 core mannoses, hybrid N-glycans contain 5 total mannoses and high mannose N-glycans contain greater than 5, all types can then be further elaborated by other types of monosaccharides. Figure 2.4 shows the putative structures of the most abundant N-glycan species present in hESC membrane fractions, further glycan structures were identified by examination of the lower abundance signals. Progressing from the 10% to 40% AcN fractions, the glycans found generally increrease in size and acidity. The 10% AcN fraction was comprised mostly of high mannose-type glycans containing GlcNAc2Man6 and GlcNAc2Man9 cores, with some that are elaborated by additional hexoses. In the 20% AcN spectrum, the glycans present are primarily complex type N-glycans that are bi-, tri- and tetra-antennary, with several containing a core fucose residue. The acidic oligosaccharides, which contain sialic acid, are found in only the 40% AcN fraction, but with relatively weaker signals. When the three fractions are combined, the resulting profile of hESCs surfaces shows mostly neutral glycans, namely high mannose and some complex type glycans (Fig. 2.4A). In this analysis, approximately 54 N-glycan compositions were identified on the hES cell membrane (Table 1).

To confirm glycan compositions and to obtain detailed structural information such as the putative glycan structures shown in Fig. 2.4, selected ions were subjected to tandem mass spectrometry using infrared multiphoton dissociation (IRMPD). Tandem MS allows observance of ions arising from sequential loss of individual monosaccharides from the native glycan structure, and the composition data obtained above via MALDI-FTICR MS is supplemented with information about how the monosaccharides are connected to one another. One representative IRMPD analysis was of the ion at m/z 2067.687 ([M+Na]+), which corresponds to 2HexNAc and 10Hex (9Man+1Hex) (Fig. 2.5A) Tandem MS afforded several fragments in a single MS/MS event (Fig. 2.5). The glycosidic bond cleavages corresponding to loss of the two core GlcNAc residues present in all N-glycans (m/z 1847 and 1643, respectively) were readily observed, along with fragments corresponding to subsequent monosaccharide losses (i.e., m/z 1847, 1685, 1523, 1361, 1198 and m/z 1643, 1481, 1319, 1157, 995, 833). The ion at m/z 833 corresponds to the trimannosyl core with twextra mannoses ([Man5-H2O+Na]+), confirming that this glycan is a high mannose type N-glycan. By contrast, the IRMPD spectrum of a complex type N-glycan (m/z 2012.719) is shown in Figure 2.5B. In summary, the fragmentation behav-
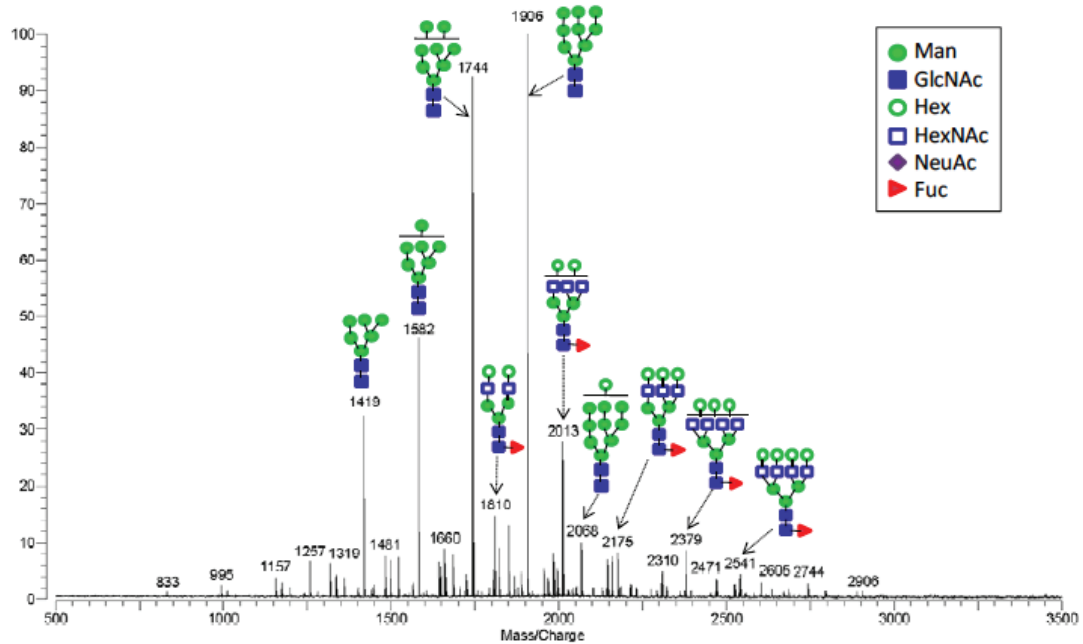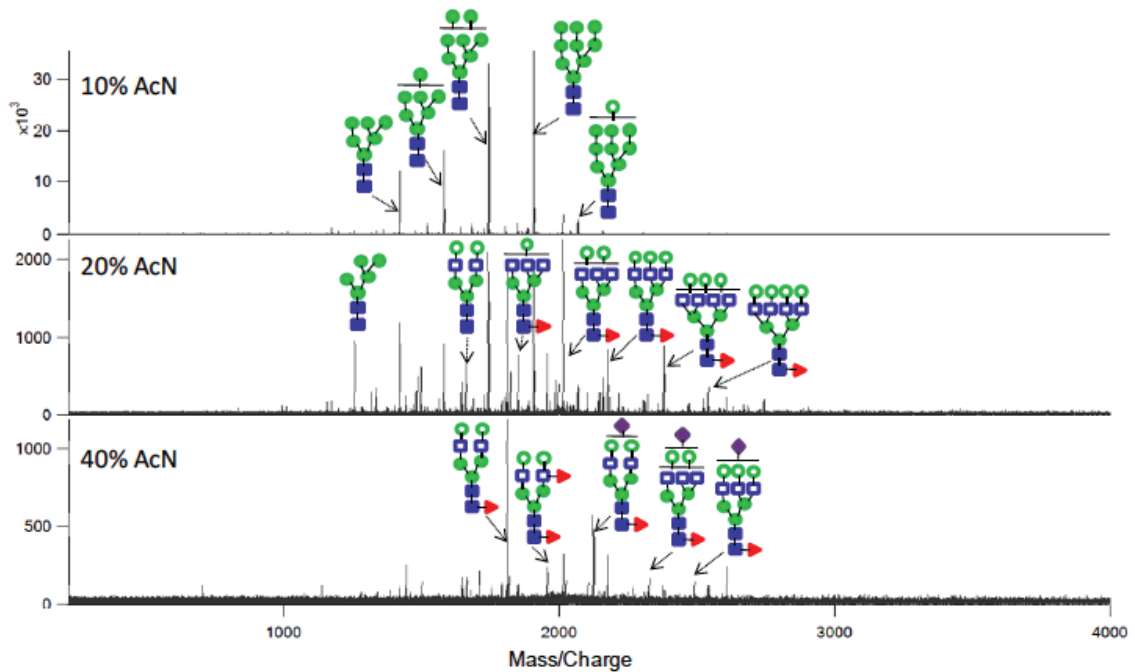
Figure 2.4. Representative MALDI-FTICR mass spectra of N-glycans found in hESC membrane fractions in the positive detection ion mode. (A) Combined fractions and (B) Each GCC fraction. 10% (top), 20% (middle), and 40% (bottom) represent glycans eluted from acetonitrile (AcN) fractions. Structures are putative and are based on accurate masses and tandem mass spectrometry.
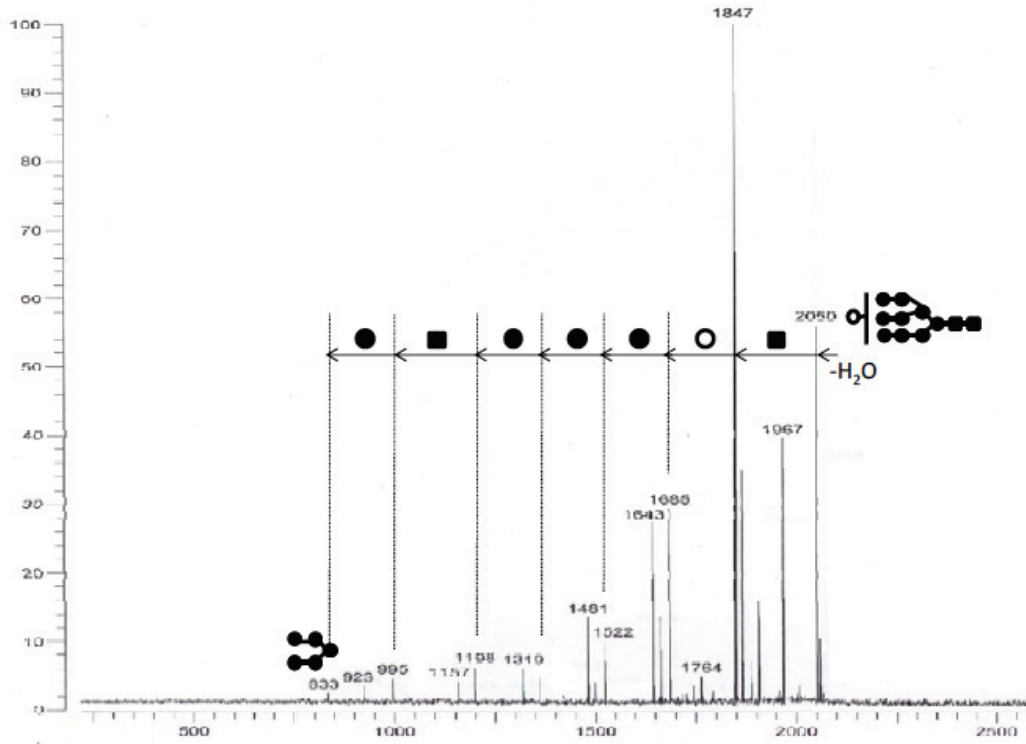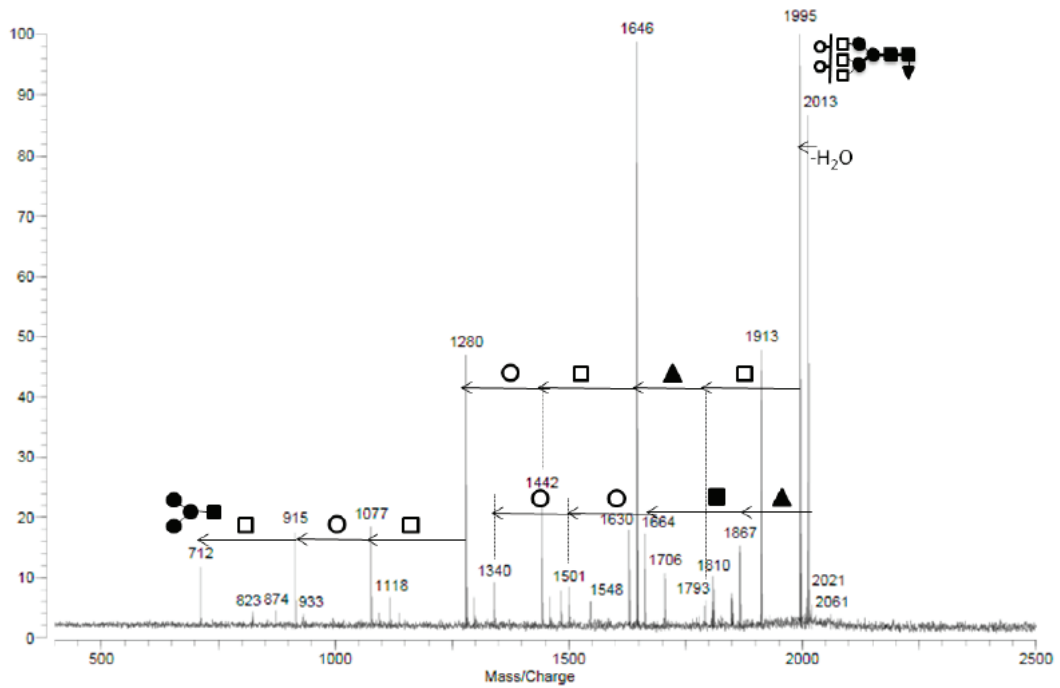
Figure 2.5. Structure elucidation of a complex N-glycans (A) (m/z 2013) and (B)(m/z 2050) found on hESC membrane by tandem mass spectrometry using IRMPD.

ior observed in the IRMPD spectrum provided confirmation of the glycan composition deduced from MALDI-FTICR MS, and also substantial additional structural information about the connectivity of the monosaccharides.

2.2.4. Quantitation of hESC membrane glycans

Glycans can be quantified using the ion intensities produced by MALDI MS if the homogeneity of the MALDI sample surface equipped with the proper matrix can be guaranteed (25, 26). Indeed, the total ion intensities of glycans obtained from MALDI-FTICR MS analysis over three biological replicates of hESCs are highly reproducible (Fig. 2.6), and thus bar graphs and error bars can be generated to represent the average of total ion intensity and standard deviation obtained from the three biological replicates.

Glycan composition can be readily obtained based solely on MALDI-FTICR MS, and the abundance can also be determined with reasonable accuracy using peak intensity, but this analysis does not provide information on the number of mass-redundant isomers associated with each mass peak. Therefore, to analyze the isomers corresponding to each composition, glycans were further examined with nanoflow liquid chromatography (nanoLC) to achieve isomer separation as well as obtain direct quantitative information. In addition, separating the glycans into individual components by chromatography further minimizes the confounding of quantitation due to ion suppression. Ion suppression is the phenomenon wherein the most ionizable species present in a MS sample dominates the spectrum, regardless of abundance or instrument sensitivity, and can confound the use of mass spectrometry for relative quantitation of glycans. Fractionating the glycans mixtures by SPE into three portions helps to minimize ion suppression by grouping glycan species of comparable ionizing efficiency with one another, but does not fully eliminate suppression (27). A microchip packed with graphitized carbon was used to chromatographically separate the glycans in this study (28). The microchip was interfaced with TOF mass analyzer that routinely provides a mass measurement accuracy of less than 5 ppm, allowing unequivocal determination of the exact molecular formula of the observed species. Therefore, aliquots of each SPE fraction were combined, and the mixture was analyzed by nanoLC MS. A representative chromatogram is shown in Fig. 2.7 with the putative structure for the most abundant glycan for each chromatographic peak. High mannoses are the most abundant glycans and elute earlier, while complex type glycans were low in abundance and eluted at later times.

Only masses above m/z 1200 were considered for possible structural isomers of high mannose N-glycans, which is the mass of the minimal common core of GlcNAc-2Man5 present in this class of N-glycans. We identified 143 distinct isomers, arising from 64 glycan compositions (Table 2). Representative extracted ion chromatograms of two of the most abundant glycans, GlcNAc2Man8 and GlcNAc2Man9, are shown in Figure 2.7B to illustrate the separation and the number of isomers that may comprise a specific composition. The extract ion chromatogram of GlcNAc2Man8 (Man8) shows two structural isomers for m/z 861.302 ([M+H]+2) with retention times of 19.50 and 20.62 min. Analogously, GlcNAc2Man9 (Man9) shows three structural isomers consisting of two major isomers with retention times of 19.21 and 20.28, and one minor isomer eluted at 21.41

min.

Chromatographic peak areas were then used for overall glycan quantitation. Putative structures were obtained based on composition to determine the proportions of the three different structural classes of N-glycans (namely high mannose, complex/hybrid, and hybrid). The relative abundance of each of the three N-glycan types is depicted in Fig. 2.8A. Interestingly, high mannose glycans are the most abundant glycans, accounting for ~85% of the total N-glycans identified, while complex/hybrid type N-glycans comprise the remaining 14%, and hybrid N-glycans (Man5) accounted for only 1%. Of the high mannose glycans, Man8 (34%) and Man9 (30%) are the major glycans present (Fig. 2.8B). The complex/hybrid type glycans are generally fucosylated, with ~70% containing at least one fucose residue (Fig. 2.8C). Importantly, the relative abundance of these three types of N-glycans was consistently observed among three biological replicates.

2.2.5. Reproducibility of method to profile membrane glycans

An important consideration in mass spectrometry to profile biomolecules is rigorously establishing the reproducibility of the method to allow routine application of the technique to various biological samples. To further evaluate our method, the reproducibility of results between biological replicates and analytical replicates was examined.
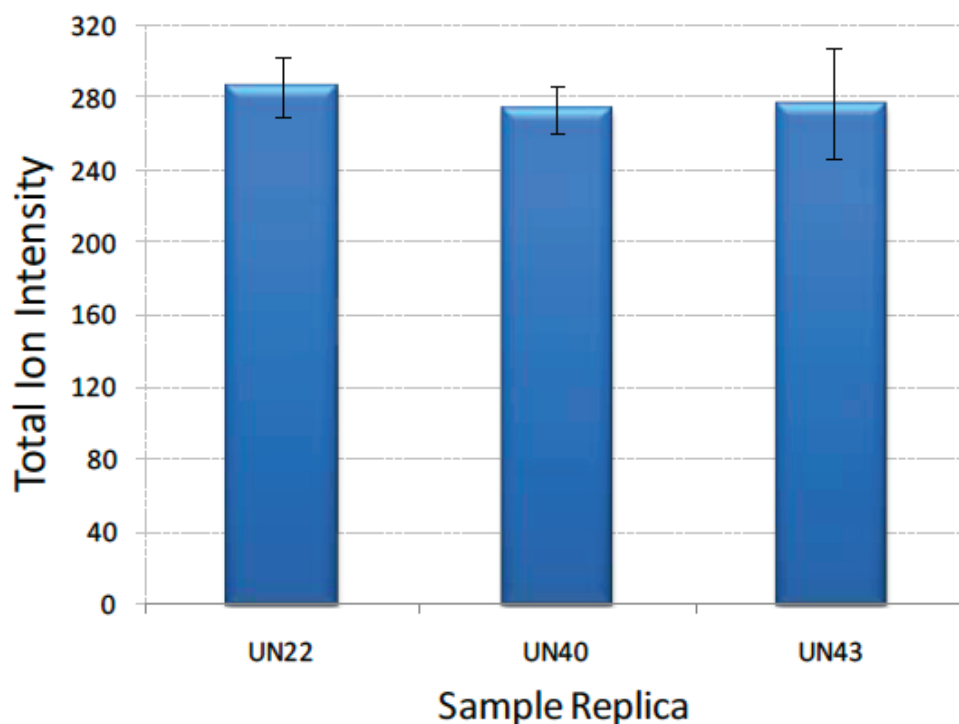
Figure 2.6. Total ion intensity of glycans obtained from MALDI-FT ICR MS analysis over three bio-replicates. Bar graph and error bar show the average of total ion intensity and standard deviation obtained from triplicates of MS analysis for each sample, respectively.
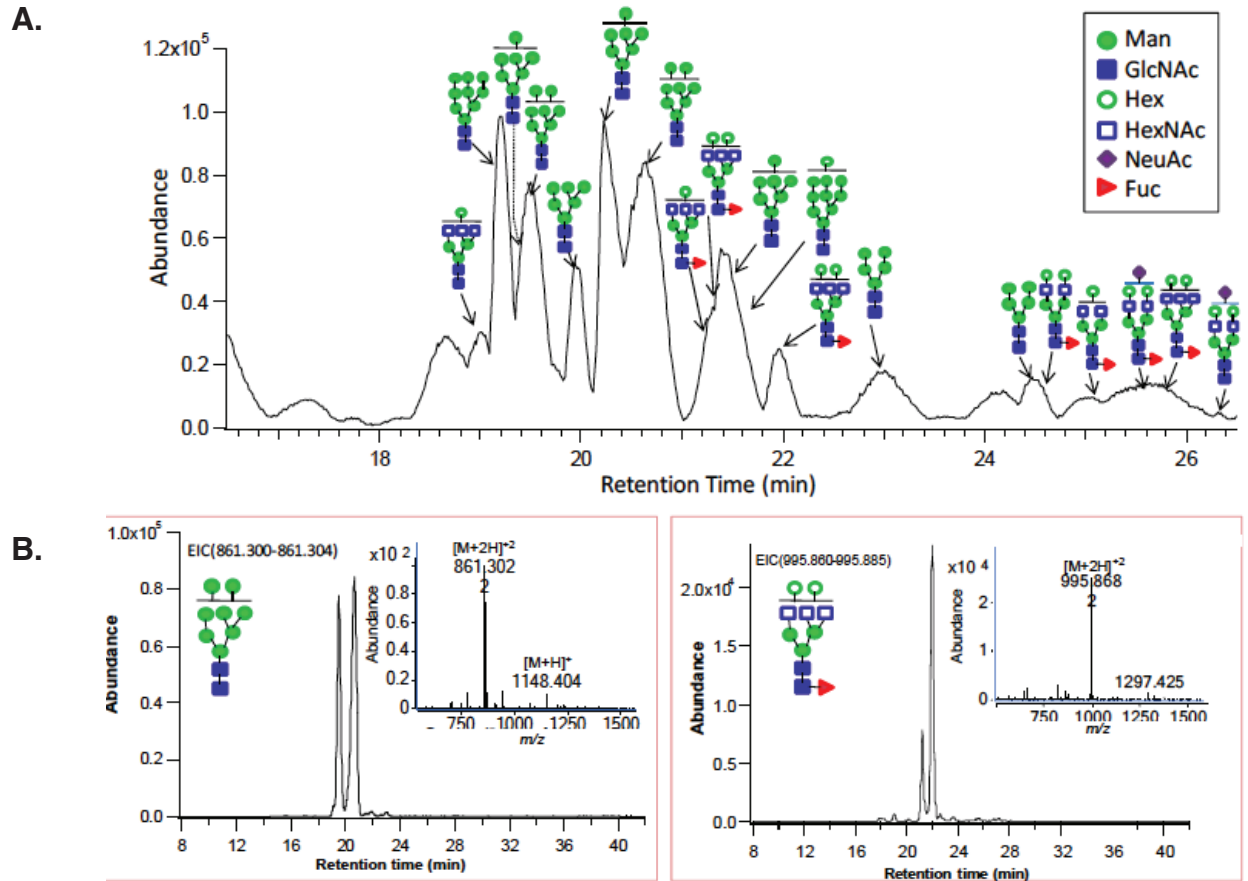
Figure 2.7. Quantitation and isomer separation of N-glycans on hESC surfaces. The combined SPE fraction (10, 20, and 40%) was analyzed by nanoLC-Chip/TOF. (A) Representative base peak chromatogram of N-glycans found on hESC membranes. Proposed structures correspond to the most abundant glycan at that retention time are provided. (B) Extracted ion chromatogram of high mannose type glycans. Left panel shows Man8 isomers and right panel shows Man9 isomers.

Biological replicates consisted of hESCs collected on different days from different passage numbers, whereas analytical replicates were from the same biological sample analyzed multiple times. For the analytical replicates, normalized absolute peak intensities measured by three MS experiments were plotted against one other (Fig. 2.9A). High correlation coefficients (r: 0.96-0.97) were obtained from three analytical replicates. The variation among biological experiments was further examined. To eliminate the biological backgrounds from the different sample batches, the intensity of only the glycan peak was compared. The correlation coefficients (r) were in the range of 0.86 to 0.92, showing good correlation between biological replicates (Fig. 2.9B). The results clearly show that this is a robust, sensitive, reproducible and reliable method for profiling cell membrane glycans.
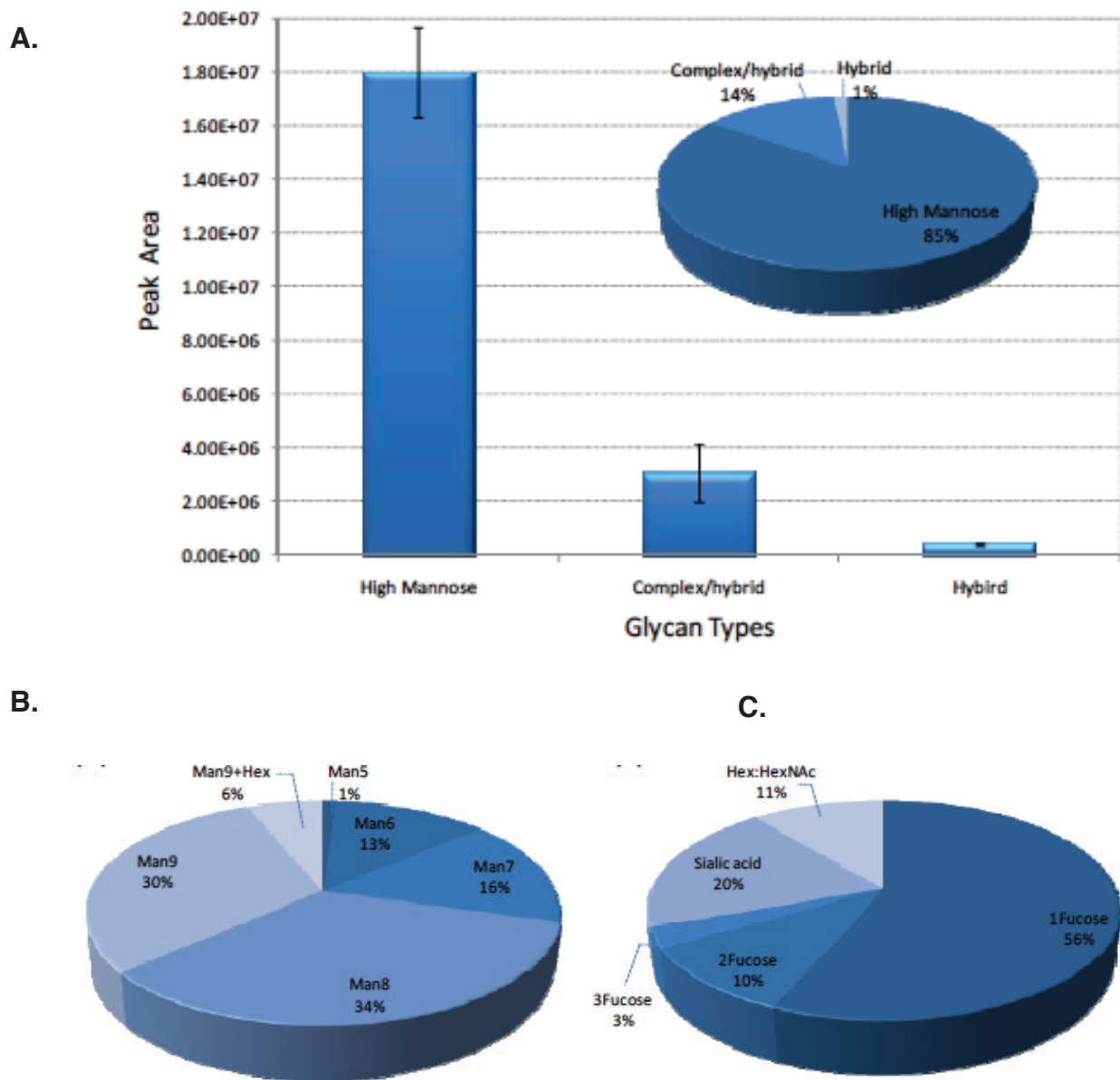
Figure 2.8. Glycan quantitation using peak areas of chromatograms from nanoLC-Chip/ TOF MS. (A) Overall abundances based on N-glycan types. Bar graph represents the sum of peak areas for three N-glycans type with error bars showing the standard deviation obtained from three biological replicates. High mannose glycans are the most abundant accounting for 85% of total glycans identified. Glycan abundance profile of (B) high mannose and (C) complex/hybrid type glycans. Man8 and Man9 are the most abundant glycans. The complex/hybrid type glycans are generally fucosylated.

2.2.6. Identification of glycan expression using lectins

Results from our MS data indicated that in the cellular membrane fraction, the majority of glycans were high mannose N-glycans. To determine whether some of these high mannose glycans were derived from the cell surface plasma membrane, hESCs were labeled with lectins, which are plant and animal proteins with natural carbohydrate binding functionality. Canavalia ensiformis (Con A) was used for identifying N-glycans generally, and Galanthus nivalis (GNA) detected high mannose N-glycans specifically. Con A recognizes branched α-mannosidic structures, high-mannose, and hybrid and biantennary complex type N-glycans. GNA is a highly specific mannose lectin used to detect terminal α 1-3 and α 1-6 linked high mannose structures. These lectins were applied on fixed and live hESCs and analyzed with microscopy and flow cytometry, respectively.

To visualize the presence of glycans via fluorescence microscopy, hESCs were fixed and labeled with an antibody against SSEA-4 (a marker for pluripotent hESCs) followed by lectins conjugated to the fluorescein isothiocyanate (FITC) fluorophore. Binding of Con A (Fig. 2.10A) and GNA (Fig. 2.10B) indicated the presence of both N-glycans and terminal high mannose glycans in the hESC colonies, respectively.

To quantify the glycans on the cell surface, live hESCs were stained with low to high concentrations of the lectins, and the pluripotent marker SSEA-4, for analysis using flow cytometry. Figure 2.10C shows the distribution of fluorescent intensities of the different cell populations after labeling with lectins and SSEA-4. With the addition of lectins to SSEA-4+ cells, double-positive cell populations (e.g. Con A+/SSEA-4+, Fig. 2.10C) were distinct from the other cell populations, allowing for the quantitation of hESCs bound with lectins on the cell surface (Fig. 2.10B-D). Live hESCs expressed dose-dependent binding of both lectins ConA and GNA (Fig. 2.11), indicating the specificity of lectin binding and presence of N-glycans and terminal high mannose glycans on the cell surface. These re sults suggest that a certain amount of high mannose glycans detected using our mass spectrometry approach may be derived from the cell surface membrane.
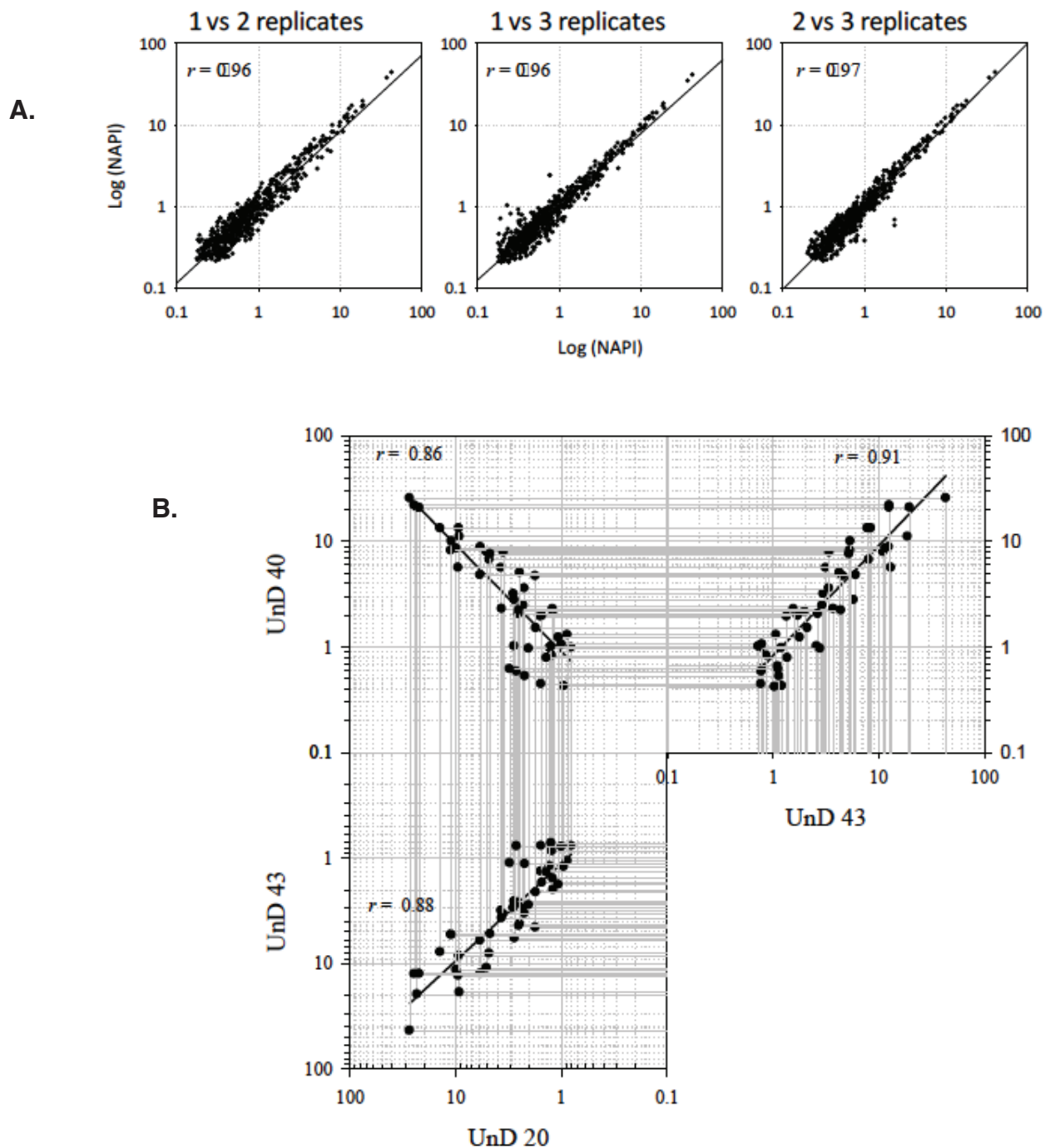
Figure 2.9. Analytical reproducibility on same sample process. Triplicate MS analyses were performed for each sample. (A) Three experiments were plotted against each other and the respective correlation coefficient R is inset. (B) Biological reproducibility of hESC membrane glycans.Bio-triplicates (Un22, Un40, Un43) of hESCs were independently prepared and membrane glycans were released and compared for the reproducibility. Only glycan peaks detected by MALDIFTICR MS were used for scatter plots and the respective correlation coefficient R is inset. NAPIrepresents normalized absolute peak intensity.
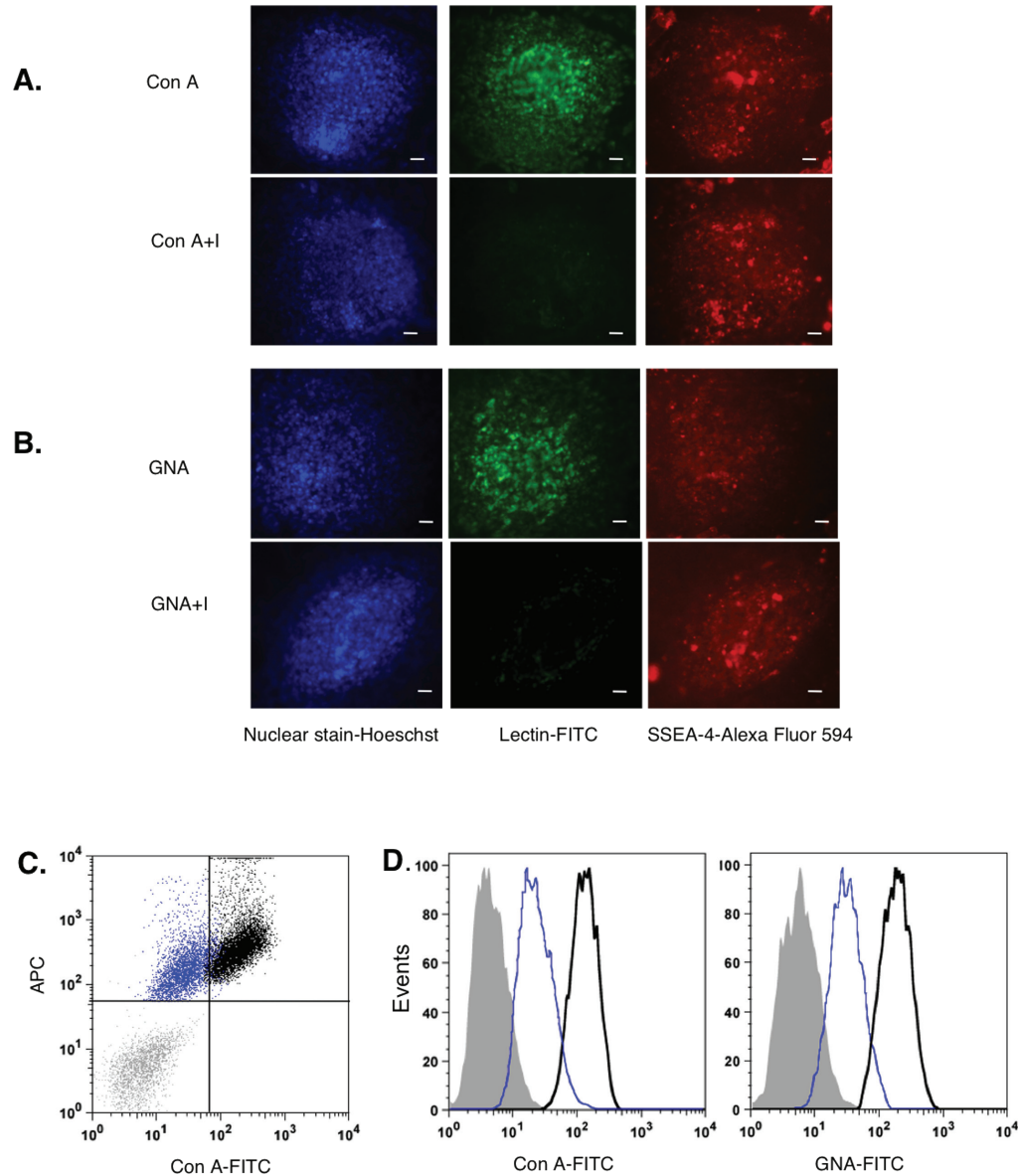
Figure 2.10. Glycan expression using lectins. (A)-(B) are fixed hESC colonies that were stained with Hoescht dye (nuclear stain), antibody against SSEA-4 with secondary antibody(depicted by Alexa Fluro 594) and Con A-FITC and GNA-FITC (20 µg/ml). All colonies were positively stained with Hoescht and expressed SSEA-4. (A) Cells bound to Con A compared to colonies that were labeled with Con A+I (inhibitory control). (B) GNA-FITC also bound to cells,compared to the inhibitory control (GNA+I). All images were taken with 10X magnification andthe scale bar: 20 µm. (C)-(D), Flow cytometry was used to quantify amount of lectin binding on live hESCs. (C) This dot plot shows the populations of cells (black) that were double-labeled with both lectin (Con A-FITC) and SSEA-4 positive (APC) compared to the unstained population (grey) and inhibitory control (blue). (D) These histrograms present the distribution of live hESCs depicted in (C) that stained with Con A-FITC and GNA- FITC (40 ug/ml) compared to unstained (grey fill) and inhibitory controls (blue).

34
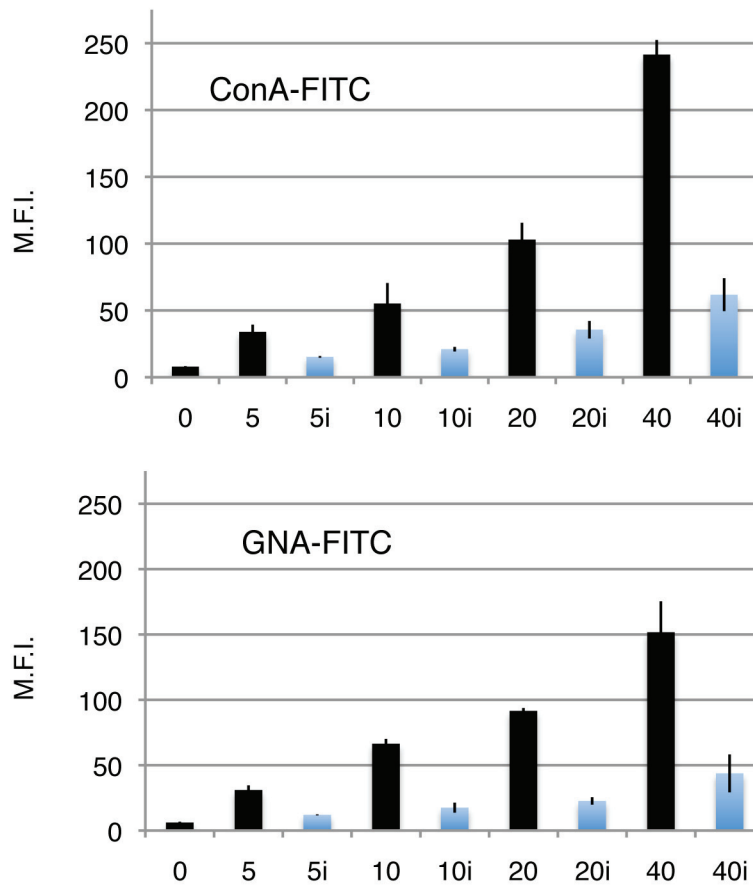
Figure 2.11. Cell surface glycan analysis using flow cytometry. To determine the presence of glycans, live hESCs labeled with antibody against SSEA-4 (stem cell marker), propidium iodide (P.I., to detect dead cells) and lectins Con A (to detect to N-glycans), GNA (to detect terminal high mannose glycans), The mean fluorescence intensity (M.F.I.) represents the quantification of live hESCs (P.I. negative and SSEA-4 positive) labeled with different concentrations (5, 10, 20 40 µg/ml) of lectins with or without inhibitory control ("+ I").

2.3. Discussion

In this study, we optimized a method to characterize the N-glycome of hESCs from membrane fractions. Isolation of membrane protein glycans followed by high performance mass spectrometry and chromatography makes this approach highly sensitive and quantitative. Using this method we were also able to analyze membrane fractions from cancer and primary cells. This approach provides comprehensive and highly quantitative structural information including isomer separation. hESC membrane fractions were found to have high levels of high mannose glycans with the specific structures of Man8 (29%) and Man9 (26%). Lectin staining with mannose binding lectins Con A and GNA and flow cytometry analyses suggested that high mannose glycans are also expressed on the cell surface of live SSEA-4 positive hESCs. Because lectins do not provide structural detail, Con A and GNA lectin staining does not necessarily coorelate with the specific presence of Man8 and Man9 structures or other high mannose glycan structures. Further analyses are needed to identify high mannose glycan structures on the cell surface. One approach, currently underway, is to identify the peptides to which the glycans are attached. Protein identification will help discern whether high mannose glycans are modifying cell surface proteins.

High mannose glycans are involved in initial steps in N-glycan processing and control of protein folding in the endoplasmic reticulum (ER). The initiating event is the processing of N-glycan precursor, Man9 and three glucoses, by glucosidases I and II to yield to Man9+Glucose, which is subsequently trimmed back in the process of generating complex-type glycans (31). If the membrane fractions were primarily plasma membrane, the abundance of Man9 from the membrane fractions may suggest that the trimming process is incomplete in hESCs, perhaps yielding "immature" glycoproteins. Indeed, the ion at m/z 2067.68, corresponding to Man9 with one extra hexose, potentially a glucose (Glc), was readily identified by tandem MS (Fig. 4C). Another possibility is that the high mannose glycans detected in our hESC studies were derived from the ER, despite the significant reduction of high mannose glycans in primary breast cell membrane fractions. Antibodies to ER integral membrane proteins will better assess ER cross-contamination (e.g. antibody against integral membrane protein ribophorin I, a subunit of the oligosaccharyltransferase complex involved in the addition of N-glycans to nascent proteins) (41). Evaluation of ER markers and glycans in nuclear and cytosolic fractions compared to the membrane fractions will also help to determine the derivation of high mannose gylcans.

Interestingly, other stem cell types such as human mesenchymal stem cells, hematopoietic stem cells and progenitor cells have been found to contain high levels of high mannose glycans (9, 19, 32). In these studies, glycans were released from whole cell lysates and characterized by NMR and MS; it is unclear what cellular components contained the high levels of high mannose glycans.

In addition to testing our method on hESC membranes, we investigated N-glycans on a colon cancer cell line called Caco-2. The FTICR MS spectrum shows a similar profile of N-glycans to hESCs, with an abundance (80%) of high mannose glycans present (Fig. 2.12). For further comparison, we used our method to evaluate the glycans on a normal primary breast cell line (Fig. 2.13). Interestingly, the glycan profile from the primary breast cell line consisted mainly of complex/hybrid glycans and only 20% high mannose glycans.
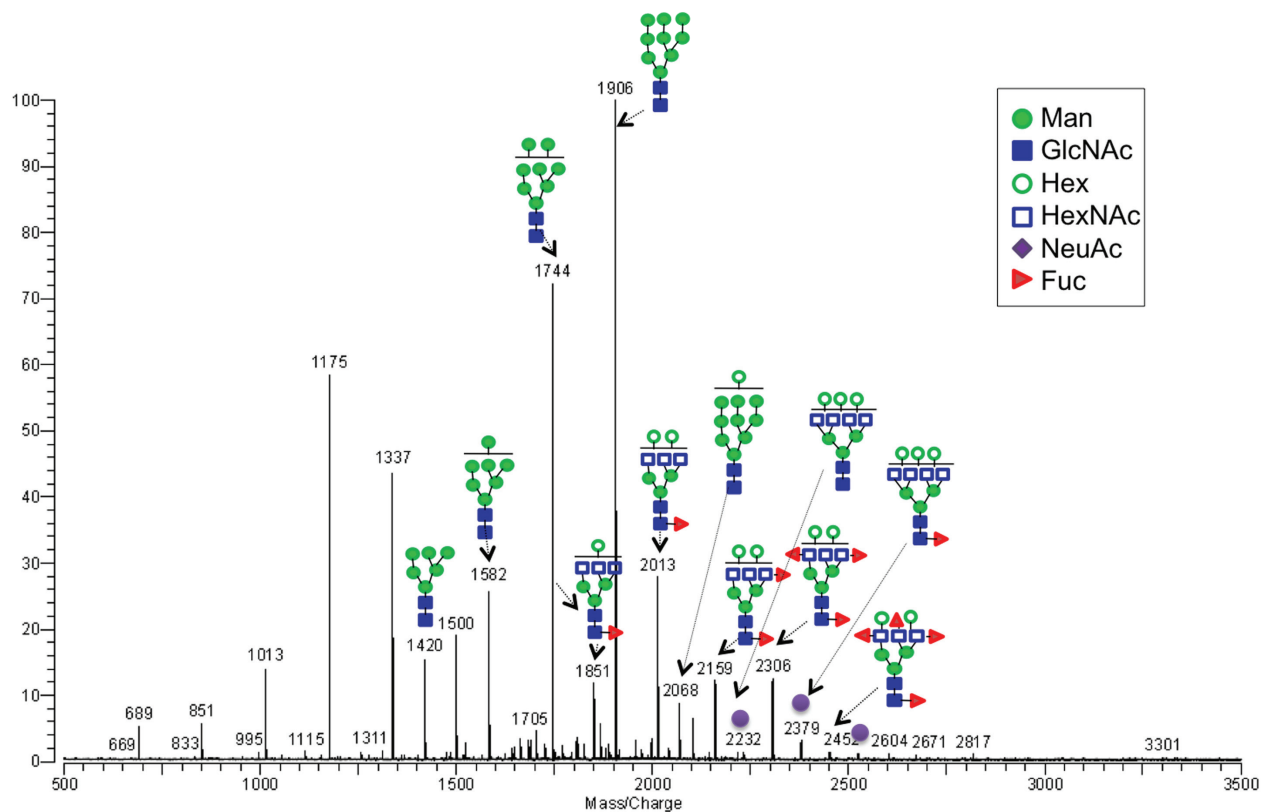
Figure 2.12. Representative MALDI-FTICR mass spectra of N-glycans found in Caco-2 prostate cancer cells in the positive detection ion mode. Structures are putative and are based on accurate masses and tandem mass spectrometry.

The findings suggest that high-mannose glycans may play important roles in stem cell and cancer biology (33). In addition, the interaction of high mannose glycans on the cell surface of macrophages and osteoclast precursors to cell surface mannose receptors has been implicated in cellular fusion, which is necessary for facilitating the differentiation of osteoclasts (34). The deep structural analysis enabled by our methodology will enable future mechanistic studies on the biological significance high mannose glycans on hESC membranes.
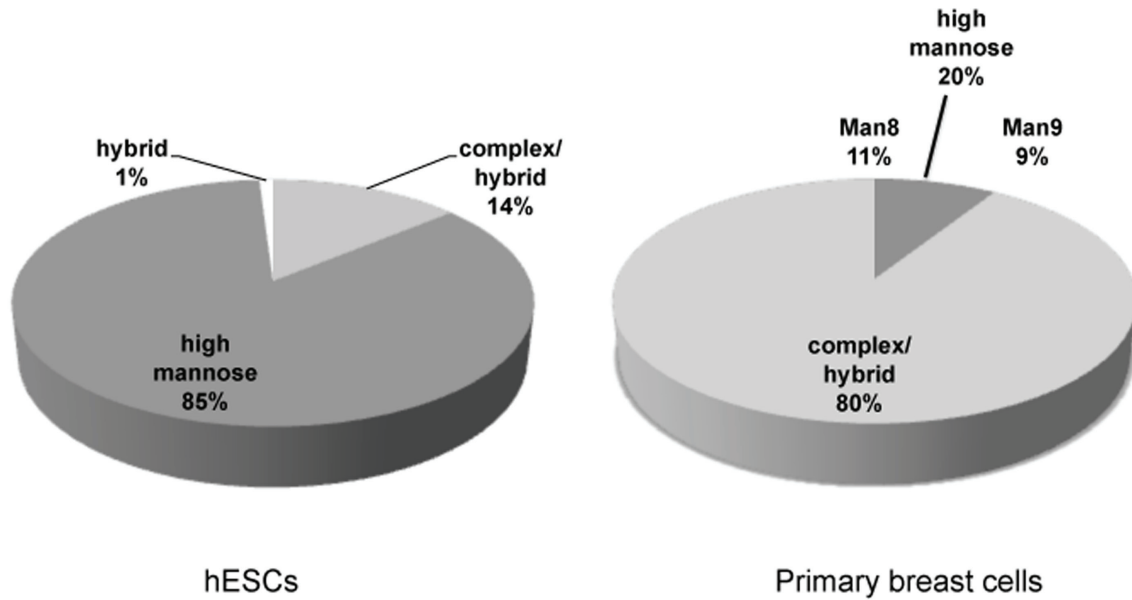
Figure 2.13. Glycan abundance profile of hESCs compared to primary breast cells (epithelial line MCF-10A). Glycan quantitation using peak areas of chromatograms from nanoLC-Chip/TOF MS. Primary breast cells have 80% complex/hybrid glycans and only 20% high mannose.

Table1 N-glycans found in hESCs membrane fractions by MALDI-FT ICR MS.

GCC fraction	Glycan type	Glycan composition[a]	m/z theoretical	m/z measured	Dm (Da)	Count[b]	Signal Intensity[c]
10%	high mannose	5H:2HN	1257.422	1257.429	0.007	2	w
		6H:2HN	1419.475	1419.476	0.001	3	m
		7H:2HN	1581.528	1581.529	0.001	3	s
		8H:2HN	1743.581	1743.570	0.011	3	s
		9H:2HN	1905.634	1905.623	0.011	3	s
		10H:2HN	2067.687	2067.705	0.018	3	m
	complex/hybrid	3H:4HN	1485.533	1485.548	0.015	3	w
		4H:4HN	1501.528	1501.552	0.023	3	w
		3H:5HN	1542.555	1542.541	0.013	2	w
		4H:5HN	1704.607	1704.623	0.016	3	w
		5H:5HN	1866.661	1866.688	0.027	3	w
		4H:3HN:1F	1589.544	1589.538	0.007	2	w
		4H:4HN:1F	1647.586	1647.606	0.020	3	w
		5H:3HN:1F	1751.597	1751.591	0.006	3	w
		6H:3HN:1F	1768.612	1768.631	0.019	2	w
		5H:4HN:1F	1809.639	1809.665	0.026	3	w
		4H:5HN:1F	1850.666	1850.686	0.020	3	w
		4H:5HN:2F	1996.724	1996.742	0.018	3	w
		5H:5HN:1F	2012.719	2012.731	0.012	3	m
		5H:5HN:2F	2158.777	2158.798	0.021	3	w
20%	hybrid	5H:3HN:1F	1606.570	1606.567	0.003	3	w
		6H:3HN	1622.560	1622.563	-0.003	3	w
	high mannose	5H:2HN	1257.424	1257.424	0.000	3	w
		6H:2HN	1419.480	1419.476	0.004	3	m
		7H:2HN	1581.540	1581.531	0.009	3	w
		8H:2HN	1743.590	1743.575	0.015	3	m
		9H:2HN	1905.640	1905.629	0.011	3	m
		10H:2HN	2067.690	2067.696	-0.006	3	w
	complex	3H:3HN:1F	1282.460	1282.456	0.004	3	w
		3H:4HN:1F	1485.540	1485.533	0.007	3	w
		3H:5HN:1F	1688.620	1688.613	0.007	3	w
		3H:5HN:2F	1834.680	1834.676	0.004	2	w
		3H:6HN:1F	1891.700	1891.697	0.003	3	w
		3H:6HN:2F	2037.760	2037.763	-0.003	3	w
		3H:6HN:3F	2183.820	2183.816	0.004	3	w
		5H:6HN:1F	2215.810	2215.800	0.010	3	w
		5H:6HN:2F	2361.860	2361.855	0.005	3	w
		6H:6HN:1F	2377.860	2377.844	0.016	3	m
		6H:6HN:2F	2523.920	2523.910	0.010	3	w
		6H:7HN:1F	2580.940	2580.940	0.000	3	w
		6H:6HN:3F	2669.970	2669.973	-	3	w

39

					0.003		
		7H:7HN:1F	2742.990	2742.994	-0.004	3	w
		7H:7HN:2F	2889.050	2889.058	-0.008	2	w
	complex/hybrid	4H:4HN	1501.540	1501.506	0.034	3	w
		5H:4HN	1663.590	1663.569	0.021	3	w
		4H:5HN	1704.620	1704.597	0.023	3	w
		5H:5HN	1866.670	1866.657	0.013	3	w
		6H:5HN	2028.714	2028.727	-0.014	3	w
		4H:3HN:1F	1444.510	1444.509	0.001	3	w
		4H:4HN:1F	1647.590	1647.587	0.003	3	w
		4H:4HN:2F	1793.650	1793.647	0.003	3	w
		5H:4HN:1F	1809.650	1809.635	0.015	3	m
		4H:5HN:1F	1850.670	1850.663	0.007	3	w
		5H:4HN:2F	1955.700	1955.701	-0.001	3	w
		4H:5HN:2F	1996.730	1996.724	0.006	3	w
		5H:5HN:1F	2012.730	2012.710	0.020	3	s
		5H:4HN:3F	2101.760	2101.765	-0.005	3	w
		4H:5HN:3F	2142.790	2142.795	-0.005	3	w
		5H:5HN:2F	2158.780	2158.778	0.002	3	m
		6H:5HN:1F	2174.780	2174.774	0.006	3	w
		5H:5HN:3F	2304.840	2304.836	0.004	3	w
		6H:5HN:2F	2320.840	2320.832	0.008	3	w
		6H:5HN:3F	2466.900	2466.895	0.005	3	w
		7H:6HN:1F	2539.910	2539.904	0.006	3	w
		7H:6HN:2F	2685.970	2685.970	0.000	3	w
		8H:7HN:1F	2905.040	2905.056	-0.016	2	w
	hybrid	5H:3HN	1460.510	1460.503	0.007	3	w
		5H:3HN:1F	1606.570	1606.562	0.008	2	w
	complex	5H:4HN:1NA	1976.658	1976.660	-0.002	3	w
		5H:4HN:1F:1NA	2122.716	2122.716	0.001	3	m
		5H:5HN:1F:1NA	2325.796	2325.777	0.018	3	w
		6H:6HN:1NA	2544.870	2544.912	-0.042	3	w
40%	complex/hybrid	4H:3HN	1298.460	1298.451	0.009	2	w
		4H:3HN:1F	1444.510	1444.506	0.004	3	m
		3H:4HN:1F	1485.540	1485.531	0.009	1	w
		4H:4HN	1501.540	1501.527	0.013	2	w
		4H:4HN:1F	1647.590	1647.586	0.004	3	m
		5H:4HN	1663.590	1663.583	0.007	3	m
		4H:4HN:2F	1793.650	1793.637	0.013	3	w
		5H:4HN:1F	1809.650	1809.634	0.016	3	s
		4H:5HN:1F	1850.670	1850.668	0.002	3	w
		5H:5HN	1866.670	1866.658	0.012	2	w
		5H:4HN:2F	1955.700	1955.699	0.001	3	m

40

5H:5HN:1F	2012.730	2012.722	0.008	3	m
6H:5HN	2028.720	2028.724	-0.004	1	w
5H:5HN:2F	2158.780	2158.782	-0.002	2	w
6H:5HN:1F	2174.780	2174.771	0.009	3	m
6H:5HN:2F	2320.840	2320.832	0.008	2	w
6H:6HN:1F	2377.860	2377.844	0.016	3	w
7H:6HN:1F	2539.910	2539.894	0.016	3	w

[a.] In glycan composition each capital letter (H, HN, F, NA) represents hexose(Hex), N-acetyl hexosamine (HexNAc), fucose(Fuc), and N-acetyl neuraminic acid (NeuAc) respectively.

[b.] Count represents the detected number from each glycan in bio-triplicates in MS analysis. The range of count is from one (1/3) to three (3/3).

[c.] Relative intensity of mass spectra was used to indicate the signal intensity. The symbol, s, m, and w, represent strong (>50%), moderate (20-50%), and weak signal (<20%), respectively.

Table 2 N-glycans found in hESCs membrane fractions by nanoLC-Chip/TOF MS.
Glycans were listed based on LC retention time (RT).

Exp Mass	Cal Mass	Error	Hex	HexNAc	Fuc	NeuAc	RT (min)	Peak Area
1681.6191	1681.6188	0.0004	4	5			17.732	126941
1234.4294	1234.4334	-0.0039	5	2			18.159	19735
1519.5628	1519.5660	-0.0032	3	5			18.267	23767
1827.6788	1827.6767	0.0021	4	5	1		18.472	16952
1843.6698	1843.6716	-0.0018	5	5			18.547	92244
1681.6165	1681.6188	-0.0023	4	5			18.900	169799
1989.7268	1989.7295	-0.0027	5	5	1		19.004	19522
1640.5905	1640.5922	-0.0017	5	4			19.048	18849
2126.7115	2126.7506	-0.0391	8	4			19.109	12299
2823.9839	2824.0048	-0.0209	8	6		1	19.205	35393
1882.6462	1882.6446	0.0016	9	2			19.211	3521394
2661.9104	2661.9520	-0.0415	7	6		1	19.287	17771
1396.4810	1396.4862	-0.0051	6	2			19.363	119676
1558.5354	1558.5390	-0.0035	7	2			19.365	1411802
1234.4279	1234.4334	-0.0055	5	2			19.415	170080
3279.1364	3279.1938	-0.0574	9	6	4		19.417	23589
2580.8791	2580.9192	-0.0401	9	4	2		19.471	24364
1720.5899	1720.5918	-0.0018	8	2			19.499	3906640
1843.6665	1843.6716	-0.0051	5	5			19.598	144840
1316.4726	1316.4866	-0.014	3	4			19.835	34114
1665.6180	1665.6239	-0.0059	3	5	1		19.855	35379
1437.5033	1437.5128	-0.0094	5	3			19.868	21095
1396.4820	1396.4862	-0.0041	6	2			19.955	1844066
1234.4266	1234.4334	-0.0067	5	2			19.957	91192
1558.5354	1558.5390	-0.0036	7	2			19.987	575937
2281.8377	2281.8453	-0.0076	5	5	3		20.081	17242
1973.7300	1973.7346	-0.0045	4	5	2		20.085	26097
1640.5912	1640.5922	-0.001	5	4			20.099	15169
2044.6942	2044.6974	-0.0032	10	2			20.106	318330
1624.5907	1624.5973	-0.0065	4	4	1		20.116	12518
2823.9638	2824.0048	-0.0409	8	6		1	20.253	54288
1882.6438	1882.6446	-0.0007	9	2			20.282	4630415
1558.5348	1558.5390	-0.0042	7	2			20.340	1948458
2661.9119	2661.9520	-0.04	7	6		1	20.340	106148
2708.8890	2708.9414	-0.0524	8	4		2	20.348	72304
1234.4238	1234.4334	-0.0096	5	2			20.375	106492
2499.8598	2499.8992	-0.0394	6	6		1	20.389	38472
1396.4832	1396.4862	-0.003	6	2			20.392	64028

3279.1348	3279.1938	-0.0589	9	6	4		20.407	36387
3522.2234	3522.2794	-0.056	8	8	2	1	20.409	40207
1234.4306	1234.4334	-0.0028	5	2			20.418	155193
1720.5892	1720.5918	-0.0026	8	2			20.620	6085126
1827.6701	1827.6767	-0.0066	4	5	1		20.652	142985
1234.4236	1234.4334	-0.0097	5	2			20.776	11802
1665.6189	1665.6239	-0.005	3	5	1		20.802	76772
2135.7802	2135.7874	-0.0072	5	5	2		20.929	57197
2281.8363	2281.8453	-0.0089	5	5	3		20.948	44679
1973.7299	1973.7346	-0.0046	4	5	2		20.985	92838
1275.4447	1275.4600	-0.0153	4	3			21.037	14168
1989.7251	1989.7295	-0.0044	5	5	1		21.197	353469
2135.7840	2135.7874	-0.0034	5	5	2		21.216	75848
1827.6713	1827.6767	-0.0053	4	5	1		21.246	522831
1437.5033	1437.5128	-0.0095	5	3			21.284	35172
1316.4795	1316.4866	-0.0071	3	4			21.305	58111
1882.6386	1882.6446	-0.006	9	2			21.413	236462
1396.4792	1396.4862	-0.0069	6	2			21.446	3256944
1234.4236	1234.4334	-0.0098	5	2			21.458	259581
1558.5327	1558.5390	-0.0063	7	2			21.487	1007669
1599.5575	1599.5656	-0.0081	6	3			21.572	33137
2044.6917	2044.6974	-0.0057	10	2			21.620	896607
2135.7813	2135.7874	-0.006	5	5	2		21.688	39356
1437.5008	1437.5128	-0.0119	5	3			21.754	13485
1843.6644	1843.6716	-0.0071	5	5			21.927	22922
1989.7228	1989.7295	-0.0067	5	5	1		21.966	1099013
1745.6135	1745.6235	-0.01	6	3	1		22.031	52007
1396.4771	1396.4862	-0.0091	6	2			22.289	75684
1640.5727	1640.5922	-0.0195	5	4			22.396	87802
1478.5246	1478.5394	-0.0148	4	4			22.422	16534
1583.5604	1583.5707	-0.0103	5	3	1		22.443	17535
1275.4472	1275.4600	-0.0128	4	3			22.474	29494
2281.8325	2281.8453	-0.0127	5	5	3		22.483	35304
1786.6414	1786.6501	-0.0087	5	4	1		22.502	48712
1462.5349	1462.5445	-0.0095	3	4	1		22.654	68592
2354.8457	2354.8617	-0.016	6	6	1		22.741	43456
1234.4226	1234.4334	-0.0108	5	2			22.797	522552
1478.5283	1478.5394	-0.0111	4	4			22.853	22436
1599.5569	1599.5656	-0.0087	6	3			22.926	107671
1729.6194	1729.6286	-0.0091	5	3	2		22.926	22244
2160.8114	2160.8191	-0.0077	3	6	3		23.009	20799
1947.7072	1947.7076	-0.0004	4	2	4	1	23.011	29569
2135.7760	2135.7874	-0.0113	5	5	2		23.014	63405

1583.5471	1583.5707	-0.0236	5	3	1		23.016	172784
1770.6447	1770.6552	-0.0105	4	4	2		23.031	47962
1624.5835	1624.5973	-0.0138	4	4	1		23.258	25300
2354.8504	2354.8617	-0.0112	6	6	1		23.350	35446
1665.6148	1665.6239	-0.0091	3	5	1		23.398	43467
1973.7274	1973.7346	-0.0072	4	5	2		23.454	22064
1932.7031	1932.7080	-0.0049	5	4	2		23.525	17049
1421.5063	1421.5179	-0.0115	4	3	1		23.663	16975
1640.5826	1640.5922	-0.0096	5	4			23.668	113364
2134.7585	2134.7670	-0.0085	5	5		1	23.713	61350
1624.5856	1624.5973	-0.0116	4	4	1		23.775	21034
1583.5618	1583.5707	-0.0088	5	3	1		23.813	81534
1259.4526	1259.4651	-0.0124	3	3	1		23.818	36551
1608.5940	1608.6024	-0.0084	3	4	2		23.898	28448
1567.5657	1567.5758	-0.01	4	3	2		23.943	15986
1462.5337	1462.5445	-0.0108	3	4	1		24.067	244494
1811.6687	1811.6818	-0.0131	3	5	2		24.139	23273
1770.6440	1770.6552	-0.0111	4	4	2		24.198	25613
2052.7057	2052.7138	-0.0081	7	3		1	24.222	18182
2119.7804	2119.7925	-0.0121	4	5	3		24.232	66460
2160.8085	2160.8191	-0.0105	3	6	3		24.314	79220
2151.7700	2151.7823	-0.0123	6	5	1		24.350	19114
1728.6003	1728.6082	-0.0078	5	3		1	24.421	37456
1234.4235	1234.4334	-0.0099	5	2			24.489	1187048
1786.6399	1786.6501	-0.0102	5	4	1		24.535	105791
2426.8699	2426.8828	-0.0128	5	5	2	1	24.568	16567
1868.6903	1868.7033	-0.013	3	6	1		24.702	29677
2014.7475	2014.7612	-0.0136	3	6	2		24.743	41481
1973.7239	1973.7346	-0.0106	4	5	2		24.842	70125
1932.6966	1932.7080	-0.0114	5	4	2		24.887	52167
2280.8132	2280.8249	-0.0117	5	5	1	1	24.897	96214
1624.5856	1624.5973	-0.0117	4	4	1		25.016	111582
2118.7609	2118.7721	-0.0112	4	5	1	1	25.089	54660
1745.6126	1745.6235	-0.0109	6	3	1		25.110	34896
1421.5062	1421.5179	-0.0117	4	3	1		25.156	58452
2426.8658	2426.8828	-0.017	5	5	2	1	25.248	41701
2151.7646	2151.7823	-0.0176	6	5	1		25.278	18896
1972.7076	1972.7142	-0.0066	4	5		1	25.314	22897
1665.6097	1665.6239	-0.0142	3	5	1		25.326	31246
1827.6673	1827.6767	-0.0093	4	5	1		25.338	40567
1932.6923	1932.7080	-0.0157	5	4	2		25.393	56144
2052.6996	2052.7138	-0.0142	7	3		1	25.407	49889
1890.6504	1890.6610	-0.0106	6	3		1	25.437	77886

2280.8112	2280.8249	-0.0137	5	5	1	1	25.548	278224
1566.5426	1566.5554	-0.0128	4	3		1	25.653	20325
2077.7349	2077.7455	-0.0106	5	4	1	1	25.723	27273
1259.4497	1259.4651	-0.0154	3	3	1		25.744	12091
1786.6384	1786.6501	-0.0116	5	4	1		25.856	476749
1728.5946	1728.6082	-0.0136	5	3		1	25.899	116152
2151.7669	2151.7823	-0.0154	6	5	1		26.257	75297
1931.6762	1931.6876	-0.0114	5	4		1	26.318	168878
1874.6544	1874.6661	-0.0117	5	3	1	1	26.422	54206
1932.6892	1932.7080	-0.0188	5	4	2		26.666	53539
1972.7033	1972.7142	-0.0109	4	5		1	26.783	18140
1890.6498	1890.6610	-0.0112	6	3		1	26.898	236085
1915.6802	1915.6927	-0.0125	4	4	1	1	26.945	21621
1769.6212	1769.6348	-0.0136	4	4		1	27.042	27963
1932.6895	1932.7080	-0.0184	5	4	2		27.075	30226
2077.7292	2077.7455	-0.0163	5	4	1	1	27.128	58432
1566.5432	1566.5554	-0.0122	4	3		1	27.186	54543
2036.7018	2036.7189	-0.0171	6	3	1	1	27.245	24679
2118.7556	2118.7721	-0.0164	4	5	1	1	27.259	46808
1259.4513	1259.4651	-0.0138	3	3	1		27.368	31604

[a]The mass corresponds to molecular mass ([M]).

2.4. Methods

2.4.1. Human embryonic stem cell (hESC) culture

The NIH approved human embryonic stem cell line HSF-6 was maintained under feeder-free conditions using a chemically defined media, X-VIVO 10 (Cambrex, Walkersville, MD) supplemented with human recombinant growth factors FGF and TGF-β1 (80 ng/mL and 0.5 ng/mL, respectively, R&D Systems, Minneapolis, MN)10. Cells were propagated on hESC-qualified Matrigel-coated plates (BD Biosciences). Media was exchanged daily after the first 48 hr in culture, and cells were passaged every 5 to 7 days using collagenase IV (200 units/ml, Invitrogen, Carlsbad, CA) and mechanically removed. Cells were centrifuged at 200 X g for 3 min and washed in PBS (Gibco/Invitrogen, Carlsbad, CA). Cells were centrifuged again and pellets were immediately frozen on dry ice. Approximately 200 million cells were counted and collected at different times and at different passage numbers to obtain biological triplicates. Karyotype analysis was routinely performed and indicated that all samples were diploid and had no chromosomal abnormalities. And cells were routinely stained with pluripotent markers Oct4 and SSEA-4.

2.4.2. Cell membrane extraction

Membrane extraction was performed using ultracentrifugation. Pellets were thawed on ice with the addition of a homogenization buffer (HB) consisting of 0.25 M sucrose, 20 mM Hepes-KOH, pH 7.4 and protease inhibitor mixture (1:100, Calbiochem/EMD Chemicals, Gibbstown, NJ). Cells were sonicated on ice, and cell lysates were centrifuged at 1,000g for 10 min to remove the nuclear fraction and debris. The supernatant was collected and additional HB was added for ultracentrifugation at 200,000g for 45 min at 4°C to remove the cytoplasmic fraction. The pellets were resuspended in 0.2 M Na_2CO_3 (pH 11) to break up the microsomes. The samples were spun twice more at 200,000g for 45 min to wash the samples of the cytoplasmic fraction. The supernatant was removed and the membrane fractions were frozen at -20 °C.

2.4.3. Western blot analysis

All fractions (nuclear, cytoplasmic and membranes) were analyzed by SDS-PAGE followed by Western blot using known organelle-specific markers for the nucleus (nuclear pore complex proteins, Covance), endoplasmic reticulum (Bip/GRP78, BD Biosciences), cytosol (α-tubulin, Sigma) and the plasma membrane (CD49b, BD Biosciences). Primary antibodies were probed with a horseradish peroxidase conjugated anti-mouse secondary antibody (HRP-anti-mouse IgG). Before Western blot analysis, membrane pellets were resuspended in 4% SDS buffer and protein concentration was determined by the BCA assay (Pierce). The samples (4ug) were separated by SDS/PAGE (4-12%, Bio-Rad).

2.4.4. Glycan release

The membrane fractions were washed twice with nanopure water and then divided into two fractions for N- and O-glycan analysis, respectively. For analysis of N-glycans, 100 μL of 100 mM ammonium bicarbonate (NH4HCO3), 5 mM dithiothreitol (DTT, from Promega) was added to the samples and heated to 100oC for 2 min to denature the protein. After cooling at room temperature, 2 μL of Peptide N-glycosidase F (PNGase F, from New England Biolabs) was added to the mixture (pH 7.5) and incubated at 37oC for 24 hours in a water bath. 800 μL of chilled ethanol was added, and the mixture was frozen at -80°C for 1 hour and then centrifuged to separate the proteins in the pellet from with the glycans in the supernatant. The supernatant was completely dried down to remove the ethanol prior to solid phase extraction (SPE) using a graphitized carbon cartridge (GCC, from Alltech).

For O-glycan analysis, alkaline borohydride solution (500μL, mixture of 1.0 M sodium borohydride and 0.1 M sodium hydroxide) was added to the membrane fraction. The mixture was incubated at 42°C for 12 hrs in a water bath. The addition of 1.0 M hydrochloric acid solution was slowly added in an ice bath to stop the reaction and destroy excess sodium borohydride.

2.4.5. Glycan enrichment

Released N- and O-glycans were purified and enriched by SPE-GCC. Prior to use, graphitized carbon cartridge (150 mg bed weight, 4 mL cartridge volume) was washed with nanopure water followed by 80% acetonitrile (AcN) in 0.05% (v/v) trifluoroacetic acid (TFA) (v/v) and again with nanopure water. Glycan solutions were applied to the GCC cartridge and subsequently washed with several cartridge volumes of nanopure water at a flow rate of 1 mL/min to remove salts. Glycans were eluted stepwise with 10% AcN in H2O (v/v), 20% AcN in H2O (v/v), and 40% AcN in 0.05% TFA in H2O (v/v). Each fraction was collected and concentrated in vacuo prior to mass spectrometry analysis. Fractions were reconstituted in nanopure water prior to MS analysis.

2.4.6. Mass spectrometric analysis

Mass spectra were recorded on a Fourier transform-ion cyclotron resonance mass spectrometer (FT-ICR MS) with an external source HiResMALDI (IonSpec Corporation, Irvine, CA) equipped with a 7.0 Tesla magnet. The HiResMALDI was equipped with a pulsed Nd:YAG laser (355 nm). 2,5-Dihydroxy-benzoic acid (DHB) was used as a matrix (5 mg/100 mL in 50% AcN:H2O) for both positive and negative modes. A saturated solution of NaCl in 50% AcN in H2O was used as a cation dopant to increase signal sensitivity. The glycan solution (0.7 μL) was applied to the MALDI probe followed by matrix solution (0.7 μL). For the negative ion spectra, DHB matrix was only used without using any dopant. The sample was dried under vacuum prior to mass spectrometric analysis.

2.4.7. Structural determination using infrared multiphoton dissociation (IRMPD)

Tandem mass spectrometry, specifically IRMPD, was used to determine the general structures of several oligosaccharides. This allowed for complete fragmentation of the ion of interest. A desired ion was readily selected in the analyzer with the use of an arbitrary-wave form generator and a frequency synthesizer. A continuous wave Parallax CO_2 laser (Waltham, MA) with 20 W maximum power and 10.6 μm wavelength was installed at the rear of the magnet and was used to provide the photons for IRMPD. The laser beam diameter is 6 mm as specified by the manufacturer. The laser beam was expanded to 12 mm by means of a 2× beam expander (Synrad, Mukilteo, WA) to ensure complete irradiation of the ion cloud through the course of the experiment. The laser was aligned and directed to the center of the ICR cell through a BaF2 window (Bicron Corporation, Newbury, OH). Photon irradiation time was optimized to produce the greatest number and abundance of fragment ions. The laser was operated at an output of approximately 13 W.

2.4.8. NanoLC mass spectrometry

Each GCC fraction was analyzed using a microfluidic HPLC-Chip-TOF MS (Agilent, CA). The microfluidic HPLC-CHIP consists of an enrichment column, a LC separation column packed with porous graphitized carbon, and a nanoelectrospray tip. Separation was performed by a binary gradient A: 3% acetonitrile in 0.1% formic acid solution and B: 90% acetonitrile in 0.1% formic acid solution. The column was initially equilibrated and eluted with the flow rate at 0.3 μL/min for nanopump and 4 μL/min for capillary pump. The 65 minute gradient was programmed as follows: 2.5-20 minute, 0%-16% B, 20-30 minute, 16%-44% B, 30-35 minute, B increased to 100%, then continued 100% B to 45 minute, finally 0% B for 20 minute to equilibrate the chip column before next sample injection. Each possible composition of N-glycans were identified with the in-house program "GlycoX" (35) according to the mass tolerance with additional retention times and abundance information noted at the same time.

2.4.9. Immunofluorescence

hESCs were fixed with 2% paraformaldehyde for 15 minutes and rinsed 3 times in PBS for 5 minutes. Cells were blocked with staining buffer (2% fetal bovine serum in PBS) for 15 minutes and then stained with pluripotent marker SSEA-4 (2.5μg/500 μL/well, Millipore) for 30 minutes at room temperature. The wells were rinsed three times in PBS before adding FITC-conjugated lectins (20 μg/ml, EY Labs) and Alexa Fluor 594-conjugated goat-anti-mouse secondary antibody to SSEA-4 (1:400, Invitrogen). Wells were rinsed three times in PBS and stained with a solution of 1X Hoechst 23187 (Sigma) as a nuclear stain, for 5 minutes. Wells were analyzed using an Olympus IX71 fluorescent microscope. Control wells were stained with hESCs with mouse IgG3 isotype (Invitrogen) and lectins incubated with their respective inhibitory sugar.

2.4.10. Flow cytometry

hESCs were collected after incubation with collagenase IV (200 units/mL, Invitrogen) and mechanically removed. Colonies were dissociated into single cell suspensions in 0.5mM EDTA, and were then filtered through a 40 micron cell strainer before they were counted. Cells were blocked with staining buffer (2% fetal bovine serum in PBS) for 15 minutes and then stained with pluripotent marker SSEA-4 (2.5µg/500 µL/500,000 cells, Milllpore) for 30 minutes on ice. Next, cells were washed, and stained with APC-conjugated goat-anti- mouse secondary antibody to SSEA-4 (1:400, Jackson ImmunoResearch Labs) and 5, 10, 20 or 40 ug/ml of the following FITC-conjugated lectins: Canavalia ensiformis (Con A), and Galanthus nivalis (GNA), (EY Labs). To validate binding specificity, hESCs were also stained with lectins pre-incubated for at least 15 minutes with sugar haptens: methy-α-mannoside and yeast mannan, respectively (Sigma). After 30 minutes on ice, cells were washed and resuspended in staining buffer with propidium iodide to distinguish dead cells from live cells. Flow cytometry (BD FACs Calibur from BD Biosciences) was performed and data was analyzed using FlowJo software (TreeStar Inc.). At least three independent assays were carried out for each lectin. The final quantitation represents live hESCs that were double-labeled with SSEA-4 and FITC-conjugated lectins. Additional controls were unstained and stained hESCs with mouse IgG3 isotype (Invitrogen).

2.5. References

1.	Spiro, R. G., Protein glycosylation: nature, distribution, enzymatic formation, and disease implications of glycopeptide bonds. Glycobiology 2002, 12, (4), 43r-56r.

2.	Lebrilla, C. B., Mahal, L. K. Post-translation modifications. Curr Opin Chem Biol 2009, 13, (4), 373-4.

3.	Ohtsubo, K., Marth, J.D. Glycosylation in cellular mechanisms of health and disease. Cell 2006, 126, (5), 855-867.

4.	Paulson, J.C., Blixt, O., Collins, B. E. Sweet spots in functional glycomics. Nature Chemical Biology 2006, 2, (5), 238-248.

5.	Dube, D. H., Bertozzi, C. R. Glycans in cancer and inflammation. Potential for therapeutics and diagnostics. Nature Reviews Drug Discovery 2005, 4, (6), 477-488.

6.	Cooke, C. L., An, H. J., Kim, J., Canfield, D. R., Torres, J., Lebrilla, C. B., Solnick, J. V., Modification of Gastric Mucin Oligosaccharide Expression in Rhesus Macaques After Infection With Helicobacter pylori. Gastroenterology 2009, 137, (3), 1061-1071.

7.	An, H. J., Kronewitter, S. R., de Leoz, M. L., Lebrilla, C. B. Glycomics and disease markers. Curr Opin Chem Biol 2009.

8.	Wearne, K. A., Winter, H. C., Goldstein, I. J. Temporal changes in the carbohydrates expressed on BG01 human embryonic stem cells during differentiation as embryoid bodies. Glycoconj J 2008, 25, (2), 121-36.

9.	Satomaa, T., Heiskanen, A., Mikkola, M., Olsson, C., Blomqvist, M., Tiittanen, M., Jaatinen, T., Aitio, O., Olonen, A., Helin, J., Hiltunen, J., Natunen, J., Tuuri, T., Otonkoski, T., Saarinen, J., Laine, J. The N-glycome of human embryonic stem cells. BMC Cell Biol 2009, 10, 42.

10.	Naka, R., Kamoda, S., Ishizuka, A., Kinoshita, M., Kakehi, K. Analysis of total N-glycans in cell membrane fractions of cancer cells using a combination of serotonin affinity chromatography and normal phase chromatography. Journal of Proteome Research 2006, 5, (1), 88-97.

11.	Yamamoto, F., Clausen, H., White, T., Marken, J., Hakomori, S. I. Molecular Genetic-Basis of the Histo-Blood Group Abo System. Nature 1990, 345, (6272), 229-233.

12.	Lovell-Badge, R., The future for stem cell research. Nature 2001, 414, (6859), 88-91.

13. Nagano, K., Yoshida, Y., Isobe, T. Cell surface biomarkers of embryonic stem cells. Proteomics 2008, 8, (19), 4025-4035.

14. McNeish, J. Embryonic stem cells in drug discovery. Nature Reviews Drug Discovery 2004, 3, (1), 70-80.

15. Lanctot, P. M., Gage, F. H., Varki, A. P. The glycans of stem cells. Curr Opin Chem Biol 2007, 11, (4), 373-80.

16. Turnbull, J. E., Field, R. A. Emerging glycomics technologies. Nature Chemical Biology 2007, 3, (2), 74-77.

17. La Belle, J. T., Gerlach, J. Q., Svarovsky, S., Joshi, L. Label-free impedimetric detection of glycan-lectin interactions. Anal Chem 2007, 79, (18), 6959-64.

18. Ito, H., Kuno, A., Sawaki, H., Sogabe, M., Ozaki, H., Tanaka, Y., Mizokami, M., Shoda, J., Angata, T., Sato, T., Hirabayashi, J., Ikehara, Y., Narimatsu, H. Strategy for glycoproteomics: identification of glyco-alteration using multiple glycan profiling tools. J Proteome Res 2009, 8, (3), 1358-67.
19. Wearne, K. A., Winter, H. C., O'Shea, K., Goldstein, I. J. Use of lectins for probing differentiated human embryonic stem cells for carbohydrates. Glycobiology 2006, 16, (10), 981-90.

20. Wu, C. C., MacCoss, M. J., Howell, K. E., Yates, J. R. A method for the comprehensive proteomic analysis of membrane proteins. Nat Biotechnol 2003, 21, (5), 532-8.

21. Wollscheid, B., Bausch-Fluck, D., Henderson, C., O'Brien, R., Bibel, M., Schiess, R., Aebersold, R., Watts, J. D. Mass-spectrometric identification and relative quantification of N-linked cell surface glycoproteins. Nature Biotechnology 2009, 27, (4), 378-386.

22. Luchansky, S. J., Hang, H. C., Saxon, E., Grunwell, J. R., Danielle, C. Y., Dube, D. H., Bertozzi, C. R. Constructing azide-labeled cell surfaces using polysaccharide biosynthetic pathways. Recognition of Carbohydrates in Biological Systems Pt A: General Procedures 2003, 362, 249-272.

23. Lebowitz, J., Lewis, M. S., Schuck, P. Modern analytical ultracentrifugation in protein science: A tutorial review. Protein Science 2002, 11, (9), 2067-2079.

24. Brockhausen, I. Biosynthesis and functions of O-glycans and regulation of mucin antigen expression in cancer. Biochem Soc Trans 1997, 25, (3), 871-4.

25. Harvey, D. J. Quantitative Aspects of the Matrix-Assisted Laser-Desorption Mass-Spectrometry of Complex Oligosaccharides. Rapid Communications in Mass Spectrometry 1993, 7, (7), 614-619.

26. Grey, C., Edebrink, P., Krook, M., Jacobsson, S. P. Development of a high performance anion exchange chromatography analysis for mapping of oligosaccharides. Journal of Chromatography B-Analytical Technologies in the Biomedical and Life Sciences 2009, 877, (20-21), 1827-1832.

27. Chu, C. S., Ninonuevo, M. R., Clowers, B. H., Perkins, P. D., An, H. J., Yin, H., Killeen, K., Miyamoto, S., Grimm, R., Lebrilla, C. B. Profile of native N-linked glycan structures from human serum using high performance liquid chromatography on a microfluidic chip and time-of-flight mass spectrometry. Proteomics 2009, 9, (7), 1939-51.

28. Ninonuevo, M., An, H., Yin, H., Killeen, K., Grimm, R., Ward, R., German, B., Lebrilla, C. Nanoliquid chromatography-mass spectrometry of oligosaccharides employing graphitized carbon chromatography on microchip with a high-accuracy mass analyzer. Electrophoresis 2005, 26, (19), 3641-9.

29. Chu, C. S., Ninonuevo, M. R., Clowers, B. H., Perkins, P. D., An, H. J., Yin, H. F., Killeen, K., Miyamoto, S., Grimm, R., Lebrilla, C. B. Profile of native N-linked glycan structures from human serum using high performance liquid chromatography on a microfluidic chip and time-of-flight mass spectrometry. Proteomics 2009, 9, (7), 1939-1951.

30. Tao, S. C., Li, Y., Zhou, J. B., Qian, J., Schnaar, R. L., Zhang, Y., Goldstein, I. J., Zhu, H., Schneck, J. P. Lectin microarrays identify cell-specific and functionally significant cell surface glycan markers. Glycobiology 2008, 18, (10), 761-769.

31. Molinari, M. N-glycan structure dictates extension of protein folding or onset of disposal. Nature Chemical Biology 2007, 3, (6), 313-320.

32. Heiskanen, A., Hirvonen, T., Salo, H., Impola, U., Olonen, A., Laitinen, A., Tiitinen, S., Natunen, S., Aitio, O., Miller-Podraza, H., Wuhrer, M., Deelder, A. M., Natunen, J., Laine, J., Lehenkari, P., Saarinen, J., Satomaa, T., Valmu, L. Glycomics of bone marrow-derived mesenchymal stem cells can be used to evaluate their cellular differentiation stage. Glycoconj J 2009, 26, (3), 367-84.

33. Reya, T., Morrison, S. J., Clarke, M. F., Weissman, I. L. Stem cells, cancer, and cancer stem cells. Nature 2001, 414, (6859), 105-11.

34. Morishima, S., Morita, I., Tokushima, T., Kawashima, H., Miyasaka, M., Omura, K., Murota, S. Expression and role of mannose receptor/terminal high-mannose type oligosaccharide on osteoclast precursors during osteoclast formation. Journal of Endocrinology 2003, 176, (2), 285-292.

35. An, H. J., Tillinghast, J. S., Woodruff, D. L., Rocke, D. M., Lebrilla, C. B., A new computer program (GlycoX) to determine simultaneously the glycosylation sites and oligosaccharide heterogeneity of glycoproteins. J Proteome Res 2006, 5, (10), 2800-8.

36. Park, Y., Lebrilla, C.B. Application of fourier transform ion cyclotron resonance mass spectrometry of oligosaccharides. Mass Spec. Rev. 2005 24, 232-264.

37. An, H.J., Miyamoto, S., Lancaster, K.S., Kirmiz. C., Li B., Lam, K.S., Leiserowitz, G.S., Lebrilla, C.B. Profiling of glycans in serum for the discovery of potential biomarkers for ovarian cancer. J. of Proteome Res 2006, 5, 1626-1635.

38. Rabilloud, T. Membrane proteins and proteomics: Love is possible, but so difficult. Electrophoresis 2009, 10, (S1), S174 - S180

39. Dunn, M.J., Cordwell, S.J. Technologies for plasma membrane proteomics Proteomics 2010, 10, (4), 611–627.

40. Ruhaak, R.L., Deelder, A.M., Wuhrer, M. Oligosaccharide analysis by graphitized carbon liquid chromatography-mass spectrometry. Analytical and Bioanalytical Chemistry 2009, 394, (1), 163-174.

41. Kelleher, D. J., Karaoglu, D., Mandon, E. C., and Gilmore, R. Mol. Cell 2003,12, 101–111.

Chapter 3:
Identification of glycans on hESCs during neural development

Chapter 3: Identification of glycans on hESCs during neural development

3.1. Introduction

Glycans on the cell surface are dynamic and they can change during cellular differentiation(1,2). Studies using lectins have already shown that glycans change during hESC development into 12-day embryoid bodies and neuroepithelial development (1). In the previous chapter, we optimized a method for the analysis of membrane glycans on undifferentiated hESCs and discovered an unusual abundance of high mannose glycans. Using our FTICR method, we analyzed membrane glycans on embryoid bodies and neural stem cells derived from hESCs to identify detailed structures of N-glycans in the neural lineage. An abundance of high mannose glycans was found on hESCs-derived embryoid bodies (EB) and neural stem cells (NS). In addition, there are potential biomarkers that could distinguish between different cell types in the neural lineage. The conservation and changes of specific glycans may reveal an essential biological function, opening the doors for further investigations and an in depth understanding of the roles that glycans play in stem cell biology and along the neural lineage.

3.2. Neural lineage

The generation of neural stem cells and neurons from hESCs provides an avenue for the discovery of unknown biomolecules and/or interactions underlying brain development. In addition, neural cells may be used for drug screening to find treatments for neurodegenerative disorders for which there is currently little hope for curing. Several hurdles exist, however, which need to be overcome before results from the field of stem cell research can be used in the clinic. For example, the factors that govern conversion of stem cells into a variety of tissue types, like the brain, are not well understood. Thus, I have chosen to identify glycoconjugates in neural differentiation as an initial area for investigation. The presence and functional significance of some glycans in the nervous system, compared to other systems, have been better characterized. In the nervous system, glycans are located at neuronal membranes and synaptic junctions, where they play essential roles in neural development, cell proliferation, neuronal migration, and axonal path finding (3-5). However, a full-scale investigation of the glycoproteins present on cell surfaces during neuronal differentaion has not been reported.

3.3. Directed in vitro differentiation of hESC

Differentiation of hESCs into the neural and neuronal lineages in culture provides a basic tool for understanding molecular and cellular mechanisms that may control cell fate during development. And reciprocally, the characterization of proteins involved in developmental biological molecular programs has facilitated the engineering of stem cells toward a specific cell type.

hESC-derived neural precursor and neuronal cell types are potential tools for cell-based therapies to treat conditions such as Parkinson's disease, spinal injury, and retinal degeneration. Significant progress has been made in developing efficient methods for

directing neural, pan-neuronal, and neuronal-subtype specification from ES cells. Neural progenitors of ES cells are mostly defined by the expression of the intermediate filament marker nestin and transcription factors such as members of the Sox family (6). It appears that Sox-positive cells give rise to most cell types in the nervous system.

Numerous procedures have been developed to enrich neural precursors from hESCs that can proliferate and differentiate into neurons, astrocytes and oligodendrocytes. hESCs are commonly induced into the neural lineages through the formation of EB in suspension (7), but can also be induced through adherent monoculture systems (8), with co-culture (9) and through spontaneous differentiation of hESCs (10,11). The main disadvantage of these approaches is the inclusion of cell populations derived from the three germ layers in the total cell population. To control ES cell differentiation, understanding the coordination and roles of intrinsic factors with extrinsic factors is a critical step to enhance the derivation of neural precursors, work that is currently being done by several groups. Obtaining an efficient and highly homogenous population of a specific cell type is still a major hurdle in stem biology.

3.3.1. Growth factors and morphogens in the induction of neural differentiation

Some of the known molecular mechanisms in directing neural differentiation of hESCs involve multiple classical pathways such as the activation of FGF and/or inhibition of BMPs and Wnts. The difficulty in directing stem cells into a homogenous population may be due to the activation of multiple parallel pathways in a specific cell response, some of which have yet to be identified. Numerous studies have analyzed the expression and roles of such developmentally important molecules in hESCs.

hESCs cells are commonly cultured in the presence of FGF-2, which is a known survival and proliferation factor for neural progenitors (12). Under the right conditions, FGF-2 has also been shown to induce neural differentiation of hESCs. Benzing et al. devised a protocol to generate neural progenitors without formation of EB or co-culture with stromal cells, but instead in the presence of FGF-2. In this protocol, hESCs were transferred to DMEM/F12 medium supplemented with FGF-2 and subsequently plated onto Matrigel and propagated as an adherent culture. The colonies were detached and cultivated in suspension culture as neural spheres. To induce neuronal differentiation, FGF-2 was removed from the culture. When the resulting cells were plated, they gave rise to neural progenitors that were able to differentiate into all three neural lineages.

Neural differentiation can also be induced by overgrowth of undifferentiated human ES cells (10,11). Reubinoff et al.(11) devised a protocol that maintained hESCs in culture for 3-4 weeks without passage or replenishment of MEFs. This led to the spontaneous differentiation of hESCs into neural progenitors. By manually transferring cells containing short processes presumptive of neural progenitors onto culture plates with defined medium supplemented with FGF-2 and EGF, a highly enriched population of neural precursors was generated. Within these neurospheres, a high proportion of cells expressed neural markers nestin and NCAM, as well as the neuronal and glial marker A2B5. These neural precursors were able to differentiate into mature neurons, astrocytes, and oligodendrocytes. A similar method published concurrently induced neural differentiation through EB formation followed by culturing in the presence of FGF-2. Following EB formation, neural

rosettes, structures that mimic neural tube formation in vivo, were generated. Rosettes were cultured in medium with FGF-2, harvested by selective dissociation and then cultured as free-floating aggregates of neural precursors (10). The advantage of the Zhang et al. method is that the time line for the generation of neural stem cells is similar to what occurs in vivo, the method that I have chosen to use for my investigations.

3.3.2. Neuronal-subtype specification

Using some of the same strategies for neural specification, several methods have been devised to direct hESCs into specific neuronal subtypes, some of which have led to recovery of symptoms in animal models of Parkinson's disease, spinal injury, and retinal degeneration after cell transplantation. Directed differentiation of hESCs toward a specific lineage can be achieved by addition of a combination of growth factors and/or their antagonists, co-culture with cell types capable of inducing specific lineages, and transfection of ES cells with transcription factors (using conventional DNA delivery, lentiviral and adenoviral vectors, or homologous recombination).

The loss of specific types of neurons underlies many neurological disorders. An approach to treating these diseases is to elucidate the inductive signals and transcription factors that can direct differentiation into specific types of neurons such as dopamine (DA) and motor neurons and use these factors to induce stem cell differentiation into desired lineages for cell replacement therapies. The field of developmental biology has identified numerous factors involved in positional specification and neural patterning during neural development, and several such factors have been found to control analogous processes of stem cell differentiation into specific neuronal phenotypes in culture. The resulting neuronal subtypes are commonly characterized by the expression of transcription factors, secretion of neurotransmitters, and the presence of transporters and synthesizing and metabolizing enzymes. Furthermore, electrophysiological characterization has demonstrated that the ESC-derived neurons are functionally active in vitro, with the potential for use in cell replacement therapy in vivo.

3.3.3. Dopaminergic specification

Mesencephalic DA neurons, which degenerate in patients with Parkinson's disease, are derived from progenitors located in the midbrain. The induction of these progenitors involves Shh and FGF8 signaling, which have been shown to promote ventral midbrain fates in neural plate explants (13,14). Likewise, Shh and FGF8 in combination with ascorbic acid increase the yield of hESC differentiation into TH-positive neurons in vitro. Ascorbic acid has been previously implicated in promoting DA neurons from primary CNS cultures (15). Mechanistically, transcription factors such as Nurr1, Pitx3, En and Lmx1b are involved in the maturation of post-mitotic DA neurons. Based on the biological roles of the aforementioned growth factors and transcription factors, several protocols have been developed to generate hESC-derived DA neurons, which have been functionally characterized by quantifying DA release upon depolarization with potassium chloride using reverse HPLC, as well as by their response to the addition of neurotransmitters such as GABA and glutamate. In addition to being electrophysiologically active, hESC-

derived DA neurons have been shown to be biologically relevant, based on studies using animal disease models, such as the animal model for Parkinson's disease. Engrafted hESC-derived DA neurons survive and are functional, alleviating some of the symptoms characteristic of Parkinson's disease.

There are two primary methods for DA differentiation. The first involves co-culturing of hESCs with feeder cells that produce factors that help direct differentiation and the second, involves the timely addition of midbrain patterning factors and neurotrophic factors that promote cell survival. The co-culture method is commonly used, which offers the advantage of more rapid differentiation and a more homogenous population of cells compared to EB-based techniques. hESCs co-cultured with PA6 stromal cells generate a high frequency of DA neurons. After 3 weeks of culture with PA6 stromal cells, 87% of the resulting colonies were TH-positive. Using RT-PCR, several dopaminergic markers were expressed, such as TH, DAT, AADC, and transcription factors Ptx3, Lmx1b, and Nurr1. The total cell population also included other non-dopaminergic neuron subtypes expressing markers for cholinergic and glutaminergic neurons (16). Co-culturing hESCs with immortalized human midbrain astrocytes derived from developing ventral midbrain has also been used as a method to induce DA differentiation (16), thus reducing the exposure to animal-derived components.

hESCs can be differentiated into DA neurons by the use of Shh and FGF-8 under more defined conditions (17). Yan et al.(17) established a chemically defined system for directing human ES cells to neuroepithelial cells in a manner that emulates human neuroectodermal development in timing and in the formation of neural tube-like structures. Early exposure to FGF-8, before precursors become SOX-1 expressing neuroepithelial cells is necessary for midbrain DA neuronal differentiation in vitro. hESCs were grown in suspension and subsequently plated on adhesive culture dishes in chemically defined neural medium supplemented with FGF-2. FGF-8 was added to promote midbrain specification, followed later by the combination of FGF8 with Shh. Early exposure to FGF-8 induced the expression of Wnt 1, midbrain-related transcription factors En1 and Pax2, and more than 95% of the neural precursors expressed nestin. After three weeks of differentiation, approximately 31.8% of cells were TH-positive, and all TH-positive neurons expressed ß -tubulin III and AADC, and most expressed VMAT2 (a protein involved in packaging DA). By using the combination of FGF-8 and Shh, hESCs can be directed to the ventral midbrain fate to generate DA neurons

Efficient and large-scale differentiation of hESCs into DA neurons has been a challenge in the stem cell field, requiring testing and development of new protocols. New protocols recently published have shown improved differentiation efficiency such as the protocol published by Cho et al. (19). The Cho et al. method has the advantage that it is feeder-free, takes 14 days and yields >77% neurons in which 86% are dopaminergic neurons.

The protocols mentioned in this section successfully enhanced DA neuron generation and increased population homogeneity by using co-culturing and the addition of exogenous molecules such as Shh and FGF-8. Choosing the appropriate differentiation protocol is important in order to address specific scientific questions. Additionally, it is important to take into account differences in hESC lines in their ability to differentiate using a particular protocol. Not all cell lines will respond under the same conditions and

initial derivation and culturing conditions may affect the efficiency and ability for neuronal differentiation. The chemically defined system for hESC derivation of DA neurons is advantageous compared to the co-culturing methods, as it doesn't involve culturing with additional cell lines and, more importantly, emulates (to a better extent) neural development in vivo.

3.4. Present investigation

In this study, hESCs were differentiated into embryoid bodies (EB) and neural stem cells/neural spheres (NS) to profile differential expression of glycans on the cell membrane surface and investigate changes in glyco-related genes. The same experimental strategy discussed in Chapter 2 was used to evaluate glycans from EB and NS derived from the hESC line, HSF-6. However, this Chapter does not include data from the isomer separation and quantitation by nanoflow liquid chromatography (nanoLC), or data from H1 cell line. These studies are currently underway as well as analysis of samples from hESC-derived neurons.

Flow cytometry analysis with GNA lectin was conducted on other cell types such as induced pluripotent cells (iPS) and primary human cells to determine the levels of high mannose glycan expression on the cell surface. Also, in a preliminary study, the function of high mannose glycans was tested using pradicimicin A, a small molecule with high specificity to terminal mannose residues.

3.4.1. Results

hESCs were differentiated into EBs and NS (Fig 3.1) and a subpopulation was stained for the expression of neural stem cell markers known to be present during neural differentiation (Fig 3.2). Cell membrane fractions from each cell type were obtained by ultracentrifugation and enriched for glycans by solid phase extraction (SPE) using a graphitized carbon column (GCC) and then profiled using MALDI-FTICR MS (Fig. 3.3). Monosaccharides present in the glycans are denoted by Hex (hexoses), HexNAc (N-acetylhexosamines), NeuAc (N-acetyl sialic acid), and Fuc (fucose), based on predicted masses for human glycans, as described in Chapter 2. The most abundant glycans were analyzed with tandem mass spectrometry using infrared multiphoton dissociation (IRM-PD) to obtain structural connectivity of the individual monosaccharides.

| | hESCs | Embryoid bodies | Rosettes | Neural spheres |

| Day 0 | Day 4 | Day 8 | Day10 |
| | - FGF | + FGF + N.I. | + FGF + N.I. |
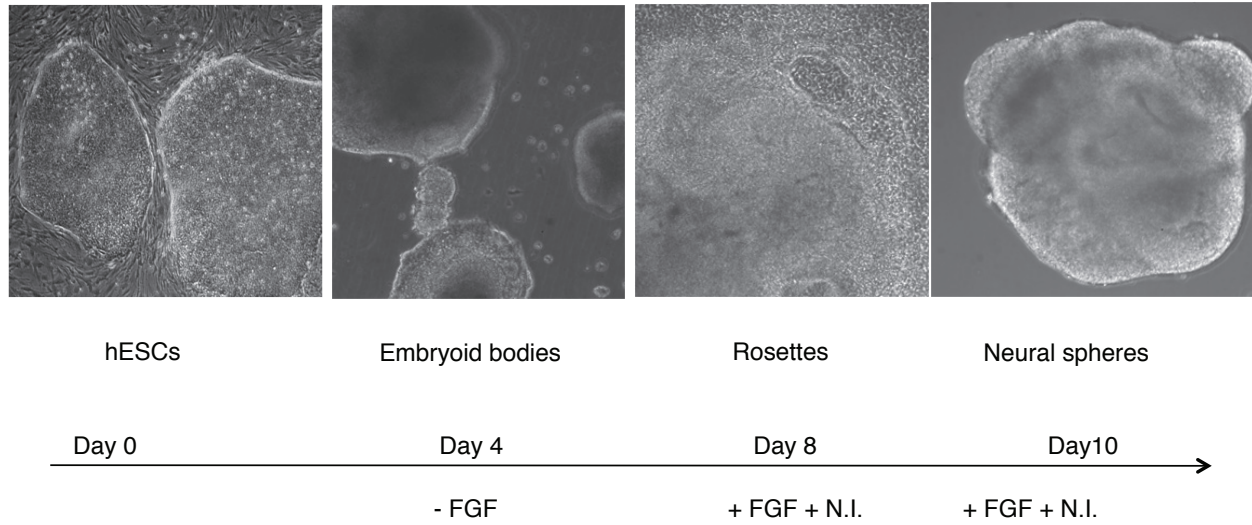
Figure 3.1. Bright-field images of hESCs, EBs, rosettes and neural sphere. Cells were differentiated using a modified protocol from Zhang et al. (10).

	Antibody	Isotype
Nestin		
Sox-2		
PSA-NCAM		
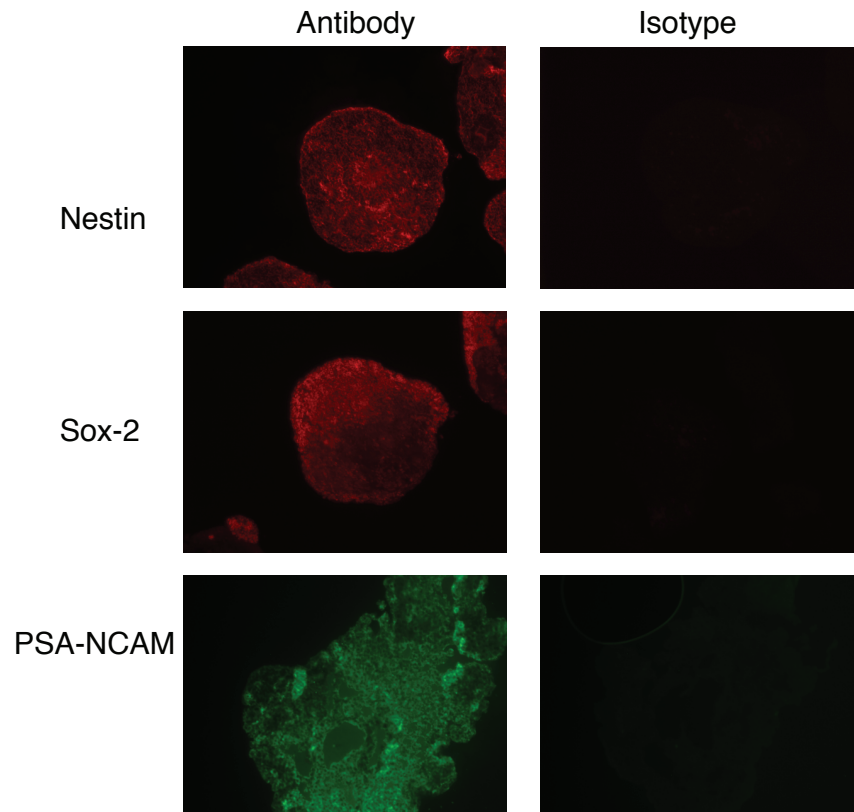
Figure 3.2. Neural spheres stained with neural stem cell markers. Cells were fixed, sectioned and stained with antibodies against neural stem cells markers nestin, sox-2 and PSA-NCAM and with respective isotype controls.

3.4.2. Mass profiling and quantitation of glycans from hESC cell membranes

Glycans were released from the graphitized carbon by successive elution with increasing concentrations of acetonitrile (AcN). Figure 3.4 shows representative mass spectra of N-glycans from all three bio-triplicates hESC, EB and NS membranes in the individual 10, 20, and 40% AcN fractions. Glycans found in each cell type were biologically and technically reproducible. When all AcN fractions were combined and analyzed, both EB and NS had an abundance of high mannose glycans, approximately 64% and 71%, respectively, compared to 54% in hESCs (Fig. 3.5) representing a trend wherein the percentage of high mannose glycans increases during differentiation. The distribution of fucosylated N-glycans analyzed from complex/hybrid glycans, however, was similar in each cell type (Fig. 3.6). The composition data obtained by MALDI-FTICR MS were supplemented with structural information using Tandem MS (Table 1). Further analysis of high mannose type glycans revealed that Man 8 and Man 9 were most abundant in all cell types, especially in NS (Fig. 3.7). In addition, assessment of the overall glycan profiles suggested that the appearance or absence of specific glycans could be possible biomarkers for a particular cell stage (Fig 3.8.)

A study by Wearne et al., using mannose-binding lectins, including GNA, reported

~200 million cells/sample → Membrane extraction

↓

Lyophilization

↓

Release of glycans

↓

Purification by solid phase extraction

↓

MALDI-FTICR MS

↓

Tandem-MS
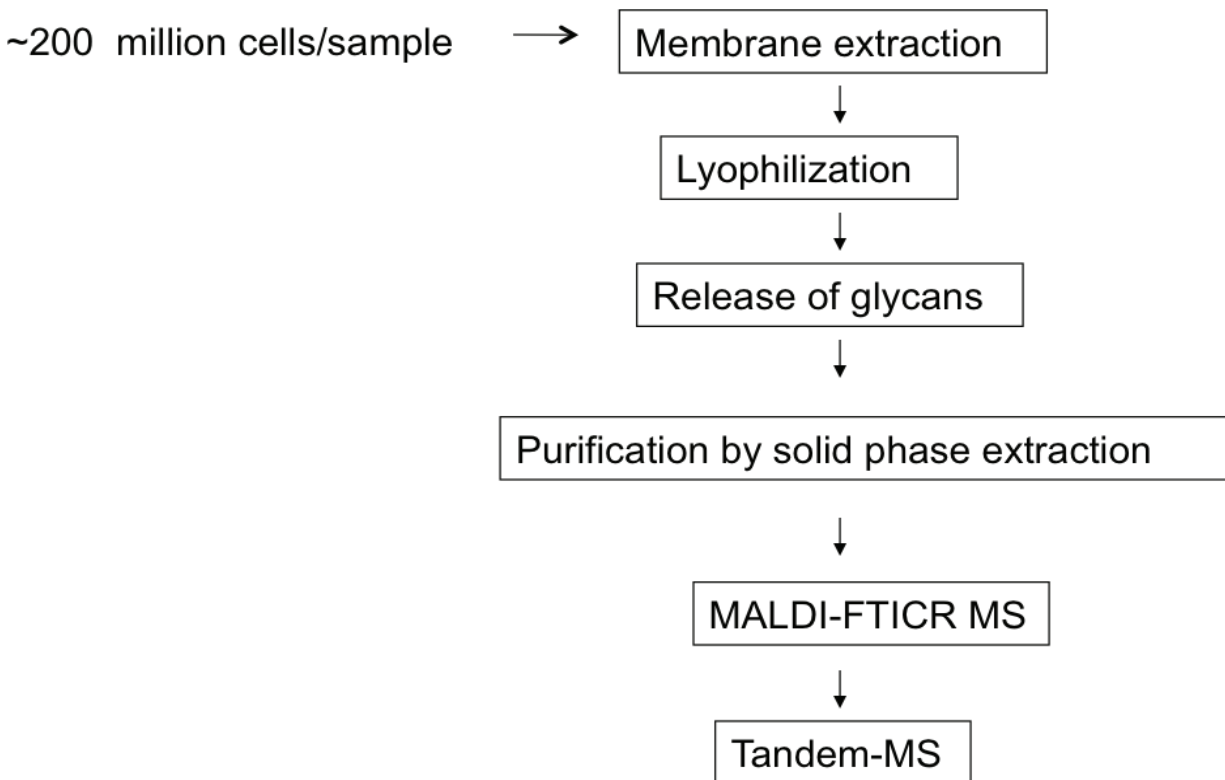
Figure 3.3. Experimental flowchart for the profiling and quantitation of N-glycans on membrane fractions. Approximately 200 million cells were used and divided for N and O-glycan analysis.
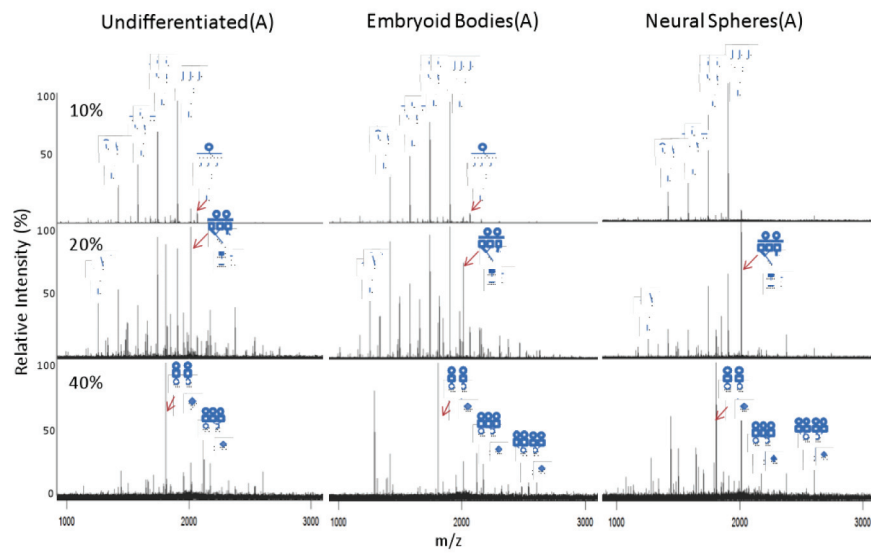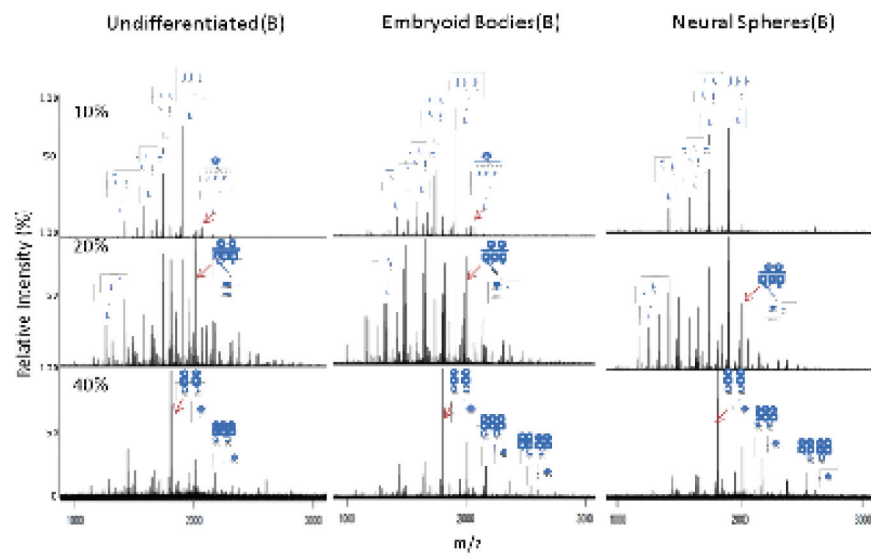
C.
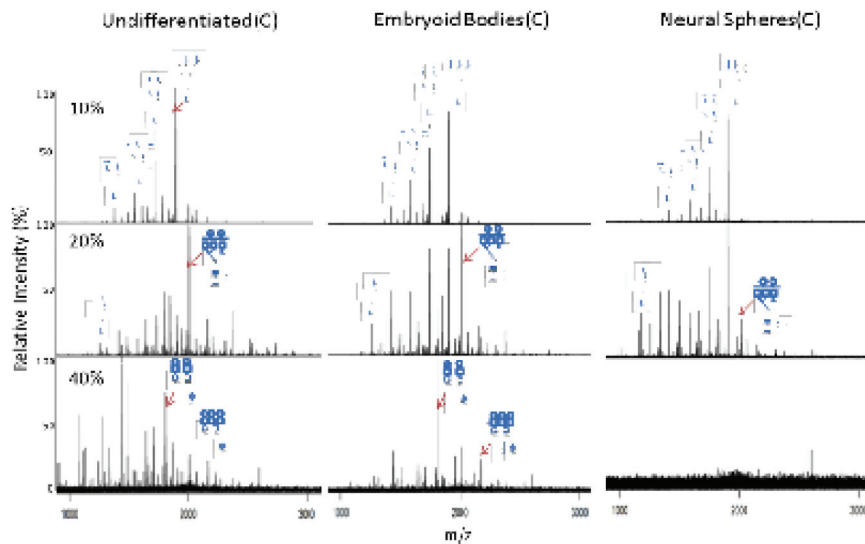
Figure 3.4. Representative MALDI-FTICR mass spectra of N-glycans found in bio-triplcates of all three cell types in the positive detection ion mode. (A) Each GCC fraction. 10% (top), 20% (middle), and 40% (bottom) represent glycans eluted from acetonitrile (AcN) fractions for the first sample of each group (A) (B) the second sample of each group (B) and (c) the third sample from each group (C). Structures are putative and are based on accurate masses and tandem mass spectrometry. Triplicate samples from each cell type produced similar mass spectra using FTICR MS.
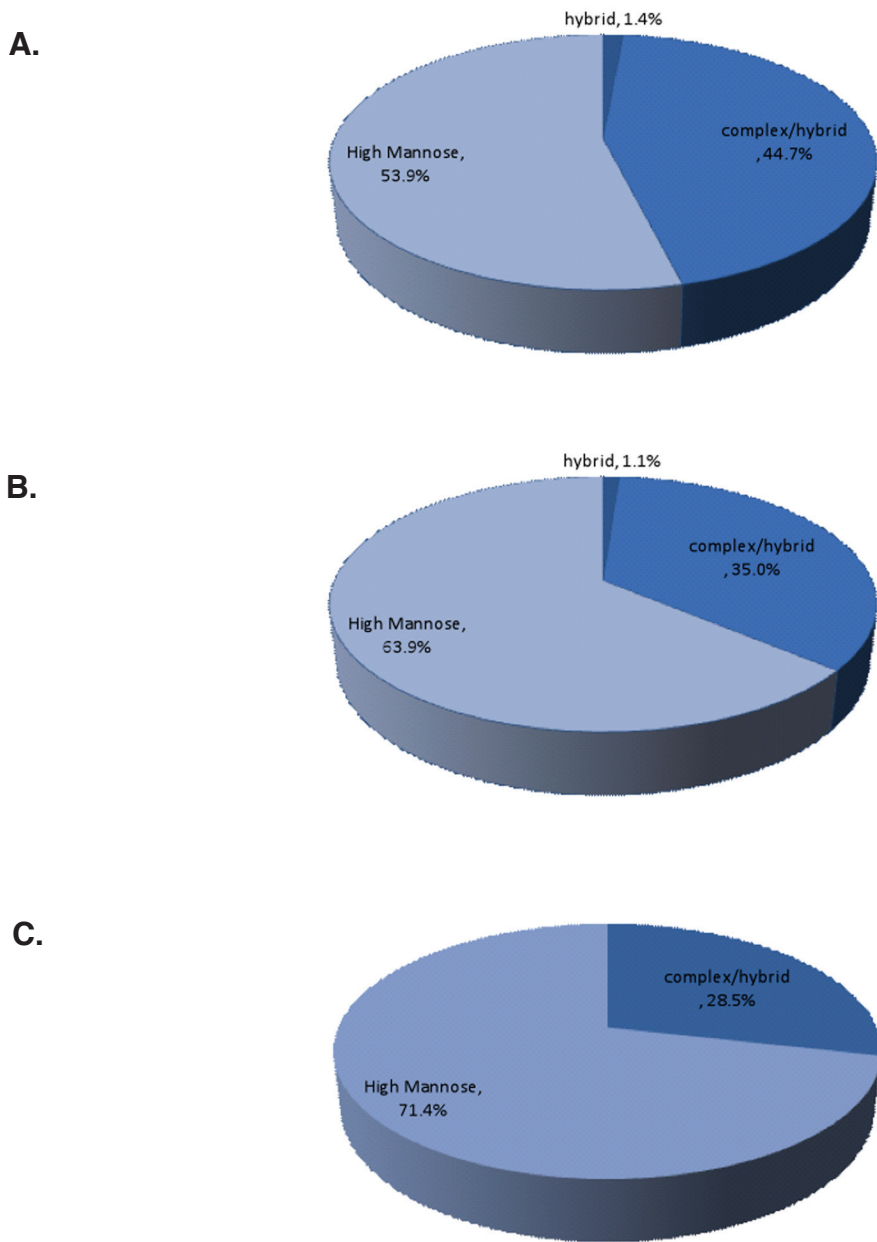
Figure 3.5. Quantitation of N-glycans analyzed from all cell types. All GCC fractions were combined prior to MS analysis and MS signals were normalized by total signal intensity. (A), (B), and (C) represent hESCs, EB, and NS, respectively. High mannose glycans are the most abundant for all cell stages. The percentage of high mannose glycans increases during differentiation, with NS having the highest percent.
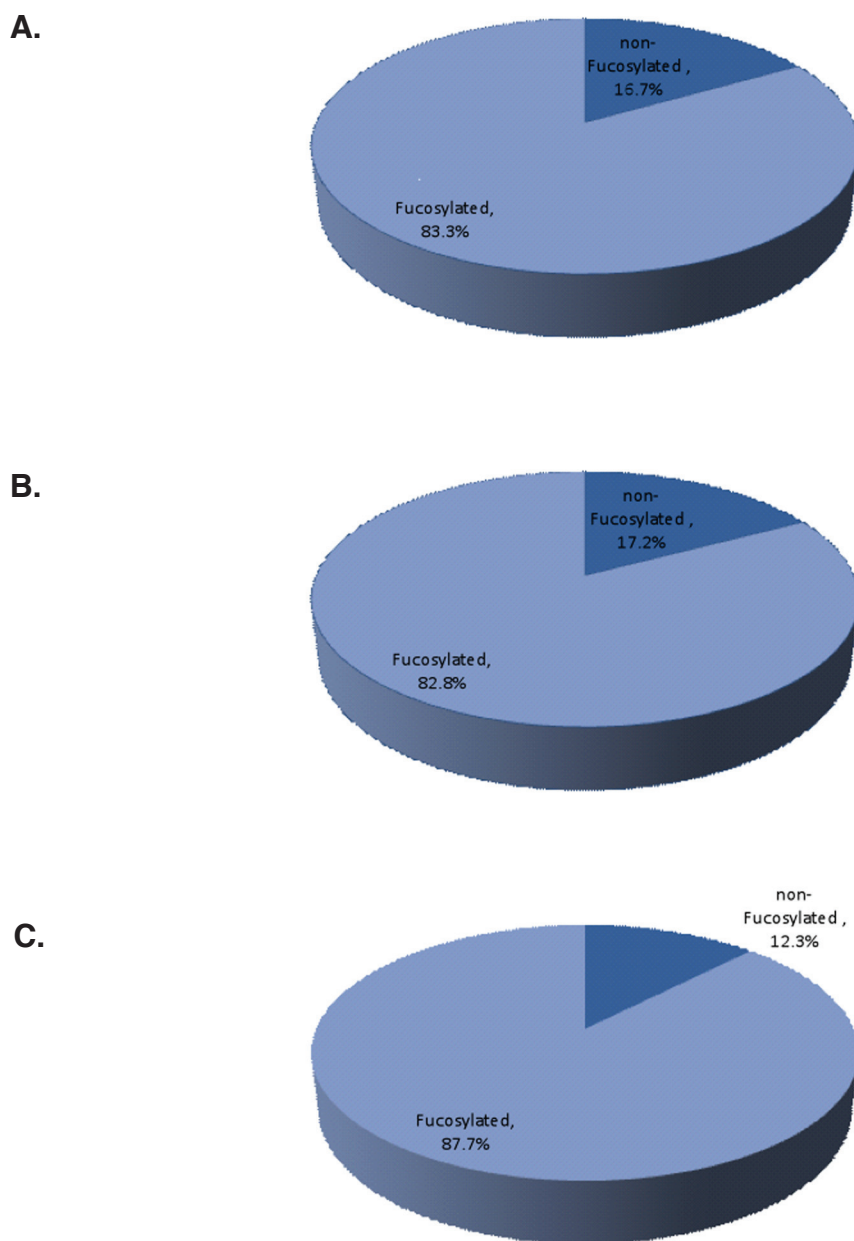
Figure 3.6. Distribution of non-fucosylated vs fucosylated glycans found in (A) hESCs, (B) EB, and (C) NS. Only hybrid and complex type glycans were considered and were found to be mostly fucosylated.
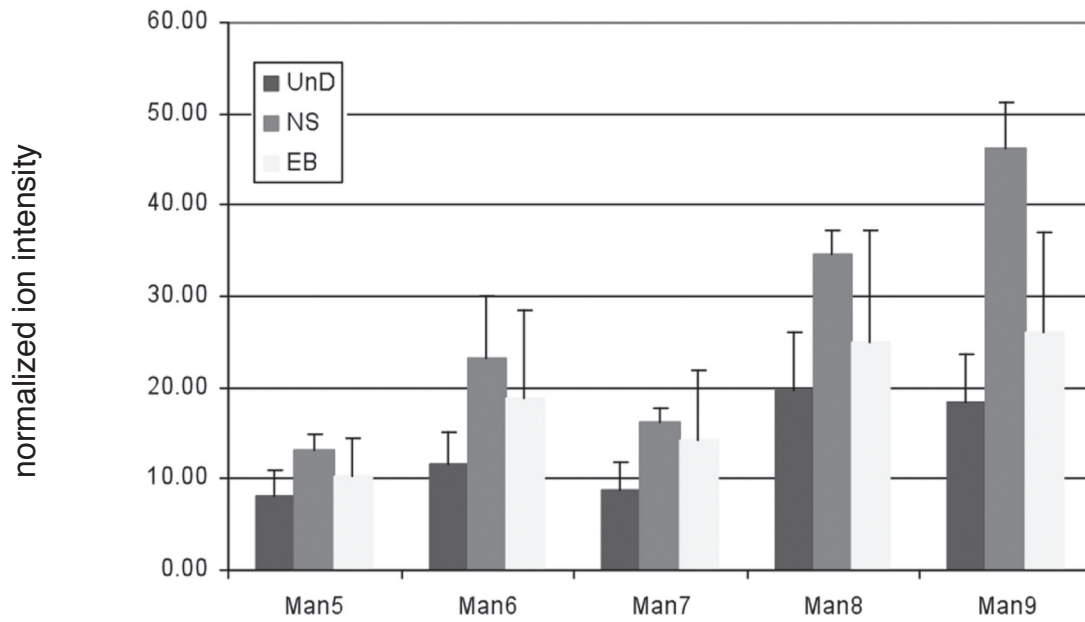
Figure 3.7. Quantification and comparison of specific high mannose glycans from hESCs (Un), EB and NS. The amount of specific mannosylated glycans changes during differentiation.
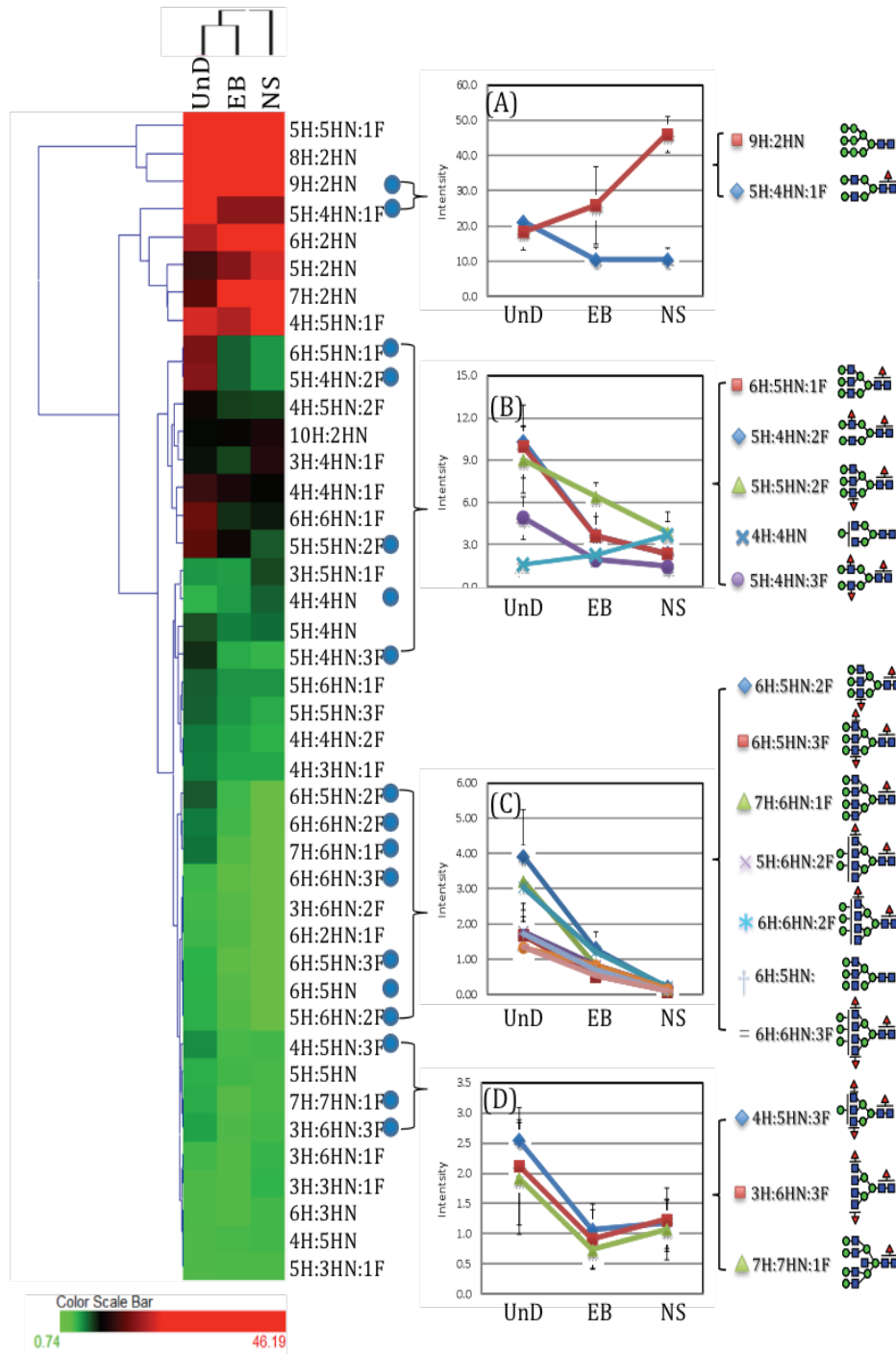
Figure 3.8. Heat map of the ion intensity distribution of glycans from the 20% fraction from each cell type. The ion intensity was averages from hESC (UnD), EB and NS. Several glycans exhibited ion intensity changes more than 2-fold (p<0.05) indicated by circle next to the composition. Figure (A), (B), and (D) represented the glycan with high, mid and low intensity but presented in all stages, respectively. Figure (C) represent the glycans disappeared in NS stage. The scale is on relative ion intensity scale, with red, representing the highest signal intensities.
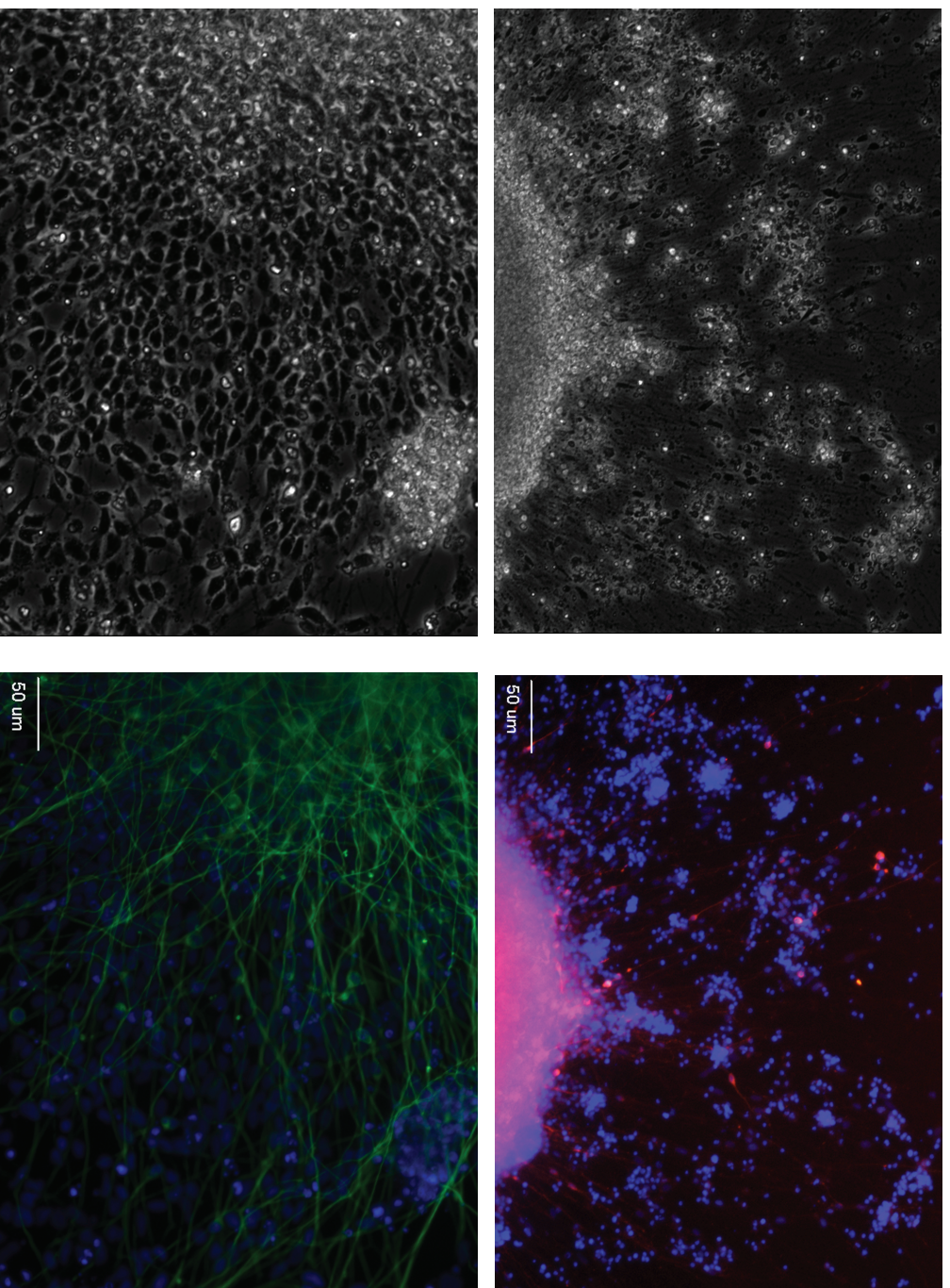
Figure 3.9. hESCs differentiated into dopaminergic neurons. Bright field (left) and fluorescent images (right) of dopaminergice neurons (A, at 20X) and neurons (B, at 4X) fixed and stained with nuclear stain dapi (blue) and antibodies against neuronal and dopaminergic marker β-tubulin III (green) and TH (red; ii), respectively. Cells were differentiated using a modified protocol from Cho et al. (19). Scale bar represents 50 um.

that hESC and hESC-derived 12-day old embryoid bodies expressed an abundance of high mannose glycans on the cell surface (1). Other studies using MS analysis found an abundance of high mannose glycans in hESCs (21), bone marrow-derived human mesenchymal stem cells (20), human hematopoientic stem and progenitor cells (22). These latter studies, however, were based on the analysis of whole cell lysates and limited cell surface analysis. In addition, N-glycan analyses of mammalian brains have revealed higher levels of high mannose glycans compared to other N-glycans and other tissue types (23,24). It will be interesting to evaluate the N-glycans from terminally differentiated hESC-derived neurons using our MS method. While existing neuronal differentiation protocols claim to efficiently generate large numbers of dopaminergic neurons (as described above in Sections 3.4.2), in our hands it has been difficult to obtain similar yields of DA neurons and therefore enough material for MS analysis. Future studies in our laboratory will instead proceed with profiling the overall neuronal population identified by the presence of ß-tubullin III (Fig. 3.9, iii), rather than just the sub-population of DA neurons. This will more easily provide larger numbers of neurons for MS analysis. Without analysis of a specific neuronal subtype, glycans conserved in all neurons will be detected.

3.4.3. Glyco-related gene expression

To evaluate the changes in glyco-related gene expression during differentiation of hESCs into EB and NS, cells from each group were collected for RNA isolation. By using microarray chips, differential gene expression could be assessed, possibly correlating associated enzymes required for glycan and glycoprotein synthesis with the glycans observed via MS. 1774 glyco-related genes were evaluated. Several genes were significantly up-regulated in hESCs compared to EBs, in EBs compared to NS, and in hESCs compared to NS (Fig. 3.10). Using the publically available DAVID software for gene ontology, glycans involved in glycan biosynthesis were evaluated. Alpha-mannosidase 1 (MANC1), an enzyme found in the endoplasmic reticulum, was differentially expressed in hESCs compared to NS and EBs compared to NS (Fig. 3.11, Fig. 3.12). NS had the highest expression, two-fold more than hESCs and EBs. This enzyme acts to cleave alpha-1,2 linkages on Man 9. There are 4 alpha-1,2 linked mannose residues present in Man 9 and exhaustive action of this enzyme would thus reduce Man 9 to Man 5. Man 5 can be further cleaved by other enzymes, ultimately trimming the glycan down to three mannoses, forming the conserved N-glycan pentacore (GlcNAc2Man3). Higher expression of alpha-mannosidase 1 suggests that NS should have higher Man 5 and less Man 9 than hESC and EB. However, NS had higher levels of Man 9 based on MS analysis and quantification.
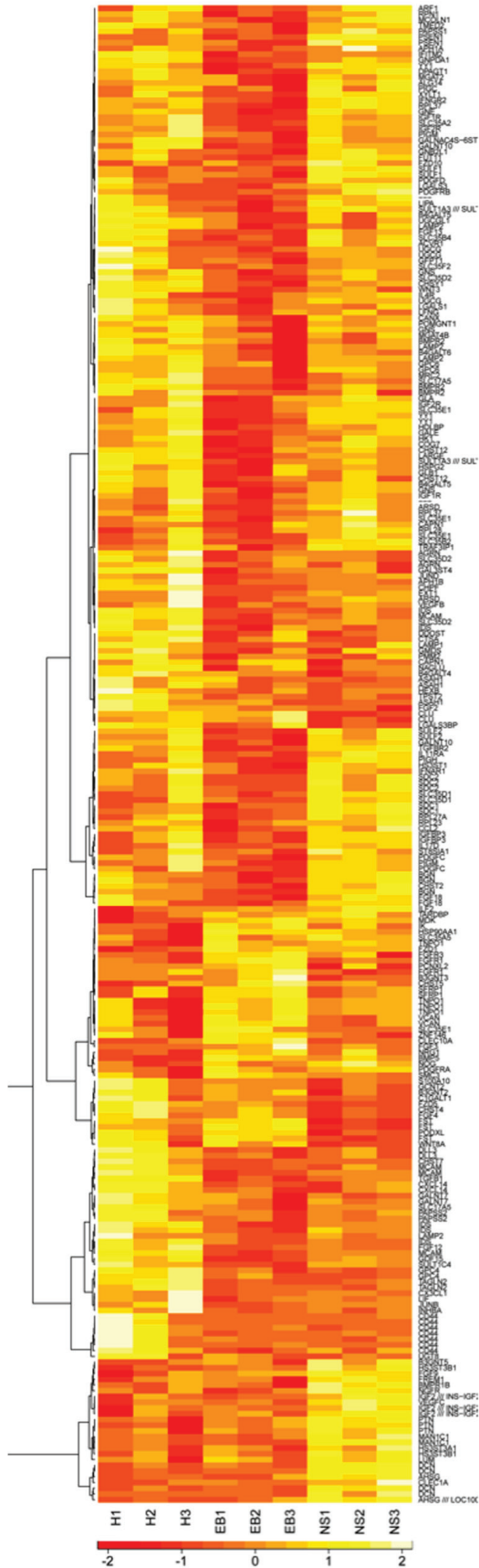
Figure 3.10. Heat map generated from the analysis of glyco-related genes (defined by the Consortium for functional glycomics) using Affymetrix human U133 microarrays. Triplicate RNA samples were collected and analyzed from hESC (H1, H2, H3), EB (EB1, EB2, EB3) and NS (NS1, NS2, NS3). Only genes with a signal intensity greater > 6 and values p<0.05 were used. The scale is based on a normal-ized relative signal intensity scale, with value 2 (yellow), representing the highest signal inten-sity.
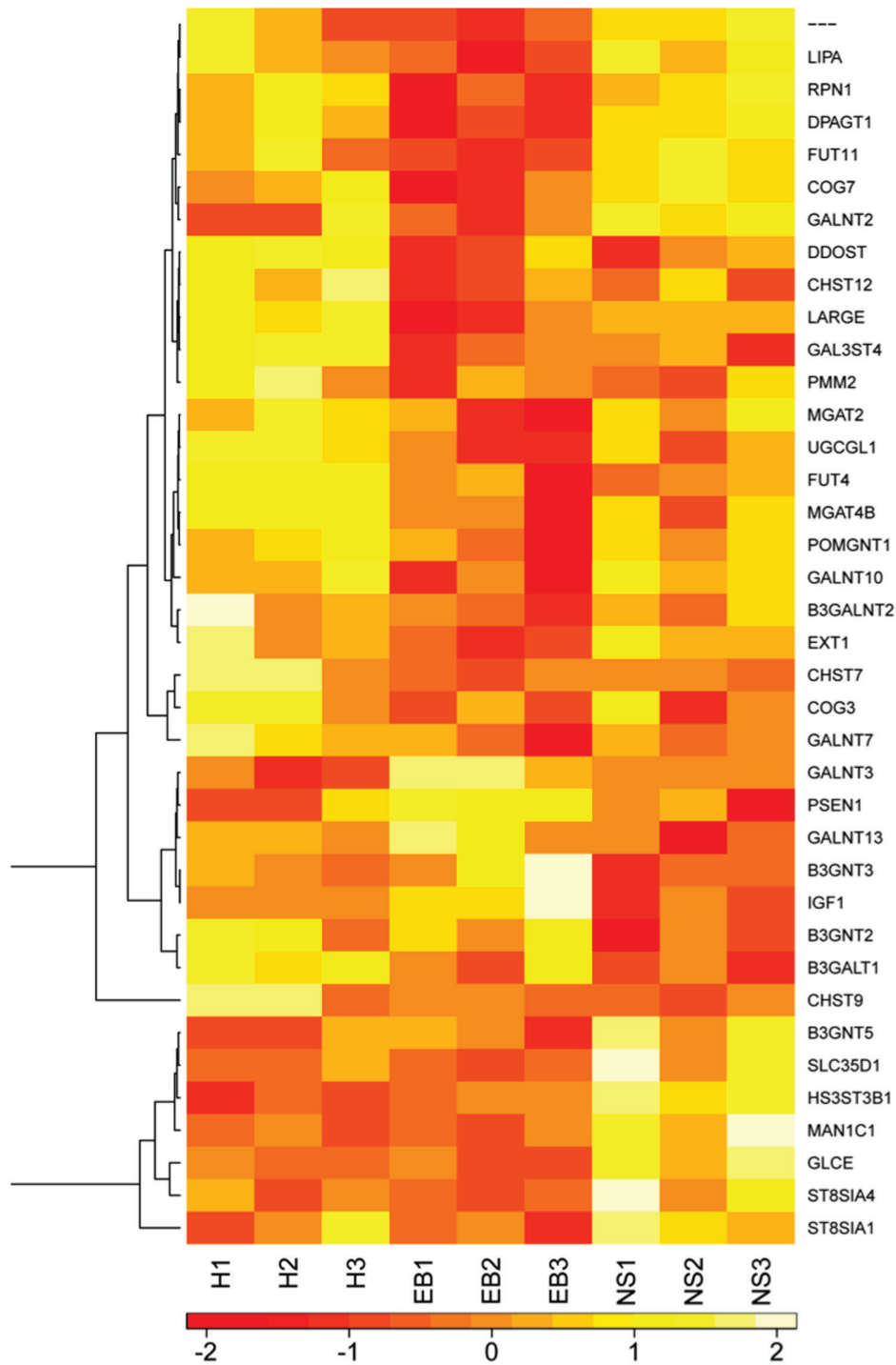
Figure 3.11. Heat map generated from the analysis of glyco-related genes specifically involved in the biosynthetic pathway of glycoconjugates using DAVID software. Only genes with a signal intensity greater > 6 and values p<0.05 were used. The scale is based on a normalized relative signal intensity scale, with value 2, representing the highest signal intensity. Triplicates from all three cell types were assessed (H1-3 = hESC; EB1-3 = embryoid bodies; NS1-3 = neural stem cells).

alpha-mannosidase	Fold change	p value
H to EB	-1.17	0.29
EB to NS	2.96	0.00004
H to NS	2.52	0.00013
mannose receptor		
H to EB	-1.93	0.11
EB to NS	1.29	0.25
H to NS	1.49	0.01

Figure 3.12. Differential expression of two genes MANC1 (alpha-mannosidase I) and MRC2 (mannose receptor 2). MANC1 is highly expressed in NS compared to hESCs and EBs. MRC2 is expressed in all cell types with no differential gene expression.

3.4.4. High mannose glycans

As previously discussed (Sections 1.3 and 2.3) high mannose glycans are usually thought of as "immature" N-glycans. Attached to nascent polypeptides, high mannose glycans undergo a series of trimming by specific glycosidases followed by elaboration by glycosyltransferases in the endoplasmic reticulum (ER) and in the Golgi apparatus to produce a variety of complex-type oligosaccharides with terminal sugars such as N-acetylglucosamine, galactose, sialic acid and fucose (25). This N-glycosylation process is specific to mammalian cells, where the majority of high mannose glycans are in the ER compartment, in the cytosol, not on the cell surface. Contrary to mammalian cells, bacteria, yeast and viruses have high mannose glycans on the cell surface. Cells in our immune system such as macrophages express mannose receptors that can bind to terminal/high mannose glycans on the surfaces of non-self entities (e.g. bacteria, yeast and viruses) to detect and initiate pathogen phagocytosis. Thus, the discovery that terminal mannose glycans are abundantly expressed on the cell surface of hESCs, and on the cellular membranes of EB and NS is particularly interesting.

3.4.5. Expression of terminal mannose on iPS and primary cells

To determine whether terminal mannose glycans are present on the surfaces of other cell types in contrast to accepted paradigms, iPS and primary human cells were labeled with GNA lectin and analyzed using flow cytometry analysis for GNA lectin binding (Fig. 3.13). T cell lymphoma cell line (Jurkats) and murine macrophage cell line (RAW), which are known to have minimal and high expression of high mannose glycans on the
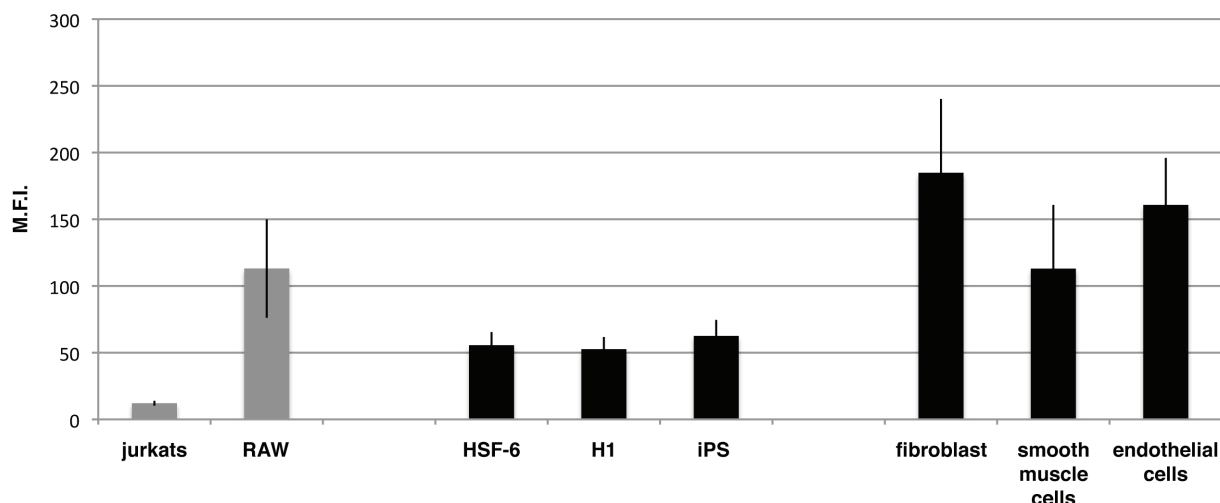
Figure 3.13. Flow cytometry analysis of different cell types using GNA lectin. Different cell types were stained with 20 ug/ml GNA lectin for the detection of terminal mannose residues, quantified by flow cytometry. At least triplicates for each cell type. The mean fluorescent intensity (M.F.I.) of the inhibitory values were subtracted from the M.F.I. experimental value, as shown.

cell surface, respectively, were used as negative and positive controls (26). iPS cells are reprogrammed somatic cells that are characteristically similar to hESCs (36). Both hESCs and iPS cells had similar levels of GNA binding, indicating terminal mannose glycan expression. Surprisingly, the primary human cells examined (lung fibroblast, aortic smooth muscle cells and aortic endothelial cells) had a higher amount of GNA staining than all cell types. MALDI-FTICR MS will be conducted to better characterize the types of high mannose glycans present on some of these primary cells, including those on iPS cells. The high level expression of terminal mannose glycans on these primary cells was surprising, especially given that primary breast cell membranes expressed lower levels of high mannose glycans compared to hESCs. Further studies will be undertaken to characterize the specific glycan structures and potential biological significance of high mannose glycans on the cell surface.

3.4.6. High mannose glycan function

Investigations of the role of high mannose glycans have been mostly directed to their involvement in protein folding in the ER. However, a few studies have suggested that high mannose glycans mediate cell-cell fusion (26,27), mediating sperm-egg fusion, myoblast fusion and osteoclast formation. In a study by Morishima et al. (26), terminal mannose residues and mannose receptors were found on the cell surfaces of osteoclast precursors and stromal cells/osteoblast precursors, two cell types involved in osteoclast differentiation. Osteoclasts are multi-nucleated, bone-resorbing cells that develop from hematopoietic cells of the monocyte/macrophage lineage through cellular fusion.

By blocking the binding of mannose receptors to high mannose glycans using pradimicin and yeast mannan, osteoclast differentiation was inhibited. Also, the addition of alpha-mannosidase inhibitor, 1-deoxymannojirimycin (DMJ), increased osteclast differentiation. Morishima et al. therefore, proposed the mechanism that high mannose glycans bind to mannose receptors, facilitating cellular adhesion and fusion and enabling osteoclast differentiation factors to bind (Fig. 3.14). By extention of these conclusions, we propose that the presence of high mannose glycans on hESCs, EB and NS may be involved in cell-cell adhesion. In addition, based on the microarray analysis, all cell types expressed the mannose receptor 1 (MRC2, Fig. 3.12).

Cell adhesion is essential in hESC viability as well as multicellular system formation, organogenesis, and morphogenesis. The presence of high mannose glycans on the cell surface of fibroblasts, smooth muscle and endothelial cells may also be involved in cellular adhesion, as these cell types are grown in culture as adherent cells. A study by Sriramarao et al. (28), using human umbilical vein endothelial cells (HUVEC) found that the forced expression of high mannose glycans using DMJ on endothelial cells resulted in a significant increase in the adhesion of activated neutrophils compared to untreated endothelial cells. The high mannose glycans were thought to interact with other adhesi-
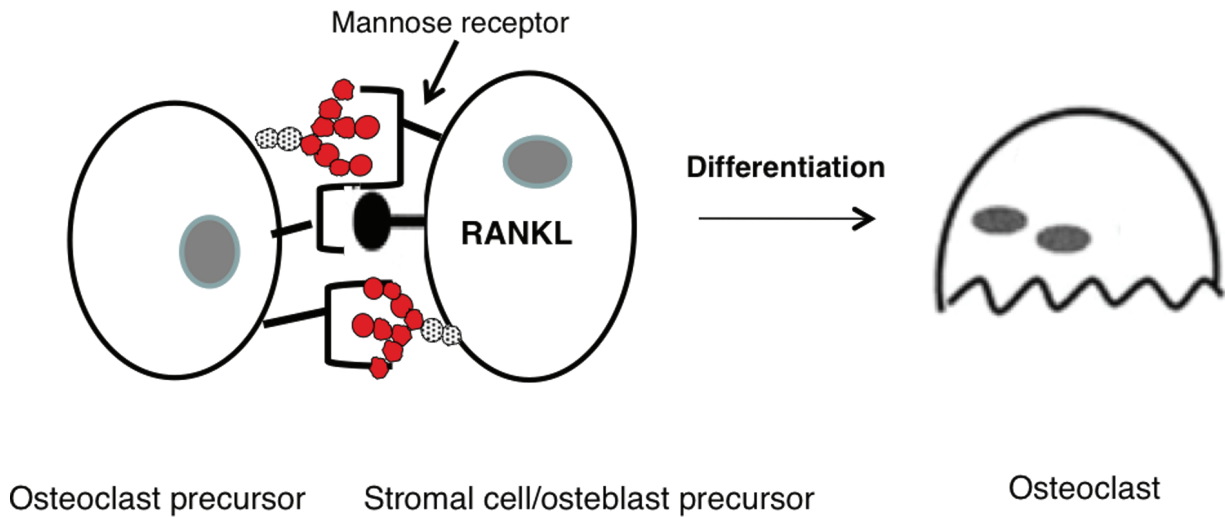
Figure 3.14. Model for high mannose glycan function. **H**igh mannose glycans are involved in cell-cell fusion and adhesion in osteoclast differentation. High mannose glycans interact with mannose receptors on osteoclast precursors and stromal cells/osteoblast cells, important for cellular fusion and adhesion, facilitating osteoclast differentiation (26).

molecules such as beta 2 integrins, since adherence was inhibited with monoclonal antibodies against integrin beta 2. Neutrophils are cells in the immune system that function as part of the acute inflammatory response in the body. They quickly mobilize to a site of infection and adhere to endothelial cells, which helps to illicit the arrival of other cells in the immune system.

74

3.4.7. Pradimicin

In a preliminary study, hESCs and EB were treated with various concentrations of a small molecule called, pradimicin A (courtesy of Drs. Yasuhiro Igarashi and Toshikazu Oki). Pradimicins (A, B and C) are antibiotics derived initially from bacteria Actinomadura hibisca in 1988 (29), consisting of 5,6-dihydrobenzo[a]naphthacenequinone structure, differing from one another by the substitutions of a D-amino acid and hexose sugar. Pradimicins are small molecules, approximately 838 Da in size compared to GNA lectin at 50,000 Da. Pradimicins specifically bind to terminal D-mannose glycans. Because of their high specificity, they are potent antifungal and antiviral agents, however they are generally non-toxic to cultured mammalian cells (30). I anticipated that pradicimin would bind to high mannose glycans on hESCs and EBs, which would result in a biological perturbation facilitated by the glycans, such as cell adhesion. Interestingly, the addition of pradimicin A at 50 and 100 ug/ml to hESCs and EBs, caused changes in cell morphology with the presence of floating hESCs and shriveled EBs (Fig. 3.15) suggesting cell death. hESCs are adherent cells that grow in colonies. With the addition of 50 and 100 ug/ml pradimicin, hESCs appeared disassociated from each other and the cell morphology of EBs were no longer in the form of tight spheres.

In addition, various concentrations of yeast mannan added to hESCs and EBs resulted in a similar phenotype (data not shown). A study by Oki et al., showed that the addition of pradimicin A to DMJ-treated human myeloid leukemia cells (U937), induced apoptosis, suggesting it was due to the specific interaction of pradimicin with mannose glycans on the cell surface (31). Quantitation of cell viability will be done to further assess this phenotype. The specificity of the action of both pradimicin and mannan on the cells will be addressed in future studies. The use of antibodies against the mannose receptors will also be used to evaluate their expression on the cell surface as well as inhibit the possible binding of high mannose glycans. Antibodies against E cadherin, an important adhesion molecule in hESCs (33-34), iPS (32) and NPs (35), will also be used as a control to test whether high mannose glycans are playing a role in cell adhesion.
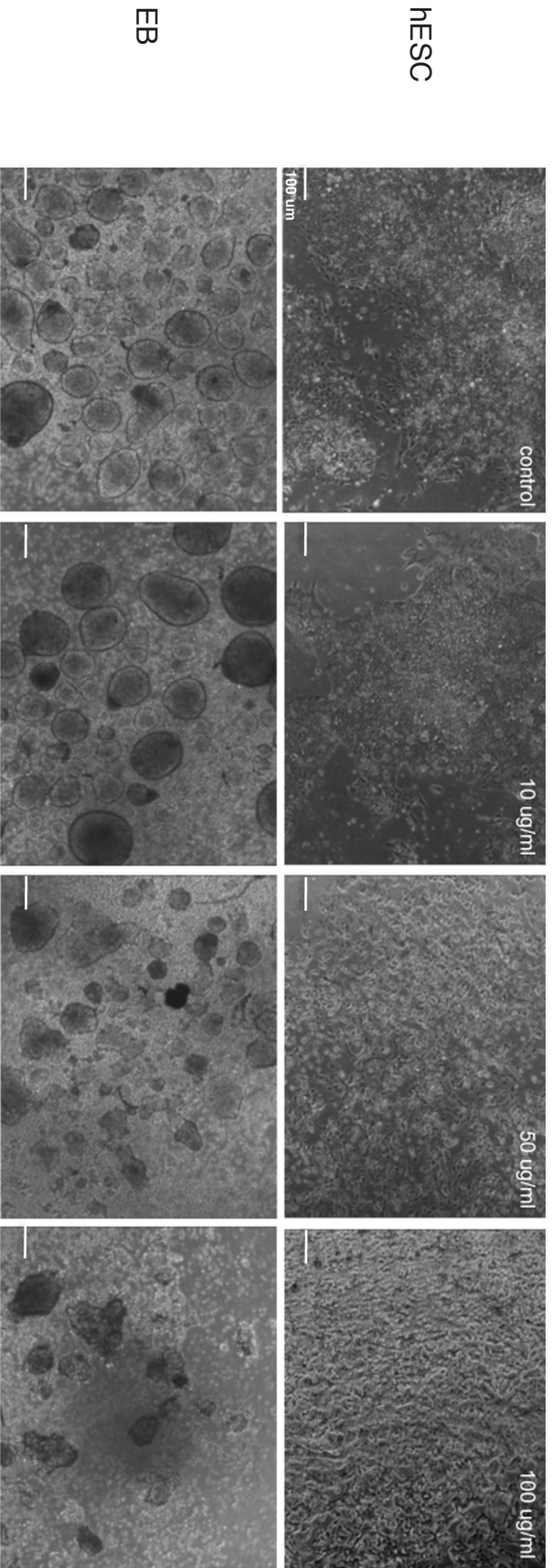
Figure 3.15. Effect of pradimicin on hESCs and EBs. Pradimicin was added the cells to determine whether it affected cell adhesion. Bright-field images of hESCs and EBs show changes in cell morphology at higher concentrations of 50 and 100 ug/ml compared to control and 10 ug/ml of pradimicin. Scale bar represents 100 um.

3.5. Discussion

In this study, hESCs were differentiated into EBs and NS in order to characterize the presence and changes in glycans during neural development. Cell membranes were evaluated with the focus of identifying glycans on the cell surface for potential biomarkers and functional significance. The N-glycans, however, were profiled and roughly quantified in each cell type based on MALDI-FTICR MS without further quantitation using nanoflow liquid chromatography (nanoLC). NanoLC is used to achieve isomer separation and thus obtain direct quantitative information. Because MALDI-FTICR MS does not provide information on the number of mass-redundant isomers associated with each mass peak and has the issue of ion suppression (only the most abundant ion species are detected), the quantitation is not as accurate as that obtained from nanoLC. This data is being currently obtained to determine the specific amounts of high mannose, complex/hybrid and hybrid glycans in all cell types. Interestingly, the current data reveals that all cell types have high levels of high mannose glycans.

Several glyco-related genes were differentially expressed between the three cell types. Further verification of the presence of proteins encoded by these genes using Western blot analysis will be important in determining their presence in the cell types. In addition to the up regulation of alpha-mannosidase in NS, there are other interesting genes to investigate. For example, genes ST8SIA1 and 4, involved in polysialic acid (PSA) synthesis, were highly expressed in NS compared to the other cell types (Fig. 3.11). This is consistent with the expression of the PSA glycan on neural cell adhesion molecule (NCAM), which is known to be a neural stem cell marker. PSA may have a role in hESC-neural differentiation.

Flow cytometry analysis with GNA lectin revealed that other cell types such as iPS and especially primary human cells have levels of high mannose glycans on the cell surface. It will be important to investigate whether this expression level is specific to adherent cells and cells that grow in colonies and cell aggregates, such as hESCs, EBs and NS. Further investigations with pradimicin A and mannose receptors may reveal that the presence of high mannose glycans on all these cell types is indicative of an essential biological function, such as cellular adhesion.

The observation that hESCs, EBs and NS grow in colonies of many cells, adhering to one another, suggests that cellular adhesion is biologically important. In fact, it has been shown that cell adhesion molecules such as E-cadherin are important in maintaining the colony morphology of ESCs, as well as cell proliferation and activates various signaling pathways (32). And in the reprogramming of iPS cells, E-cadherin-mediated cell-cell contact helps to increase reprogramming efficiency, presumably, important in sensing adhesion dependent signals from neighboring cells. E-cadherin is also expressed in the developing and adult brain as well as on NPs and has a role in regulating NP self-renewal (35). It would be interesting to determine whether high mannose glycans interact or act in concert with E-cadherins.

Table 2.1.

Fraction	Glycan type	Glycan composition	m/z theoretical	m/z measured	Δm (Da)	Count[a] UnD	Count[a] EB	Count[a] NS	Ratio UnD	Ratio EB	Ratio NS	AVE_NAI UnD	AVE_NAI EB	AVE_NAI NS
10%	high mannose	5H:2HN	1257.42	1257.429	0.007	2	3	2	1.00	0.87	1.21	1.23 ± 1.51	1.07 ± 0.81	1.49 ± 0.30
		6H:2HN	1419.48	1419.476	0.001	3	3	3	1.00	1.24	1.03	25.14 ± 13.08	31.08 ± 18.42	25.92 ± 6.74
		7H:2HN	1581.53	1581.529	0.001	3	3	3	1.00	1.10	1.01	41.04 ± 12.19	45.33 ± 14.11	41.29 ± 6.58
		8H:2HN	1743.58	1743.570	0.011	3	3	3	1.00	0.93	1.08	96.46 ± 13.27	89.63 ± 14.30	103.85 ± 17.41
		9H:2HN	1905.63	1905.623	0.011	3	3	3	1.00	0.97	1.18	119.92 ± 7.57	115.96 ± 8.67	140.93 ± 8.02
		10H:2HN	2067.69	2067.705	0.018	3	3	3	1.00	0.76	0.34	9.73 ± 0.98	7.43 ± 1.27	3.29 ± 1.15
		7H:2HN:1F	1727.59	1727.596	0.011	3	3	2	1.00	1.31	1.37	1.31 ± 0.46	1.72 ± 0.82	1.80 ± 0.46
		8H:2HN:1F	1889.64	1889.660	0.021	3	3	2	1.00	1.33	1.25	2.01 ± 1.48	2.66 ± 1.56	2.52 ± 0.67
	complex/hybrid	3H:4HN	1485.53	1485.548	0.015	3	3	0	1.00	1.10		0.42 ± 0.17	0.45 ± 0.04	
		4H:4HN	1501.53	1501.552	0.023	3	1	0	1.00	0.83		0.43 ± 0.15	0.36	
		3H:5HN	1542.55	1542.541	0.013	2	2	0	1.00	2.52		0.13 ± 0.00	0.32 ± 0.03	
		4H:5HN	1704.61	1704.623	0.016	3	3	3	1.00	0.80	1.57	1.89 ± 0.64	1.51 ± 0.45	2.96 ± 0.98
		5H:5HN	1866.66	1866.688	0.027	3	3	3	1.00	0.60	1.16	2.60 ± 1.07	1.57 ± 0.91	3.02 ± 1.25
		4H:3HN:1F	1589.54	1589.538	0.007	2	1	0	1.00	2.83		0.14 ± 0.02	0.38	
		4H:4HN:1F	1647.59	1647.606	0.020	3	3	1	1.00	0.84	1.05	1.01 ± 0.41	0.85 ± 0.39	1.07
		5H:3HN:1F	1751.60	1751.591	0.006	3	3	0	1.00	0.80		0.52 ± 0.13	0.42 ± 0.21	
		6H:3HN:1F	1768.61	1768.631	0.019	2	2	1	1.00	1.34	4.50	0.22 ± 0.11	0.29 ± 0.06	0.97
		5H:4HN:1F	1809.64	1809.665	0.026	3	2	1	1.00	0.88	3.64	0.51 ± 0.09	0.45 ± 0.05	1.87
		4H:5HN:1F	1850.67	1850.686	0.020	3	3	3	1.00	0.77	0.90	7.23 ± 3.38	5.57 ± 0.92	6.48 ± 2.01
		4H:5HN:2F	1996.72	1996.742	0.018	3	3	2	1.00	0.81	0.81	1.94 ± 1.04	1.57 ± 0.14	1.58 ± 0.14
		5H:5HN:1F	2012.72	2012.731	0.012	3	3	3	1.00	0.58	0.72	11.52 ± 0.72	6.71 ± 1.47	8.34 ± 4.19
		5H:5HN:2F	2158.78	2158.798	0.021	3	3	2	1.00	0.78	0.57	3.24 ± 1.73	2.53 ± 0.37	1.84 ± 0.16
	complex / hybrid	4H:4HN	1501.54	1501.506	0.034	3	3	3	1.00	1.40	2.26	1.61 ± 0.30	2.25 ± 0.98	3.65 ± 1.06
		5H:4HN	1663.59	1663.569	0.021	3	3	3	1.00	0.70	0.81	4.15 ± 1.28	2.89 ± 0.40	3.35 ± 0.82
		4H:5HN	1704.62	1704.597	0.023	3	2	3	1.00	1.26	1.45	0.85 ± 0.11	1.08 ± 0.54	1.24 ± 0.60
		5H:5HN	1866.67	1866.657	0.013	3	3	2	1.00	0.66	0.59	1.78 ± 0.52	1.17 ± 0.52	1.06 ± 0.53
		6H:5HN	2028.71	2028.727	-0.014	3	2	1	1.00	0.42	0.18	1.74 ± 0.22	0.73 ± 0.22	0.31
		4H:3HN:1F	1444.51	1444.509	0.001	3	3	3	1.00	0.66	0.66	3.00 ± 0.17	1.98 ± 0.36	1.99 ± 0.26
		4H:4HN:1F	1647.59	1647.587	0.003	3	3	3	1.00	0.85	0.74	8.01 ± 3.00	6.84 ± 3.38	5.92 ± 0.19
		4H:4HN:2F	1793.65	1793.647	0.003	3	3	3	1.00	0.69	0.55	3.06 ± 0.73	2.11 ± 0.65	1.67 ± 0.08
		5H:4HN:1F	1809.65	1809.635	0.015	3	3	3	1.00	0.49	0.50	21.21 ± 1.77	10.48 ± 3.67	10.54 ± 3.51

	Composition												
complex/hybrid-fucose	4H:5HN:1F	1850.67	1850.663	0.007	3	3	3	1.00	0.91	1.17	13.01 ± 5.10	11.80 ± 6.22	15.28 ± 5.70
	5H:4HN:2F	1955.70	1955.701	-0.001	3	3	3	1.00	0.36	0.23	10.34 ± 2.57	3.68 ± 1.32	2.38 ± 0.42
	4H:5HN:2F	1996.73	1996.724	0.006	3	3	3	1.00	0.69	0.67	6.51 ± 1.64	4.46 ± 1.72	4.38 ± 1.74
	5H:5HN:1F	2012.73	2012.710	0.020	3	3	3	1.00	0.86	1.10	32.05 ± 9.78	27.54 ± 13.28	35.13 ± 29.73
	5H:4HN:3F	2101.76	2101.765	-0.005	3	3	3	1.00	0.39	0.30	4.92 ± 2.52	1.93 ± 0.32	1.48 ± 0.30
	4H:5HN:3F	2142.79	2142.795	-0.005	3	3	3	1.00	0.42	0.46	2.55 ± 0.33	1.06 ± 0.43	1.17 ± 0.40
	5H:5HN:3F	2158.78	2158.778	0.002	3	3	3	1.00	0.71	0.43	9.03 ± 3.35	6.44 ± 3.02	3.91 ± 1.44
	6H:5HN:1F	2174.78	2174.774	0.006	3	3	3	1.00	0.37	0.24	9.97 ± 1.51	3.69 ± 1.85	2.41 ± 1.43
	5H:5HN:3F	2304.84	2304.836	0.004	3	3	3	1.00	0.66	0.52	3.67 ± 1.66	2.42 ± 1.04	1.92 ± 0.37
	6H:5HN:2F	2320.84	2320.832	0.008	3	3	1	1.00	0.33	0.16	3.92 ± 1.33	1.31 ± 0.17	0.64
	6H:5HN:3F	2466.90	2466.895	0.005	3	3	1	1.00	0.32	0.20	1.68 ± 0.55	0.54 ± 0.07	0.34
	7H:6HN:1F	2539.91	2539.904	0.006	3	3	1	1.00	0.26	0.15	3.22 ± 0.81	0.85 ± 0.26	0.47
	7H:6HN:2F	2685.97	2685.970	0.000	3	1	0	1.00	0.34	0.00	1.08 ± 0.21	0.37	
	8H:7HN:1F	2905.04	2905.056	-0.016	2	1	0	1.00	0.39	0.00	0.71 ± 0.13	0.28	
complex-fucose	3H:3HN:1F	1282.46	1282.456	0.004	3	3	3	1.00	0.78	1.62	0.97 ± 0.22	0.76 ± 0.14	1.57 ± 0.56
	3H:4HN:1F	1485.54	1485.533	0.007	3	3	3	1.00	0.79	1.29	5.57 ± 0.69	4.40 ± 1.25	7.20 ± 2.17
	3H:5HN:1F	1688.62	1688.613	0.007	3	3	3	1.00	0.92	1.77	2.41 ± 0.32	2.21 ± 0.69	4.27 ± 1.45
	3H:5HN:2F	1834.68	1834.676	0.004	2	2	1	1.00	0.78	0.75	0.88 ± 0.32	0.68 ± 0.31	0.66
	3H:6HN:1F	1891.70	1891.697	0.003	3	3	2	1.00	0.65	1.27	1.15 ± 0.16	0.75 ± 0.32	1.47 ± 0.04
	3H:6HN:2F	2037.76	2037.763	-0.003	3	2	1	1.00	0.61	0.51	1.18 ± 0.34	0.72 ± 0.12	0.60
	3H:6HN:3F	2183.82	2183.816	0.004	3	3	2	1.00	0.43	0.58	2.13 ± 0.97	0.92 ± 0.49	1.24 ± 0.52
	5H:6HN:1F	2215.81	2215.800	0.010	3	3	3	1.00	0.66	0.65	3.78 ± 1.75	2.49 ± 1.14	2.46 ± 1.47
	5H:6HN:2F	2361.86	2361.855	0.005	3	3	1	1.00	0.47	0.32	1.79 ± 0.31	0.83 ± 0.31	0.57
	6H:6HN:1F	2377.86	2377.844	0.016	3	3	3	1.00	0.52	0.58	9.38 ± 3.74	4.92 ± 2.41	5.46 ± 5.38
	6H:6HN:2F	2523.92	2523.910	0.010	3	3	1	1.00	0.40	0.24	3.05 ± 1.19	1.23 ± 0.57	0.72
	6H:7HN:1F	2580.94	2580.940	0.000	3	1	1	1.00	0.55	0.32	0.86 ± 0.40	0.47	0.28
	6H:6HN:3F	2669.97	2669.973	-0.003	3	2	1	1.00	0.39	0.25	1.36 ± 0.38	0.54 ± 0.12	0.34
	7H:7HN:1F	2742.99	2742.994	-0.004	3	3	3	1.00	0.38	0.56	1.93 ± 0.92	0.74 ± 0.31	1.07 ± 0.49
	7H:7HN:2F	2889.05	2889.058	-0.008	2	2	0	1.00	0.48	0.00	0.73 ± 0.43	0.35 ± 0.00	
hybrid	5H:3HN:1F	1606.57	1606.567	0.003	3	3	2	1.00	1.06	1.11	0.94 ± 0.14	1.00 ± 0.21	1.05 ± 0.28
	6H:3HN	1622.56	1622.563	-0.003	3	3	2	1.00	0.77	1.21	0.99 ± 0.26	0.76 ± 0.14	1.19 ± 0.51
	6H:2HN:1F	1565.54	1565.501	0.039	3	3	1	1.00	0.63	0.39	1.33 ± 1.14	0.84 ± 0.53	0.52
	7H:2HN:1F	1727.59	1727.582	0.004	1	1	3	1.00	1.72	2.72	0.51	0.87	1.38 ± 0.58
	8H:2HN:1F	1889.64	1889.645	-0.006	1	2	2	1.00	1.40	3.38	0.38	0.52 ± 0.28	1.27 ± 0.55

20%

	Composition	Theor. m/z	Meas. m/z	Error	UnD	EB	NS	UnD	EB	NS	Ave NAI (UnD)	Ave NAI (EB)	Ave NAI (NS)
high mannose	9H:2HN:1F	2051.70	2051.665	0.035	3	2	1	1.00	0.51	0.31	0.92 ± 0.56	0.47 ± 0.34	0.28
	5H:2HN	1257.42	1257.424		3	3	3	1.00	1.26	1.60	8.19 ± 2.85	10.28 ± 4.19	13.12 ± 1.71
	6H:2HN	1419.48	1419.476	0.004	3	3	3	1.00	1.60	1.98	11.70 ± 3.37	18.75 ± 9.64	23.11 ± 6.94
	7H:2HN	1581.54	1581.531	0.009	3	3	3	1.00	1.61	1.85	8.79 ± 2.98	14.18 ± 7.71	16.26 ± 1.56
	8H:2HN	1743.59	1743.575	0.015	3	3	3	1.00	1.26	1.75	19.71 ± 6.28	24.89 ± 12.44	34.56 ± 2.78
	9H:2HN	**1905.64**	**1905.629**	**0.011**	**3**	**3**	**3**	**1.00**	**1.41**	**2.50**	**18.48 ± 5.15**	**25.99 ± 10.94**	**46.19 ± 5.09**
	10H:2HN	2067.69	2067.696	-0.006	3	3	3	1.00	1.06	1.16	5.84 ± 1.53	6.21 ± 2.11	6.78 ± 2.82
40%	3H:4HN:1F	1485.54	1485.531	0.009	1	2	1	1.00	2.11	1.14	2.08	4.39 ± 0.28	2.37
	4H:3HN	1298.46	1298.451	0.009	2	2	2	1.00	0.87	0.69	5.80 ± 1.00	5.07 ± 2.39	3.99 ± 0.55
	4H:3HN:1F	1444.51	1444.506	0.004	3	2	3	1.00	1.10	0.88	11.97 ± 1.33	13.11 ± 2.11	10.56 ± 2.67
	4H:4HN	1501.54	1501.527	0.013	2	2	2	1.00	1.27	0.76	3.66 ± 1.26	4.63 ± 1.56	2.77 ± 0.15
	4H:4HN:1F	1647.59	1647.586	0.004	3	2	3	1.00	1.54	1.07	9.93 ± 0.94	15.34 ± 1.32	10.58 ± 4.08
	4H:4HN:2F	1793.65	1793.637	0.013	3	2	2	1.00	0.93	0.81	5.37 ± 1.88	4.99 ± 1.38	4.37 ± 0.81
	4H:5HN:1F	1850.67	1850.668	0.002	3	2	3	1.00	1.66	1.48	5.43 ± 2.21	9.04 ± 3.81	8.05 ± 0.52
	5H:4HN	1460.51	1460.503	0.007	3	2	2	1.00	1.00	0.70	4.90 ± 0.35	4.88 ± 1.47	3.44 ± 0.38
	5H:3HN:1F	1606.57	1606.562	0.008	2	1	2	1.00	1.34	0.79	3.05 ± 1.45	4.08	2.40 ± 0.66
	5H:4HN	1663.59	1663.583	0.007	3	2	3	1.00	1.19	1.09	10.53 ± 3.26	12.56 ± 1.21	11.48 ± 6.51
	5H:4HN:1F	1809.65	1809.634	0.016	3	2	3	1.00	1.19	1.21	54.60 ± 24.79	64.80 ± 22.53	65.92 ± 2.11
	5H:4HN:2F	1955.70	1955.699	0.001	3	2	3	1.00	1.08	1.20	10.47 ± 4.89	11.31 ± 6.43	12.62 ± 3.93
	5H:5HN	1866.67	1866.658	0.012	2	2	2	1.00	1.68	0.89	3.26 ± 1.35	5.47 ± 0.64	2.91 ± 0.35
	5H:5HN:1F	2012.73	2012.722	0.008	3	2	3	1.00	1.98	1.45	16.06 ± 5.26	31.77 ± 0.91	23.24 ± 5.85
	5H:5HN:2F	2158.78	2158.782	-0.002	2	2	3	1.00	1.48	1.41	3.82 ± 1.76	5.64 ± 2.90	5.37 ± 0.39
	5H:6HN:1F	2215.81	2215.803	0.007	0	1	1		1.00	0.58		3.22	1.88
	6H:5HN	2028.72	2028.724	-0.004	1	1	2	1.00	0.89	0.71	4.97	4.40	3.55 ± 0.91
	6H:5HN:1F	2174.78	2174.771	0.009	3	2	3	1.00	1.22	1.46	14.43 ± 4.44	17.57 ± 11.40	21.09 ± 7.16
	6H:5HN:2F	2320.84	2320.832	0.008	2	1	3	1.00	0.73	0.82	5.51 ± 1.09	4.00	4.53 ± 0.79
	6H:6HN:1F	2377.86	2377.844	0.016	3	2	3	1.00	2.14	1.36	4.66 ± 1.42	9.97 ± 1.11	6.35 ± 1.60
	7H:6HN	2393.85	2393.836	0.014	0	1	0		1.00			3.10	
	7H:6HN:1F	2539.91	2539.894	0.016	3	1	3	1.00	2.19	1.53	4.56 ± 2.28	10.01	6.99 ± 2.50
	9H:2HN	1905.64	1905.637	0.003	0	2	0		1.00			3.56 ± 0.31	

Table 1. N-glycans found in hESC (UnD), EB and NS membrane fractions by MALDI-FT ICR MS. Highlighted rows represent the glycans found to be potential markers shown in Fig. 3.8. Glycan composition: each capital letter (H, HN, F, NA) represents hexose(Hex), N-acetyl hexosamine (HexNAc), fucose(Fuc), and N-acetyl neuraminic acid (NeuAc) respectively. Count represents the detected number from each glycan in bio-triplicates in MS analysis. The range of count is from one (1/3) to three (3/3). Ave NAI represents the normalized absolute peak intensity.

3.6 Methods

3.6.1. Neural differentiation

hESC lines HSF-6's and H1's were differentiated into neural progenitors (or neural spheres) that have the capacity to become neurons and glia. The differentiation protocol is based on a modified version of the method reported by Zhang et al. (10). The process of differentiation entails culturing undifferentiated hESCs in growth media without growth factors to form embryoid bodies. To initiate neural induction, embryoid bodies were then cultured in neural induction media comprising DMEM/F12 media with N2 supplement and FGF-2. These additives caused cells to adhere and differentiate into neuroectodermal cells (rosettes). The rosettes formed neural spheres when maintained in suspension culture in neural induction media. The phenotypes of the neural spheres were confirmed by observation of the neural stem cell markers nestin, sox-2 and PSA-NCAM, via immunohistochemistry (Fig. 3.2), their ability to propagate in culture (> 2 months) and to differentiate into neurons (Fig. 3.9) and glia (data not shown). Three biological samples were collected from each cell type: n=1 from each group is derived from respective hESCs differentiated into EB into NS.

3.6.2. Neuronal differentiation

hESCs were differentiated into dopaminergic neurons using a modified Cho et al. protocol (19) (Fig. 3.9). Neural stem cells/neural spheres were maintained on poly-ornithine/laminin coated plates in neural induction media for 14 days consisting of DMEM/F12 media supplemented with N2, 1mM L-glutamine, 1 uM cAMP, 0.1 mM b-ME, 2 ug/mL heparin, 200 uM Ascorbic Acid, 0.1 mM NEAA, 10 ng/mL GDNF, 100 ng/mL FGF-8 and 200 ng/mL Shh.

3.6.3. Cell membrane extraction

Membrane extraction was performed using ultracentrifugation. Pellets were thawed on ice with the addition of a homogenization buffer (HB) consisting of 0.25 M sucrose, 20 mM Hepes-KOH, pH 7.4 and protease inhibitor mixture (1:100, Calbiochem/EMD Chemicals, Gibbstown, NJ). Cells were sonicated on ice, and cell lysates were centrifuged at 1,000g for 10 min to remove the nuclear fraction and debris. The supernatant was collected and additional HB was added for ultracentrifugation at 200,000g for 45 min at 4°C to remove the cytoplasmic fraction. The pellets were resuspended in 0.2 M Na2CO3 (pH 11) to break up the microsomes. The samples were spun twice more at 200,000g for 45 min to wash the samples of the cytoplasmic fraction. The supernatant was removed and the membrane fractions were frozen at -20 °C.

3.6.4 Glycan release

The membrane fractions were washed twice with nanopure water and then divided into two fractions for N- and O-glycan analysis, respectively. For analysis of N-glycans,

100 µL of 100 mM ammonium bicarbonate (NH4HCO3), 5 mM dithiothreitol (DTT, from Promega) was added to the samples and heated to 100oC for 2 min to denature the protein. After cooling at room temperature, 2 µL of Peptide N-glycosidase F (PNGase F, from New England Biolabs) was added to the mixture (pH 7.5) and incubated at 37oC for 24 hours in a water bath. 800 µL of chilled ethanol was added, and the mixture was frozen at -80°C for 1 hour and then centrifuged to separate the proteins in the pellet from with the glycans in the supernatant. The supernatant was completely dried down to remove the ethanol prior to solid phase extraction (SPE) using a graphitized carbon cartridge (GCC, from Alltech).

3.6.5. Glycan enrichment

Released N- and O-glycans were purified and enriched by SPE-GCC. Prior to use, graphitized carbon cartridge (150 mg bed weight, 4 mL cartridge volume) was washed with nanopure water followed by 80% acetonitrile (AcN) in 0.05% (v/v) trifluoroacetic acid (TFA) (v/v) and again with nanopure water. Glycan solutions were applied to the GCC cartridge and subsequently washed with several cartridge volumes of nanopure water at a flow rate of 1 mL/min to remove salts. Glycans were eluted stepwise with 10% AcN in H2O (v/v), 20% AcN in H2O (v/v), and 40% AcN in 0.05% TFA in H2O (v/v). Each fraction was collected and concentrated in vacuo prior to mass spectrometry analysis. Fractions were reconstituted in nanopure water prior to MS analysis.

3.6.6. Mass spectrometric analysis

Mass spectra were recorded on a Fourier transform-ion cyclotron resonance mass spectrometer (FTICR MS) with an external source HiResMALDI (IonSpec Corporation, Irvine, CA) equipped with a 7.0 Tesla magnet. The HiResMALDI was equipped with a pulsed Nd:YAG laser (355 nm). 2,5-Dihydroxy-benzoic acid (DHB) was used as a matrix (5 mg/100 mL in 50% AcN:H2O) for both positive and negative modes. A saturated solution of NaCl in 50% AcN in H2O was used as a cation dopant to increase signal sensitivity. The glycan solution (0.7 µL) was applied to the MALDI probe followed by matrix solution (0.7 µL). For the negative ion spectra, DHB matrix was only used without using any dopant. The sample was dried under vacuum prior to mass spectrometric analysis.

3.6.7. Structural determination using infrared multiphoton dissociation (IRMPD)

Tandem mass spectrometry, specifically IRMPD, was used to determine the general structures of several oligosaccharides. This allowed for complete fragmentation of the ion of interest. A desired ion was readily selected in the analyzer with the use of an arbitrary-wave form generator and a frequency synthesizer. A continuous wave Parallax CO2 laser (Waltham, MA) with 20 W maximum power and 10.6 µm wavelength was installed at the rear of the magnet and was used to provide the photons for IRMPD. The laser beam diameter is 6 mm as specified by the manufacturer. The laser beam was expanded to 12 mm by means of a 2× beam expander (Synrad, Mukilteo, WA) to ensure complete irradiation of the ion cloud through the course of the experiment. The laser was aligned

and directed to the center of the ICR cell through a BaF2 window (Bicron Corporation, Newbury, OH). Photon irradiation time was optimized to produce the greatest number and abundance of fragment ions. The laser was operated at an output of approximately 13 W.

3.6.8. Microarray analysis

Total RNA was isolated from all cell types using Trizol and RNA isolation kit (Qiagen). RNA quality was assessed using the Agilent 2100 Bioanalyzer. Subsequent steps included Oligo-dT based affinity purification of mRNA to selectively enrich poly (A)+ RNA, reverse transcription using Superscript III (SSIII, Invitrogen) and labeling of Cy3 and Cy5 dyes using Ambion labeling kit. Processing of the Affymetrix (Santa Clara, CA) HG-U133 A&B Human genome GeneChip® for each sample (n=3/ cell type) and microarray data extraction, and quality control (using RMA and Mas 5.0) and statistical analyses (using R package) were conducted by the Functional glycomics lab at University of California, Berkeley. A change in gene expression was considered to be significant if $p<0.05$ relative to the expression level in the hESC group with fold change ≥ 2, and present calls $\geq 80\%$ as defined by MAS 5.0.

Based on the database provided by the Consortium for functional glycomics, there are approximately 1774 glyco-gene probes representing 833 unique glyco-related genes on their glyco-gene chips similar to the ones on Affymetrix HG-U133 A&B Human genome GeneChips.

The 1774 genes were filtered so that only IDs where at least one of the p values was < 0.05 were included with M value >1, leaving approximately 305 genes. The heatmaps were generated by filtering genes with signal intensity >6 and $p<0.05$. The signal intensities were normalized ranging from -2 to 2 values.

3.6.9. Immunofluorescence

Neural spheres were fixed with 4% paraformaldehyde for overnight at 4°C. Paraformaldehye was removed and 30% sucrose v/w was added and left overnight at 4°C. Neural spheres were embedded in OCT freezing medium and frozen and sectioned into 40 micron sections onto glass slides using a cryostat. Slides were rinsed in PBS and blocked with 2% BSA in PBS for 30 minutes at room temperature. Primary antibodies nestin (1:50 ,Invitrogen), sox-2 (1:50, Millipore) and PSA-NCAM (1:50, BD Bioscience) were in 2% BSA in PBS + 0.3% Triton solution and added to individual slides and left overnight at 4°C. Slides were rinsed with PBS and secondary antibodies were added (1:200 dilution, Invitrogen) and incubated for 2h at room temperature. Slides were rinsed with PBS, and Dapi (Sigma) was added and left to dry.

Neurons were fixed with 4% paraformaldehyde for 15 minutes and rinsed 3 times in PBS for 5 minutes. Cells were blocked with staining buffer (2% fetal bovine serum + 0.3% Triton in PBS) for 15 minutes and then stained with antibodies against neuronal and dopaminergic marker ß-tubullin III (1: 1000, Millipore) and TH (1:250, Millipore), respectively, overnight at 4°C. The wells were rinsed three times in PBS. Alexa Fluor 488 conjugated-goat-anti-mouse secondary antibody for ß-tubullin III (1:400, Invitrogen) and Alexa Fluor 594-conjugated goat-anti-rabbit secondary antibody to TH (1:400, Invitrogen)

were incubated in the wells for 2 h at room temperature. Wells were rinsed three times in PBS and Dapi (Sigma) was added for 5 minutes before analysis using an Olympus IX71 fluorescent microscope. Control wells were stained with mouse IgG and rabbit IgG iso-type (Invitrogen, data not shown).

3.6.10. Flow cytometry

hESCs (HSF-6 and H1), induced pluripotent stem cell (iPS), Jurkats (human T cell lymphoma, ATCC) RAW (murine RAW 264.7 macrophages, ATCC) and primary hu-man lung fibroblasts (IMR-90, ATCC), smooth muscle cells (aorta smooth muscle cells, Lonza) and aorta endothelial cells (HAEC, courtesy of Dr. Andrew Wursmer) were col-lected for analysis. hESCs and iPS cells were collected after incubation with collagenase IV (200 units/mL, Invitrogen) and mechanically removed. Colonies were dissociated into single cell suspensions in 0.5mM EDTA, and were then filtered through a 40 micron cell strainer before they were counted. Jurkats and RAW cells were cultured in RPMI media (Invitrogen) supplemented with 10% FBS and 0.5% penicillin and streptomycin (Invitro-gen). Fibroblast, smooth muscle cells and endothelial cells were grown in DMEM media (Invitrogen) supplement with 10% FBS and 0.5% penicillin and streptomycin (Invitrogen) and smooth muscle (SmGM-2-smooth muscle a, Lonza) and endothelial growth media (EGM-2MV-microvascular endothelial cell Medium, Lonza), respectively (Lonza). All cells were blocked with staining buffer (2% fetal bovine serum in PBS) for 15 minutes and then hESCs and iPS cells were stained with pluripotent marker SSEA-4 (1:200/500,000 cells, Milllpore) for 30 minutes on ice. Next, cells were washed, and hESCs and iPS cells were stained with APC-conjugated goat-anti- mouse secondary antibody to SSEA-4 (1:400, Jackson ImmunoResearch Labs) and the addition of 20 ug/ml of Galanthus nivalis (GNA) conjugated to FITC (EY Labs). All other cells (250,00 to 500,000) were stained only with 20 ug/ml of Galanthus nivalis (GNA) conjugated to FITC (EY Labs). To validate binding specificity, cells were also stained with lectins pre-incubated for at least 15 minutes with 10 mg/ml inhibitory sugar, yeast mannan (Sigma). After 30 minutes on ice, cells were washed and resuspended in staining buffer with propidium iodide to distinguish dead cells from live cells. Flow cytometry (BD FACs Calibur from BD Biosciences) was performed and data was analyzed using FlowJo software (TreeStar Inc). At least three indepen-dent assays were carried out. Only hESCs and iPS cells double-labeled with SSEA-4 and FITC-conjugated GNA were quantified. Additional controls were unstained cells from each cell type and hESCs were stained with isotype control mouse IgG3 isotype (Invit-rogen). The final quantitation was derived from the subtraction of the mean fluorescence intensity (M.F.I.) of the inhibitory controls for each cell type from the M.F.I. obtained from the GNA-labeled cells.

3.7. References

1. Wearne, K. A., Winter, H.C., O'Shea, K., Goldstein, I.J. Temporal changes in the carbohydrates expressed on BG01 human embryonic stem cells during differentiation a embryoid bodies. Glycoconj J, 2006, 25,(2), 121-36.

2. Varki, A., Cummings, R.D., Esko, J.D., Freeze, H.H., Stanley, P., Bertozzo, C.R., Hart, G.W., Etzler, M.E. Essentials of Glycobiology: Cold Spring Harbor Laboratory Press. 2009

3. Yanagisawa, M. et al. Characterization of glycoconjugate antigens in mouse embryonic neural precursor cells. J of Neurochem, 2005, 95, 1311-1320.

4. Yamaguchi, Y. Glycobiology of the synapse: the role of glycans in the formation, maturation and modulation of synapses. Biochim et Biophys Acta, 2002, 1573, 369-376.

5. Best, T., Kemps, E., Bryan, J. Effects of saccharides on brain function and cognitive performance. Nutrition Rev, 2005, 63, 409-418.

6. Li, M., Pevny,L., Lovell-Badge, L., Smith, A. Generation of purified neural precursors from embryonic stem cells by lineage selection. Curr Biol, 1998, 8, 971-4.

7. Zhang, X., Cai,J., Klueber, K. M. , Guo, Z., Lu, C., Winstead, W.I., Qiu, M., Roisen, F.J. Role of transcription factors in motoneuron differentiation of adult human olfactory neuroepithelial-derived progenitors. Stem Cells, 2006, 24, 434-42.

8. Benzing, C., Segschneider,M., Leinhaas, A., Itskovitz-Eldor, J., Brustle O. Neural conversion of human embryonic stem cell colonies in the presence of fibroblast growth factor-2. Neuroreport 2006, 17, 1675-81.

9. Ueno, M., Matsumura, M., Watanabe, K., Nakamura, T., Osakada, F., Takahashi, M., Kawasaki, H., Kinoshita, S., Sasai, Y. Neural conversion of ES cells by an inductive activity on human amniotic membrane matrix. Proc Natl Acad Sci, 2006, 103, 9554-9.

10. Zhang, S. C., Wernig,M., Duncan, I.D., Brustle, O., Thomson, J.A. In vitro differentiation of transplantable neural precursors from human embryonic stem cells. Nat Biotechnol, 2001, 19, 1129-33.

11. Reubinoff, B. E., Itsykson,P., Turetsky, T., Pera,M.F., Reinhartz,E., Itzik, A., Ben Hur, T. Neural progenitors from human embryonic stem cells. Nat Biotechnol, 2001,19, 1134-40.

12. Palmer, T. D., Markakis, E.A., Willhoite, A.R., Safar, F., Gage, F.G. Fibroblast growth factor-2 activates a latent neurogenic program in neural stem cells from diverse regions of the adult CNS. J Neurosci, 1999, 19, 8487-97.

13. Roussa, E., Krieglstein, K. Induction and specification of midbrain dopaminergic cells: focus on SHH, FGF8, and TGFbeta. Cell Tissue Res, 2004, 318, 23-33.

14. Ye, W., Shimamura, K., Rubenstein, J.L., Hynes, M.A., Rosenthal, A. FGF and Shh signals control dopaminergic and serotonergic cell fate in the anterior neural plate. Cell, 1998, 93, 755-66.

15. Lee, J. Y., Chang, M.Y., Park, C.H., Kim, H.Y., Kim, J.H., Son, H., Lee, Y.S., Lee, S.H. Ascorbate-induced differentiation of embryonic cortical precursors into neurons and astrocytes. J Neurosci Res, 2003, 73, 156-65.

16. Zeng, X., Cai, J., Chen, Y. , Luo, Z. B., You, E., Fotter, Y. , Wang, B., Harvey, T., Miura, C., Backman, G. , Chen, J., Rao, M.S., Freed, W.J. Dopaminergic differentiation of human embryonic stem cells. Stem Cells, 2004, 22, 925-40.

17. Roy, N. S., Cleren,C., Singh, S.K., Yang, L., Beal, M.F., Goldman, S.A. Functional engraftment of human ES cell-derived dopaminergic neurons enriched by coculture with telomerase-immortalized midbrain astrocytes. Nat Med, 2006, 12, 1259-68.

18. Yan, Y., Yang,D., Zarnowska, E.D., Du, Z., Werbel, B., Valliere, C., Pearce, R.A., Thomson., J.A., Zhang, S.C. Directed differentiation of dopaminergic neuronal subtypes from human embryonic stem cells. Stem Cells, 2005, 23, 781-90.

19. Cho, M. S., Lee, Y.E., Kim, J.Y., Chung, S., Cho, Y.H., Kim, D.S., Kang, S.M., Lee, H., Kim, M.H., Kim, J.H., Leem, J.W., Oh, S.K., Choi, Y.M., Hwang, D.Y., Chang, J.W., Kim, D.W. Highly efficient and large-scale generation of functional dopamine neurons from human embryonic stem cells. PNAS, 2008, 105(9), 3392-3397.

20. Heiskanen, A., Hirovonen, T., Salo, H., Impola, U., Olonen, A., Laitinen, A., Tiitinen, S., Natunen, S., Aitio, O., Miller-Podraza, H., Wuhrer, M., Deelder, A.M.,, Natunen, J., Laine, J.,, Lehenkari, P., Saarinen, J., Satomaa, T., Valmu, L., Glycomics of bone marrow-derived mesenchymal stem cells can be used to evaluate their cellular differentiation stage. Glycoconj J, 2009, 26, 367-384.

21. Satomaa, T., Heiskanene, A., Mikkola, M., Olsson, C., Blomqvist, M., Tiittanen, M., Jaatinen, T., Aitio, O., Olonen, A., Helin, J., Hiltunen, J., Natunen, J., Tuuri, T., Otonkosku, T., Saarinen, J., Laine, J. The N-glycome of human embryonic stem cells. BMC Cell Biol, 2009, 10, (42), 1-18.

22. Hemmoranta, H., Satomaa, T., Blomqvist, M., Heiskanen, A., Aitio, O., Saa-rinen, J., Natunen, J., Partanen, J., Laine, J., Jaatinen, T. N-glycan structures and associated gene expression reflect the characteristic N-glycosylation pattern of human hematopoietic stem and progenitor cells. Exp. Hematol, 2007, 35, 1279-1292.

23. Chen, Y.J., Wing, D., Guile, G.R., Dwek, R.A., Harvey, D.J., Zamze, S. Neutral N-glycans in adult rat brain tissue. Eur J Biochem, 1998, 251, 691-703.

24. Ye, Z., Marth, J. N-glycan branching requirement in neuronal and postnatal viability. Glycobiology, 2004, 14, (6), 547-558.

25. Kornfeld, R., Kornfeld, S. Assembly of asparagine-linked oligosaccharides. Annu Rev Biochem, 1985, 54, 631-64.

26. Morishima, S., Morita, I., Tokushima, T., Kawashima, H., Miyasaka, M., Omura, K., Murota, S. Expression and role of mannose receptor/terminal high-mannose type oligosaccharides on osteoclast precursors during osteoclast formation. J of Endocrinol, 2003, 176, 285-292.

27. Kurachi, T., Morita, I., Toshikazu, O., Ueki, T., Sakaguchi, K., Enomoto, S., Mrota, S. Expression on outer-membranes of mannose residues, which are involved in osteclast formation via cellular fusion event. J of Biol Chem, 1994, 269, (26), 17572-17576.

28. Sriramarao, P., Berger, E., Chambers, J.D., Arfors, K.E., Gehlsen, K.R. High manse type N-linked oligosaccharides on endothelial cells may influence beta 2 intergrin mediated neutrophil adherence in vitro. J Cell Biochem, 1993, 51, (3), 360-8.

29. Oki, T., Konishi, K., Tomatsu, K., Tomita, K., Saitoh, M., Tsuanakawa, M., Nishio, T., Miyaki, T., Kawaguchi, H. Pradimicin, a novel class of potent antifungal antibiotics. J of Antibiotics, 1988, 41, 1701-1704.

30. Oki, T., Tenmyo, O., Hirano, M., Tomatsu, K., Kamei, H. Pradimicins A, B, and C: New antifungal antibiotics. In vitro and In vivo biological activities. J of Antibiotics, 1990, 43, 763-770.

31. Oki, T., Yamazaki, Y., Nomura, N., Furumai, T., Igarashi, Y. High mannose type oligosaccharide-dependent apoptosis in U937 cells induced by pradimicin, mannose-binding antibiotic. J of Antibiotics 1999, 52, (5), 449-454.

32. Chen, T., Yuan, D., Wei, B., Jiang, J., Kang, J., Ling, K., Gu1,Y., Li, K., Xiao, L., Pei, G. E-cadherin-mediated cell-cell contact is critical for induced pluripotent stem cell generation. Stem cell, 2010 [Epub ahead of print]

33. Li, Z., Qiu, D., Sridharan, I., Qian, X., Zhang, H., Zhang, C., Wang, R. Spatially resolved quantification of E-cadherin on target hES cells. J Phys Chem B 2010, 114: 2894-2900.

34. Li, L., Wang, S., Jezierski, A., Moalim-Nour, L., Mohib, K., Parks, R.J., Retta, S.F., Wang, L. A unique interplay between Rap1 and E-cadherin in the endocytic pathway regulates self-renewal of human embryonic stem cells. Stem Cells 2010, 28, 247-257.

35. Karpowicz,P., Willaime-Morawek, S., Balenci, L., DeVeale, B., Inoue, T., van der Kooy, D. E-Cadherin regulates neural stem cell self-renewal. J of Neurosci, 2009, 29(12), 3885–3896.

36. Takahashi K, Tanabe K, Ohnuki M, Narita M, Ichisaka T, Tomoda K, Yamanaka S. Induction of pluripotent stem cells from adult human fibroblasts by defined factors. Cell. 2007,131,(5),861-72.